

**STRATIGRAPHY AND VOLCANIC FACIES IN
KHAO NOI AREA, THA TAKIAP DISTRICT,
CHACHOENGSAO PROVINCE**



Miss Amporn Chaikam

**จุฬาลงกรณ์มหาวิทยาลัย
CHULALONGKORN UNIVERSITY**

**A Thesis Submitted in Partial Fulfillment of the Requirements
for the Degree of Master of Science in Geology
Department of Geology
FACULTY OF SCIENCE
Chulalongkorn University
Academic Year 2020
Copyright of Chulalongkorn University**

ลำดับชั้นหินและชุดลักษณะหินภูเขาไฟในบริเวณพื้นที่เขาน้อย
อำเภอท่าตะเียบ จังหวัดฉะเชิงเทรา



วิทยานิพนธ์นี้เป็นส่วนหนึ่งของการศึกษาตามหลักสูตรปริญญาวิทยาศาสตรมหาบัณฑิต
สาขาวิชาธรณีวิทยา ภาควิชาธรณีวิทยา
คณะวิทยาศาสตร์ จุฬาลงกรณ์มหาวิทยาลัย
ปีการศึกษา 2563
ลิขสิทธิ์ของจุฬาลงกรณ์มหาวิทยาลัย

อัมพร ไชยคำ : ลำดับชั้นหินและชุดลักษณะหินภูเขาไฟในบริเวณพื้นที่เขาน้อยอำเภอท่าตะเกียบ จังหวัดฉะเชิงเทรา. (STRATIGRAPHY AND VOLCANIC FACIES IN KHAO NOI AREA, THAKIAP DISTRICT, CHACHOENSAO PROVINCE) อ.ที่ปรึกษาหลัก : ดร.อภิสิทธิ์ ชาล้า

ภูเขาไฟเขาน้อย ตั้งอยู่ในอำเภอท่าตะเกียบ จังหวัดฉะเชิงเทรา ภาคตะวันออกของไทย ภูเขาไฟนี้เป็นส่วนหนึ่งของแนวหินภูเขาไฟลำปาง ซึ่งเป็นหินที่มีศักยภาพในการสะสมตัวของแร่ โดยเฉพาะแหล่งแร่ทองคำและพลวงแบบอพิเทอรัล (Au-Sn epithermal style) จากการศึกษาภาคสนาม ข้อมูลแท่งตัวอย่าง และการศึกษาสิลาวรรณภาพ พบว่าลำดับชั้นหินภูเขาไฟเขาน้อยมีความหนาไม่น้อยกว่า 150 เมตร ลำดับชั้นหินแบ่งออกเป็น 3 หน่วยหิน ประกอบด้วย 1) หน่วยหินตะกอน 2) หน่วยหินภูเขาไฟสีเข้ม-ปานกลาง (mafic-intermediate volcanic unit) และ 3) หน่วยหินภูเขาไฟสีจาง (felsic volcanic unit) หน่วยหินที่ 1 เป็นหินฐานของลำดับชั้นหินภูเขาไฟเขาน้อย ประกอบด้วยหินปูนแสดงชั้นบาง หินทรายแสดงชั้นบาง หินกรวดเหลี่ยมปูน และหินโคลนแสดงชั้นบาง หน่วยหินที่ 2 ประกอบด้วยหินแพลจิโอเคลสแอนดีไซต์ และหินกรวดเหลี่ยมแอนดีไซต์ หน่วยหินนี้มีลักษณะเป็นลาวาและไซยาโลกลาสไต์ หน่วยหินที่ 3 ประกอบด้วยหินกรวดเหลี่ยมพิมมิชเนื้อเศษหิน (lithic-rich pumice breccia) หินกรวดเหลี่ยมพิมมิชเนื้อผลึก (crystal-rich pumice breccia) และหินควอตซ์ไรโอไลต์ ลักษณะของหินกรวดเหลี่ยมพิมมิชเนื้อเศษหินและหินกรวดเหลี่ยมพิมมิชสามารถแปลผลได้ว่ามีการเกิดจากการระเบิดของภูเขาไฟและมีการสะสมตัวได้ทะเลในระดับต่ำกว่าอิทธิพลของคลื่นทะเล

ในการศึกษาธรณีเคมีได้นำตัวอย่างหินภูเขาไฟ (ลาวา) จากหน่วยหินสีเข้ม-ปานกลาง (หน่วยหินที่ 2) มาทำการศึกษาหาปริมาณของธาตุร่องรอยและธาตุหายาก พบว่าหน่วยหินสีเข้ม-ปานกลางมีองค์ประกอบเป็นหินแอนดีไซต์จนถึงหินทราไคต์-แอนดีไซต์ซึ่งมีความสัมพันธ์กับแมกมาชนิดแคลก์-แอลคาไล หินภูเขาไฟนี้สามารถแบ่งออกเป็นสองชุด โดยชุดที่หนึ่งมีปริมาณความเข้มข้นของธาตุนิกเกิล (Ni) ไทเทเนียม (Ti) และวานาเดียม (V) ที่สูงกว่า และชุดที่สองมีปริมาณความเข้มข้นของธาตุอิตเทรียม (Y) และเซอร์โคเนียม (Zr) ที่สูงกว่า หินทั้งสองชุดแสดงค่าคิดปกติเชิงลบของธาตุยูโรเพียม (Eu) และสตรอนเชียม (Sr) ขณะเดียวกันยังมีความสมบูรณ์ของธาตุ LILE และ LREE สูง และมีปริมาณธาตุไนโอเบียม (Nb) ต่ำ ซึ่งบ่งชี้ถึงหินต้นกำเนิดมาจากเปลือกโลกอัตราส่วนของธาตุแทนทาลัมต่ออิตเทรียม (Ta/Yb) และอัตราส่วนของธาตุทอเรียมต่ออิตเทรียม (Th/Yb) บ่งชี้ว่าหินทั้งสองชุดมีการเกิดในธรณีแปรสัณฐานแบบแนวโค้งภูเขาไฟทวีปหรือแนวเกาะโค้งภูเขาไฟแอลคาไลมหาสมุทร จากการเปรียบเทียบกับแนวหินภูเขาไฟปัจจุบันที่เกิดสัมพันธ์กับการมุดตัวของแผ่นเปลือกโลก พบว่าหินชุดที่หนึ่งมีรูปแบบคล้ายกับหินแคลก์-แอลคาไลที่มีโพแทสเซียมสูง (High-K calc-alkaline) จากบริเวณ Riggitt-Beser complex อาบูโพลสโตซิน ในจังหวัดชาวตะวันออก ประเทศอินโดนีเซีย ในขณะที่หินชุดที่สองมีรูปแบบคล้ายกับหินแคลก์-แอลคาไลที่มีโพแทสเซียมสูง จากบริเวณเกาะเอโอเลียน (Aeolian island) อาบูโพลสโตซิน ตอนใต้ของทะเลดีร์เรเนียน (Tyrrhenian sea) ประเทศอิตาลี นอกจากนี้หินทั้งสองชุดยังมีลักษณะคล้ายกับหินภูเขาไฟจากพื้นที่ลำปางซึ่งเกิดขึ้นในสภาพแวดล้อมที่เกี่ยวข้องกับการมุดตัวในช่วงยุคไทรแอสซิกตอนกลาง ดังนั้นหินภูเขาไฟเขาน้อยอาจมีการก่อตัวขึ้นในธรณีแปรสัณฐานแบบแนวโค้งภูเขาไฟและเป็นส่วนหนึ่งของแนวภูเขาไฟลำปาง

สาขาวิชา ธรณีวิทยา

ปีการศึกษา 2563

ลายมือชื่อผู้จัดทำ

ลายมือชื่อ อ.ที่ปรึกษาหลัก

6172102023 : MAJOR GEOLOGY

KEYWORD: volcanic facies, Lampang volcanic belt, Chachoengsao province, Sukhothai arc, Khao Noi

Amporn Chaikam : STRATIGRAPHY AND VOLCANIC FACIES IN KHAO NOI AREA, THA TAKIAP DISTRICT, CHACHOENGSAO PROVINCE.
Advisor: ABHISIT SALAM, Ph.D.

The Khao Noi volcanics is in Tha Takiap district, Chachoengsao province, eastern Thailand. This volcanics is a part of the Lampang volcanic belt, a potential host rocks for mineralizations, especially gold and antimony epithermal style deposits. Based on field investigation, drill core logging, and petrographic study, the Khao Noi host volcanic sequence has a thickness of at least 150 meters. The sequence can be divided into three units, namely 1) Sedimentary unit (Unit 1), 2) Mafic-intermediate volcanic unit (Unit 2), and 3) Felsic volcanic unit (Unit 3). Unit 1 forms as a basement of the Khao Noi volcanic sequence and is characterized by laminated limestone, laminated sandstone, limestone breccia, and laminated mudstone. Unit 2 consists of plagioclase-phyric andesite, monomictic andesitic breccia, and mafic volcanic facies. This unit is mainly characterized by lava and hyaloclastite facies. Unit 3 consists of lithic-rich pumice breccia, crystal-rich pumice breccia, and quartz-phyric rhyolite facies. Both lithic-rich pumice breccia and crystal-rich pumice breccia facies were interpreted to form from the explosive eruption and deposited in the submarine environment below the wave-base.

The volcanic rocks (lava) from the mafic-intermediate volcanic unit (Unit 2) were selected for geochemistry study. Based on trace elements and REEs, the mafic-intermediate volcanic rocks range in composition from andesite to trachyte-andesite with calc-alkaline magma affinity. These volcanic rocks can be separated into two suites; Suite I shows a higher concentration of Ni, Ti, and V, and Suite II shows a higher concentration of Y and Zr. Both Suites I and II have negative Eu and Sr anomalies. Besides, they are characterized by enrichment of LILE and LREE with depleted Nb indicating the crust-derived magmatic source. A ratio of Ta/Yb vs. Th/Yb indicates that both suites originate in a continental arc or alkaline oceanic arc setting. According to the modern analogs of subduction-related settings, Suite I resembles a high-K calc-alkaline rock from the Riggitt-Beser complex, Pleistocene age, East Java Indonesia. While Suite II similar to the high-K calc-alkaline rocks from the Aeolian islands of Pleistocene age from the southern part of the Tyrrhenian Sea, Italy. Furthermore, both Suites I and II are similar to the Lampang area's volcanic rocks, which occur in subduction-related settings during the Middle Triassic age. Thus, the Khao Noi volcanic rocks might be formed in an arc tectonic setting as a part of the Lampang volcanic belt.

Field of Study: Geology
Academic Year: 2020

Student's Signature
Advisor's Signature

ACKNOWLEDGEMENTS

I would like to thank my supervisor, Dr. Abhisit Salam, for his supervision, for his help in the field, and for his thorough, constructive reviews and comments.

I also would like to extend deep appreciation to the Department of Mineral resources for drill core samples, XRF analyses, and financial supports.

Thanks are also too many people who assisted during this study, in particular, Dr. Takayuki Manaka for his suggestion and revision; Dr. Punya Charusiri for useful comment; Mr. Tanaz Watcharamai, Miss Maythira Srivichai, Mr. Sirawit Keawpaluk, and Miss Saowaphap Uthairat for their advice. All staff and members of the Department of Geology, Faculty of Science, Chulalongkorn University include Ms. Sopit Poompuan, Mr. Prajin Thongprachum, Mr. Suriya Chokmo, Ms. Jiraprapa Niampan, and Ms. Bunjong Puanthong for preparing thin-section, sample powder, and many facility supports. And Dr. Somboon Khositanont for inspired me to this study.

Finally, I would like to give special thanks to my family, who support my studies.

Amporn Chaikam

TABLE OF CONTENTS

	Page
ABSTRACT (THAI)	iii
ABSTRACT (ENGLISH).....	iv
ACKNOWLEDGEMENTS.....	v
TABLE OF CONTENTS.....	vi
LIST OF TABLES.....	ix
LIST OF FIGURES	x
CHAPTER 1 INTRODUCTION.....	1
1.1 Introduction	1
1.2 Location and accessibility	2
1.3 Objective of the study.....	2
1.4 Physiographic description	3
1.5 Thesis structure.....	4
CHAPTER 2 TECTONIC SETTING AND REGIONAL GEOLOGY	5
2.1 Introduction	5
2.2 Tectonic setting of Thailand.....	5
2.3 The pre-Cenozoic volcanic rocks in Thailand.....	7
1) Chiang Mai volcanic belt.....	7
2) Lampang volcanic belt.....	9
3) Nan river volcanic belt.....	10
4) Phetchabun volcanic belt	10
2.4 Regional geology of study area	12
CHAPTER 3 STRATIGRAPHY, VOLCANIC FACIES AND ARCHITECTURE ..	14
3.1 Introduction	14
3.2 Stratigraphy of the Khao Noi area.....	14
3.2 Facies and Facies associations of Khao Noi volcanic	16

1) Laminated limestone facies	16
2) Laminated sandstone facies	20
3) Limestone breccia facies.....	20
4) Laminated mudstone facies	24
5) Plagioclase-phyric andesite facies association	24
6) Monomictic andesitic breccia facies.....	27
7) Plagioclase-phyric basalt facies	27
8) Aphyric trachyte facies	30
9) Quartz-phyric rhyolite facies association	30
3.4 Interpretation of volcanic facies	35
3.5 Facies architecture of the Khao Noi area succession	36
CHAPTER 4 GEOCHEMISTRY	38
4.1 Introduction	38
4.2 Sample preparation and analytical techniques	38
1) Major element analyses	38
2) Trace and Rare earth element analyses.....	39
4.3 Rock types and Magmatic affinities	40
1) Plagioclase-phyric andesite	40
2) Plagioclase-phyric basalt dyke	45
3) Aphyric trachyte dyke.....	48
4.4 Tectono-magmatic Discrimination Diagrams	50
CHAPTER 5 DISCUSSION AND CONCLUSION	52
5.1 Introduction	52
5.2 Stratigraphy	52
5.3 Volcanism.....	52
5.4 Magmatic suite at Khao Noi volcanic	55
5.5 Tectonic setting	56
5.6 Regional tectonic setting	57
5.7 Conclusion.....	58

REFERENCES60
VITA.....66



LIST OF TABLES

	Page
Table 3.1 List of selected drill holes and outcrop description of the Khao Noi volcanic	15
Table 4.1 List of rock sample from Khao Noi area for whole-rock geochemistry.....	39
Table 4.2 Whole-rock major element oxide (wt. %), trace and rare earth elements (ppm).	41



LIST OF FIGURES

	Page
Fig. 1.1 Google image showing accessibility and the location of the study area (modified from Google map data ©2020).....	3
Fig. 1.2 Topographic map of the Khao Noi area (modified from The Royal Thai Survey Department, 2008).....	4
Fig. 2.1 Tectonic map showing the location of the study area (red square) in eastern Thailand, and five tectonic terranes comprise (1) Sibumasu terrane; (2) Inthanon zone; (3) Sukhothai arc; (4) Loei-Phetchabun fold belt; (5) Indochina terrane (after Bunopas and Khositantont, 2008; Sone and Metcalfe, 2008).	6
Fig. 2.2 Map showing the location of study area (red square) and the distribution of pre-Cenozoic volcanic rocks in Thailand (after Barr and Macdonald, 1991; Sone and Metcalfe, 2008).	8
Fig. 2.3 Geological map of the Khao Noi area (modified from Tiyaipirach, 1996).....	13
Fig. 3.1 (A) The Khao Noi volcanic located in east of Thailand. (B) Geological map showing outcrop location and (C) Drill holes location of the Khao Noi volcanic, Tha Takiap district, Chachoengsao province.	17
Fig. 3.2 Simplify graphic log of selected drill holes, in geographic order from northernmost at the left to the southernmost at the right. See Fig. 3.1C for location of drill holes.	18
Fig. 3.3 Preliminary schematic cross-section (A-A') of the Khao Noi volcanic, showing lithofacies relationships, and somewhat oblique to be trends, display east-trending inclining in cross-section. See Fig. 3.1C for location of drill holes (after DMR, 2007).	19
Fig. 3.4 Simplify composite stratigraphy of the Khao Noi volcanic, Chachoengsao province, eastern Thailand.	19
Fig. 3.5 Graphic log for drill holes DDH08, DDH26, DDH16 and lower part of DDH24, which intersects a thick interval of quartz-phyric rhyolite, aphyric trachyte, laminated sandstone and limestone. (A) Hand specimen of limestone interbedded with mud layer and inclined bed (40°, dip angle; DDH24 at depth 124.4 m). (B) Polarized photomicrograph of fossil fragment (foraminifera?) set in less carbonate cement. (C) Photograph of boundstone in Wat Tham Raet (KN13) adjacent area contains abundant of coral mounds. See Fig. 3.1C for location of drill holes and outcrops.	21
Fig. 3.6 (A) Photographs showing core sample laminated sandstone and limestone breccia (B) Hand specimen showing laminated sandstone interlayer with mud layer and inclined bed (60°, dip angle; DDH24 at depth 111.5 m). (C) Cross-polarized photomicrograph showing subangular sand size-grains with mostly clear quartz, feldspar, and clay. (D)	

- Hand specimen of fine sandstone associated with fossil fragments. (E) Photograph of an outcrop of fine sandstone at the north of Khao Noi. See Fig. 3.1C for location of drill holes and outcrops. 22
- Fig. 3.7 The graphic log of lower part of drill hole DDH24, which interbedded a thick interval of limestone breccia, laminated sandstone and laminated limestone. (A) Hand specimen showing clast-supported of limestone breccia, mostly clasts of irregular limestone clasts, sandstone and few of mudstone surrounded by mud-matrix breccia (at depth 106.5 m). (B) Polarized photomicrograph showing fossils fragment (foraminifera?) in limestone clasts. See Fig. 3.1C for location of drill holes. 23
- Fig. 3.8 The graphic log upper part of drill hole DDH24 through a laminated mudstone intersected by Quartz-phyric rhyolite with sharp contacts. (A) Hand specimen of laminated mudstone with fine-grains layers. (B) Cross-polarized photomicrograph laminated mudstone in normal graded fine-grained of crystal and lithic fragment and minor opaque mineral and pyrite crystal (arrow). (C) Beds of lithic and volcanoclastic clasts rich at basal at interval 65-70 meters. See Fig. 3.1C for location of drill holes. 25
- Fig. 3.9 The graphic log through a plagioclase-phyric andesite. (A) Plagioclase-phyric andesite showing fine-grain, that contains plagioclase phenocrysts. (B) Cross-polarized photomicrograph showing hornblende (hbl) and plagioclase phenocrysts (pl) in microlite plagioclase groundmass. (C) Cross-polarized photomicrograph of plagioclase phenocrysts (pl) in a holocrystalline groundmass and vesicle (V) and quartz. (D) Hand specimen of plagioclase-phyric andesite containing plagioclase phenocrysts. See Fig. 3.1C for location of drill holes. 26
- Fig. 3.10 Characteristics of coherent monomictic andesitic breccia in the graphic log of drill holes DDH17 and DDH23 (A) Glassy margins of irregular shape. (B) Subangular clasts exhibiting jigsaw-fit within coarse-grained lithic and crystal fragments. (C) Cross-polarized photomicrograph showing plagioclase phenocrysts with fine-grained matrix. (D) Fine-grained margin showing flow-banded crystals (E) Cross-polarized photomicrograph showing flame texture and flow-banded of glass shard and crystals. See Fig. 3.1C for location of drill holes. 28
- Fig. 3.11 The graphic log through plagioclase-phyric basalt and aphyric trachyte intersected limestone (drill hole DDH09). (A) Fine-grained margins of aphyric trachyte (up) showing aphanitic texture and plagioclase-phyric basalt (down) showing sparsely phenocrysts with medium grained. (B) Cross-polarized photomicrograph aphyric trachyte showing microlite plagioclase of trachytic texture. (C) Cross-polarized photomicrograph of plagioclase-phyric basalt showing mafic mineral phenocrysts which is partly pseudomorphs by chlorite (chl) with felty-texture groundmass of plagioclase. See Fig. 3.1C for location of drill holes. 29
- Fig. 3.12 The graphic log in drill hole DDH26 through lithic-rich pumice breccia overlying on quartz-phyric rhyolite with sharp contacts. The sequence of the pumice-rich unit base on breccia grading to the finer grain of sand size rich. (A) The uppermost sequence of lithic-rich pumice breccia showing fine-grained lamination interlayer coarse-grained

and breccia. (B) Hand specimen of lithic-rich pumice breccia, clasts mainly of pumice clast (P) and lithic clasts (L). Large silicified quartz-plagioclase-phyric rhyolite clast (J) with sericite alteration (at depth 44.6 m). See Fig. 3.1C for location of drill holes. ... 31

Fig. 3.13 Hand specimen of crystal-rich pumice breccia showing many pumice clasts have an irregular shape, surrounding by crystal fragments. (A) Polarized Photomicrograph showing phyric pumice (pp) contains quartz, feldspar, and tube pumice (tp) (arrow). (B) Cross-polarized photomicrograph of pumice clast and fluorite (fl) infill within the association of the fine-grained matrix and shard. (C) Polarized Photomicrograph showing glass shard and fine-grained pumice fragments. 33

Fig. 3.14 (A) Fine-grained quartz-phyric rhyolite containing an abundance of quartz (qtz) and plagioclase (pl) phenocrysts. (B) Cross-polarized photomicrograph showing large subhedral quartz xenocrysts with irregular embayed edges set in the cryptocrystalline groundmass. (C) Coarse-grained composed of quartz xenocrysts and plagioclase phenocrysts with iron oxide. (D) Cross-polarized photomicrograph showing plagioclase phenocrysts, cluster of quartz xenocrysts with an irregular resorbed layer in quartz microcrystalline groundmass and zircon grain (zrn). See Fig. 3.1C for location of drill holes. 34

Fig. 3.15 Schematic cross-section through the Khao Noi area. (A) Subaqueous, andesite lava domes and sills volcano; Unit 2. (B) The syn-volcanic intrusion of the basalt dykes and aphyric trachyte dykes (Unit 2). (C) Subaerial to shallow marine pyroclastic eruptions generate subaqueous syn-volcanic mass-flow deposits; Unit 3, and (D) The syn-volcanic intrusion of rhyolite sills (Unit 3)..... 37

Fig. 4.1 Discrimination diagram of Nb/Y and Zr/TiO₂ (after Winchester and Floyd, 1977)..... 43

Fig. 4.2 Major element bivariate diagrams plotted against MgO for volcanic rocks from Khao Noi area. (A) SiO₂ vs. MgO showing a slightly negative trend to more mafic composition, (B) TiO₂ vs. MgO showing low concentrate and relatively high Ti for dykes, (C) Fe₂O₃ (total) vs. MgO showing low Fe concentrate and high Fe concentrate in dykes, (D) CaO vs. MgO showing slightly low Ca and relatively high for plagioclase-phyric basalt dyke, (E) K₂O vs. MgO showing low concentrate for the volcanic rocks, and (F) Al₂O₃ vs. MgO showing low concentrate for the volcanic rocks..... 44

Fig. 4.3 AFM diagram for tholeiite and calc-alkaline magma series with divide line from Irvine and Baragar (1971); dash gray line) showing trend to calc-alkaline and tholeiite series for the volcanic rocks. 45

Fig. 4.4 Trace element bivariate diagrams plotted against MgO for coherent rocks from the Khao Noi area. (A) Zr vs. MgO showing low Zr concentrate, (B) Ni vs. MgO showing low concentrate except the Suite I of plagioclase-phyric andesite showing a negative trend, (C) V vs. MgO showing high V for Suite I and low concentrate for all volcanic rocks, (D) Sr vs. MgO showing a slightly positive trend for volcanic rocks, (E) Y vs. MgO showing low concentrate, and (F) Zn vs. MgO showing low concentrate. 46

- Fig. 4.5 Chondrite-normalized REE patterns for the plagioclase-phyric andesite, the Chondrite-normalized value from Sun and McDonough (1989). 47
- Fig. 4.6 N-MORB normalized multi-element for plagioclase-phyric andesite, the N-MORB normalized value from Sun and McDonough (1989). 47
- Fig. 4.7 Chondrite-normalized REE patterns for the plagioclase-phyric basalt dyke, the Chondrite-normalized value from Sun and McDonough (1989). 47
- Fig. 4.8 N-MORB normalized multi-element for plagioclase-phyric basalt dyke, the N-MORB normalized value from (Sun and McDonough, 1989). 48
- Fig. 4.9 Chondrite-normalized REE patterns for the aphyric trachyte, the Chondrite-normalized value from Sun and McDonough (1989). 49
- Fig. 4.10 N-MORB normalized multi-element for aphyric trachyte, the N-MORB normalized value from Sun and McDonough (1989). 49
- Fig. 4.11 (A) Al_2O_3 vs. TiO_2 (after Müller et al., 1992); (B) Ta/Yb vs. Th/Yb diagram (after Pearce, 1983) the volcanic rocks are distinguishing all group generally shonshonitic series show the field for Continental arcs and alkaline oceanic arcs. 50
- Fig. 4.12 (A) N-MORB normalized multi-element patterns and (B) Chondrite-normalized REE patterns for the studied, least-altered volcanic rocks and their modern analogue. 51
- Fig. 5.1 Schematic of facies modal for the depositional environment. (A) The sedimentary rocks (Unit 1) were deposited after the Early Carboniferous age. (B) During the late Permian age, the first plagioclase-phyric andesite lava was effusive overlying basement sedimentary rocks and associated hyaloclastite (Unit 2). Then (C) the second of andesitic lava was effusive. (D) Emplacement of mafic-intermediate dykes. 54
- Fig. 5.2 Schematic of facies modal for depositional environment. (E) Syn-eruptive pyroclastic flow, pyroclastic surge and resedimented pyroclasts from distal source. (F) At least of three sequence of felsic volcanism that deposited in the Khao Noi volcanic. And (G) the last events is syn-volcanic rhyolite dyke and sills. 55
- Fig. 5.3 N-MORB normalized multi-element diagram of Sun and McDonough (1989) displaying the patterns for two suite representative Khao Noi volcanic rocks compared with surrounding volcanic belt. Note; black dotted line data from Barr et al. (2000), purple dotted line data from Srichan et al. (2009), red dotted line data from Salam et al. (2014), orange dotted line data from Arboit et al. (2016). 58

CHAPTER 1

INTRODUCTION

1.1 Introduction

Gold is an important ore metal for the world economy, along with ore metal associated such as copper, lead, zinc. It occurs in many mineral deposit types such as volcanic hosted massive sulfide deposits (VMS), porphyry and epithermal deposits. Moreover, Gold is often the predominant metal in epithermal deposits, providing more than a kilogram of gold per ton, as it does in New Zealand, Indonesia, Papua New Guinea, North America, and Japan. The Wairakei and Broadlands deposits in New Zealand are large epithermal gold deposits in the world, along with arsenic, cadmium, copper, lead, and zinc associated with quartz veins in the Taupo volcanic host and formed in Neogene. They also volcanic-related mineral deposits and for that reason, volcanic rocks are a key point of interest when discussing gold deposits.

In Thailand, the volcanic rocks mainly distribute in the northern part, the upper central part, and the eastern part of the country. They are mainly confined to the Sukhothai Arc (SA) and the Loei Fold Belt (LFB; Fig. 1.1). Volcanic rocks play an essential role in hosting mineral deposits, for instance, volcanic massive deposits (VMS), epithermal gold deposits (both high- and low sulfidation epithermal gold deposits). Moreover, skarn deposits are often associated with intermediate volcanic rocks. In Thailand, the best example of an epithermal gold deposit hosted in volcanic rocks is the Chatree epithermal gold-silver deposits in Phetchabun province. Ten kilometers to the west of the Chatree deposits is the Khao Phanom Pha gold skarn deposits in Phichit province hosted by Late Permian to Early Triassic volcanic rocks. Moreover, small mineral occurrences have been reported in association with volcanic rocks in the Sukhothai Arc, such as the Huai Kham On orogenic gold prospect in Lampang-Phrae province (Khositanont et al., 2009).

Khao Noi volcanic (study area) locates in Chachoengsao province that lies within the southern part of the Lampang volcanic belt also hosts epithermal antimony-fluorite-gold mineralization (Fig. 1.1; Khin Zaw et al., 2014; Paipana, 2014). Most studies of volcanic rocks in the region focus on petrochemistry including in the Sukhothai Arc, where the Khao Noi volcanic rock is located. At the Khao Noi, Paipana, (2014) study

focused on general geology, geochemistry, and mineralization of antimony-fluorite-gold mineralization. There is no detailed study of volcanic rocks, particularly on volcanic facies and facies architecture has been done. To define the characteristics of Khao Noi volcanic and its environment of deposition. Therefore, this study focuses on detailed volcanic facies and volcanic architectures, and whole-rock geochemistry to present the possible tectonic setting and compare the data with those of modern analogue of volcanic suites.

1.2 Location and accessibility

The study area is at Khao Noi (13°22'02.7" latitude 101°41'36.6" longitude), Tha Takiap district, Chachoengsao province (Fig. 1.1). It is about 170 kilometers east of Bangkok and about 100 kilometers east of Chachoengsao township. The area is in geological map sheet ND47-12 (Bangkok) at a scale of 1:250,000 and on geological map sheet 5335 IV (Amphoe Tha Takiap) and covers an area of approximately 5 square kilometers.

The study area can access many routes. From Bangkok, the journey can be comfortable using the highway toll Route 7 (Bangkok-Baan Chang), following Route 7 about 65 km to Chachoengsao province. Then turn left onto Route 315 (Chachoengsao-Chonburi), and turning right onto Route 3259 following about 10 km, and turn right to the northern part of study area (Khao Noi) (Fig. 1.1).

1.3 Objective of the study

1. To determine the relationship between volcanic facies from stratigraphy, petrography, and geochemistry.
2. To describe the tectonic setting in relation to volcanic rocks in the Khao Noi area.

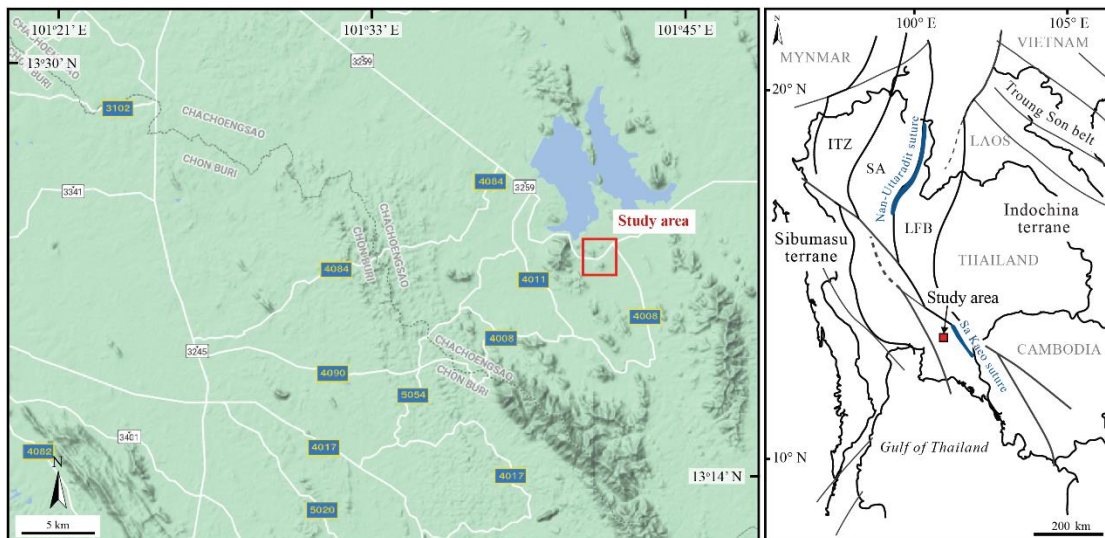


Fig. 1.1 Google image showing accessibility and the location of the study area (modified from Google map data ©2020).

1.4 Physiographic description

The study area composes of a low hill and undulating terrain between NNW-SSE trending (Fig. 1.2). The hill in the western part of the study area includes Khao Yai Mo Noi and Khao Noi, whereas those in the eastern part, about 60 % of the area covered by undulating terrain. The highest hill in the western is Khao Yai Mo Noi (343 meters above mean sea level) and Khao Noi (177 meters above mean sea level). The Takao River is the primary drainage system with a dendritic pattern that develops on low terrain. The north of the study area is represented by the Khlong Si Yat reservoir (Fig. 1.2).

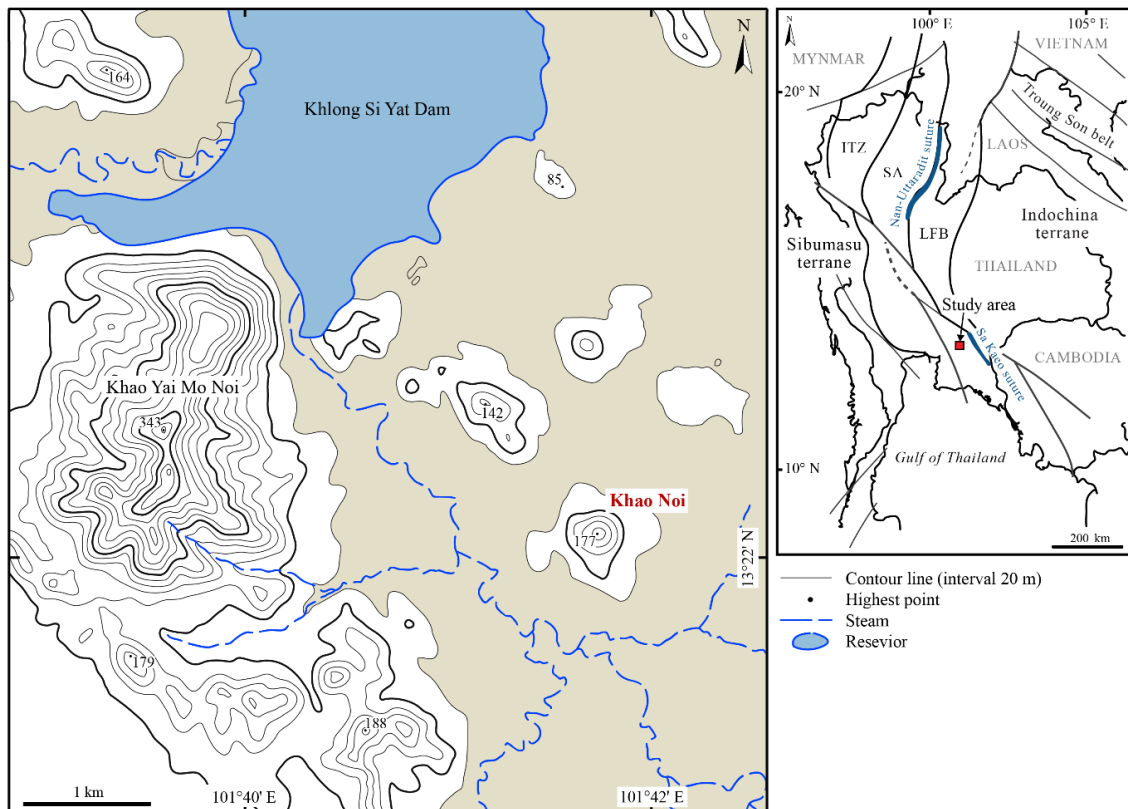


Fig. 1.2 Topographic map of the Khao Noi area (modified from The Royal Thai Survey Department, 2008).

1.5 Thesis structure

The thesis divided into the following chapters:

Chapter 2 (Tectonic setting and Regional geology) includes the tectonic setting of Thailand, the pre-Cenozoic volcanic rocks in Thailand, and the regional geology of the study area.

Chapter 3 (Stratigraphy, Volcanic facies, and Facies architecture) presents the detailed stratigraphy, the characteristics of volcanic facies, and a discussion of the volcanic architecture of the study area.

Chapter 4 (Geochemistry) presents the characteristics of volcanic rocks by geochemistry, and explain their tectonic settings in the Khao Noi area.

Chapter 5 (Discussion and Conclusion) involves the discussion and summarization of all the collected data in this study.

CHAPTER 2

TECTONIC SETTING AND REGIONAL GEOLOGY

2.1 Introduction

This chapter reviews the tectonic evolution of Thailand and its adjacent areas as well as the characteristics and distribution of pre-Cenozoic volcanic rocks in Thailand.

2.2 Tectonic setting of Thailand

Thailand and its adjacent area comprise of two major terranes, namely, Sibumasu terrane (the northern part previously known as Shan-Thai; Bunopas, 1981) in the west and Indochina terrane in the east (Fig. 2.1). In between, there are the Inthanon zone, a zone representing old Paleo-Tethys on the eastern edge of Sibumasu terrane, and Sukhothai Arc; an island arc lay to the east of the Inthanon zone. The Loei Fold Belt represents a zone predominantly of volcano-plutonic rocks on the western edge of the Indochina terrane (Fig. 2.2). The Sibumasu terrane and Indochina terrane separated from Gondwana during the Pre-Cambrian and lower Paleozoic ages, respectively (Bunopas, 1981; Bunopas and Vella, 1983). Later, these two tectonic terranes moved together, collided, and amalgamated during the Carboniferous to Middle Triassic (Barr and Macdonald, 1991; Bunopas, 1981; Bunopas and Khositanont, 2008). Sone and Metcalfe, 2008) proposed the tectonic model explaining the relationships between Sibumasu terrane and Indochina terrane during the closure of Paleo-Tethys and the formation of the Sukhothai Arc. Based on stratigraphy correlations, fauna, igneous, and geological history indicated that the Sukhothai arc could be correlated with southwest China (Lincang region). The Sukhothai Arc also correlated with the East Malaya (Barr et al., 2006; Barr and Macdonald, 1991; Gillespie et al., 2019; Sone et al., 2012; Sone and Metcalfe, 2008; Ueno and Hisada, 2001). The Chiang Mai-Chiang Rai tectonic line separates the Sukhothai Arc in the north and the Klaeng fault in the south from the Inthanon zone. The Jinhong suture is a north extension of the Nan-Uttaradit-Sa Kaeo suture, representing a back-arc basin that separated the Sukhothai Arc from the Loei Fold Belt (Barr and Macdonald, 1987; Singharajwarapan and Berry, 2000; Ueno and Hisada, 2001).

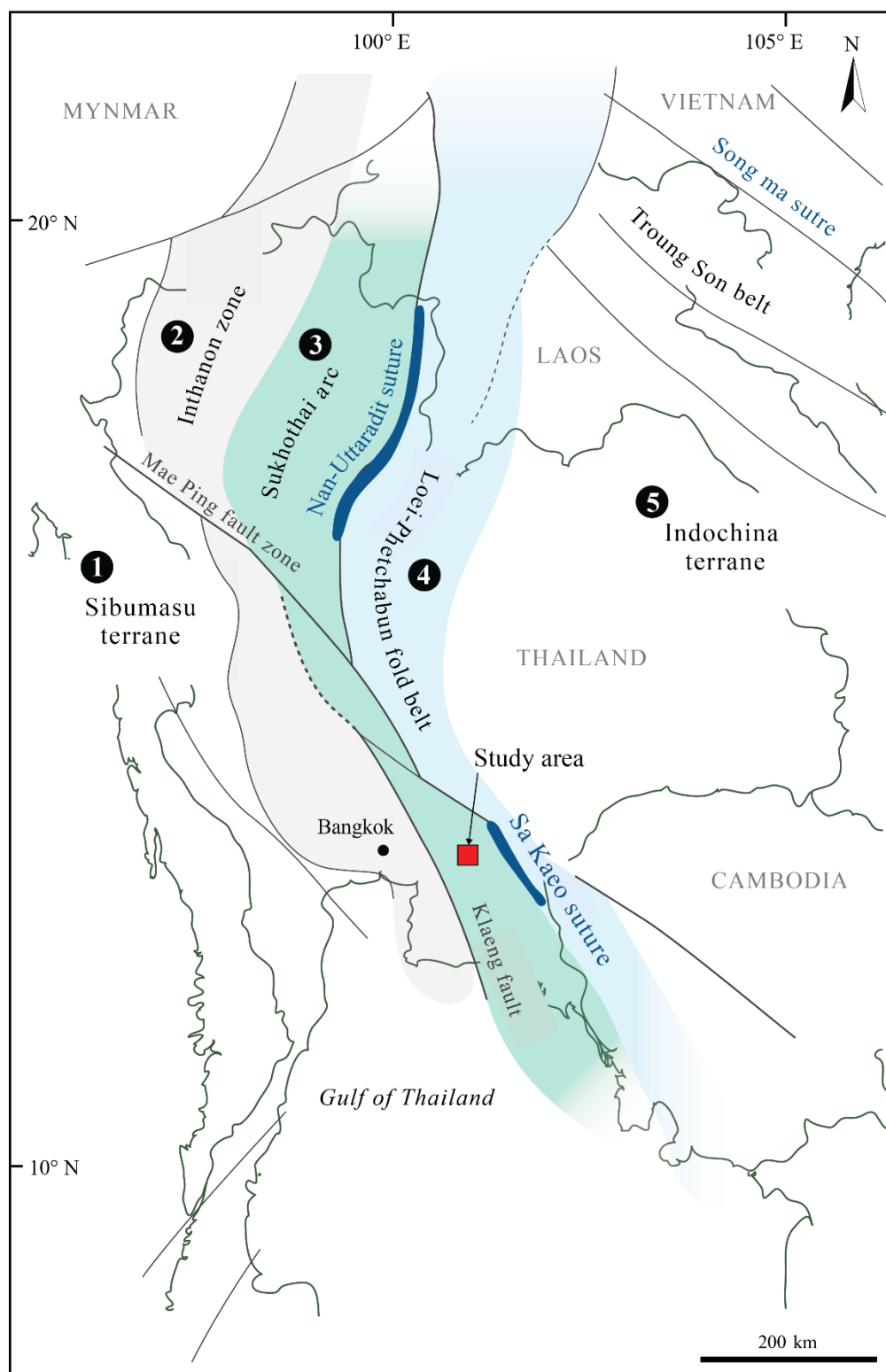


Fig. 2.1 Tectonic map showing the location of the study area (red square) in eastern Thailand, and five tectonic terranes comprise (1) Sibumasu terrane; (2) Inthanon zone; (3) Sukhothai arc; (4) Loei-Phetchabun fold belt; (5) Indochina terrane (after Bunopas and Khositant, 2008; Sone and Metcalfe, 2008).

2.3 The pre- Cenozoic volcanic rocks in Thailand

In Thailand, pre-Cenozoic volcanic rocks mainly distribute in the northern, upper central, north eastern part (e.g., Loei, Nong Khai), and eastern part of the country (Fig. 2.2). On the other hand, the Cenozoic volcanic rocks are predominantly comprised of basalt and rhyolite. Some basalts of the Cenozoic age are gems bearing particularly those found in Chanthaburi (eastern Thailand) and Kanchanaburi (western Thailand). However, in this review focus will be given to the pre-Cenozoic volcanic consistency with the focus of this study. Based on the tectonic setting, geochemistry, and ages, they can be divided into four belts, namely 1) Chiang Mai volcanic belt, 2) Lampang volcanic belt, 3) Nan river volcanic belt, and 4) Phetchabun volcanic belt (Barr and Macdonald, 1991) (Fig. 2.2).

1) Chiang Mai volcanic belt

The Chiang Mai volcanic belt (or Chiang Mai-Chiang Rai volcanic belt of Panjasawatwong, 2003) locates in the Inthanon zone, and its zone trending almost N-S. The volcanic rocks of this belt are exposed in the northern part of Mae Chan district, Chiang Rai province. In Chiang Mai province, the rocks of this belt are exposed in Fang, Chiang Dao, Doi Saket, San Kamphaeng districts. Moreover, the rocks of this belt are also exposed in the Lamphun province, south of Chiang Mai. The volcanic rocks in this belt are inferred of Carboniferous to Permian ages (Barr et al., 2000; Barr and Macdonald, 1979; Phajuy et al., 2005)

Barr et al. (1990) suggested that the volcanic rocks in the San Kamphaeng area (east of Chiang Mai province) comprise mainly basaltic flow and lithic crystal tuff. They are identified as transitional tholeiite and alkaline affinities. They formed in an extensional continental setting (back-arc).

Panjasawatwong et al., (1995) studied volcanic rocks in the Li basin and reported that the volcanic rocks in this area mainly comprise basaltic flows, pillow breccia hyaloclastite with a transitional tholeiite affinity. Besides, Phajuy et al., (2005) studied volcanic rocks in the Phrao district, north of the Chiang Mai volcanic belt, and suggesting that the rocks include mafic lava flow, pillow lava, and dykes of tholeiite that forming in the oceanic basin. Moreover, Phajuy (2008) concluded that the Chiang Mai volcanic belt comprises at least two generations, namely, the Silurian-Devonian and Carboniferous-

Triassic ages comprising mafic to ultramafic compositions. They occur as a lava flow, pillow lava, and hyaloclastite. Subsequently, Shen et al., (2009) suggested that the basaltic rocks have an alkaline affinity with high Ti, and P interpreted as formed in an oceanic island setting. Zhang et al., (2016) provides an age of these volcanic rocks of 283 Ma (Wang et al., 2017) and suggesting that in the Chiang Dao area they are ocean island basalt with high-Fe, Ti forming in Seamount setting.

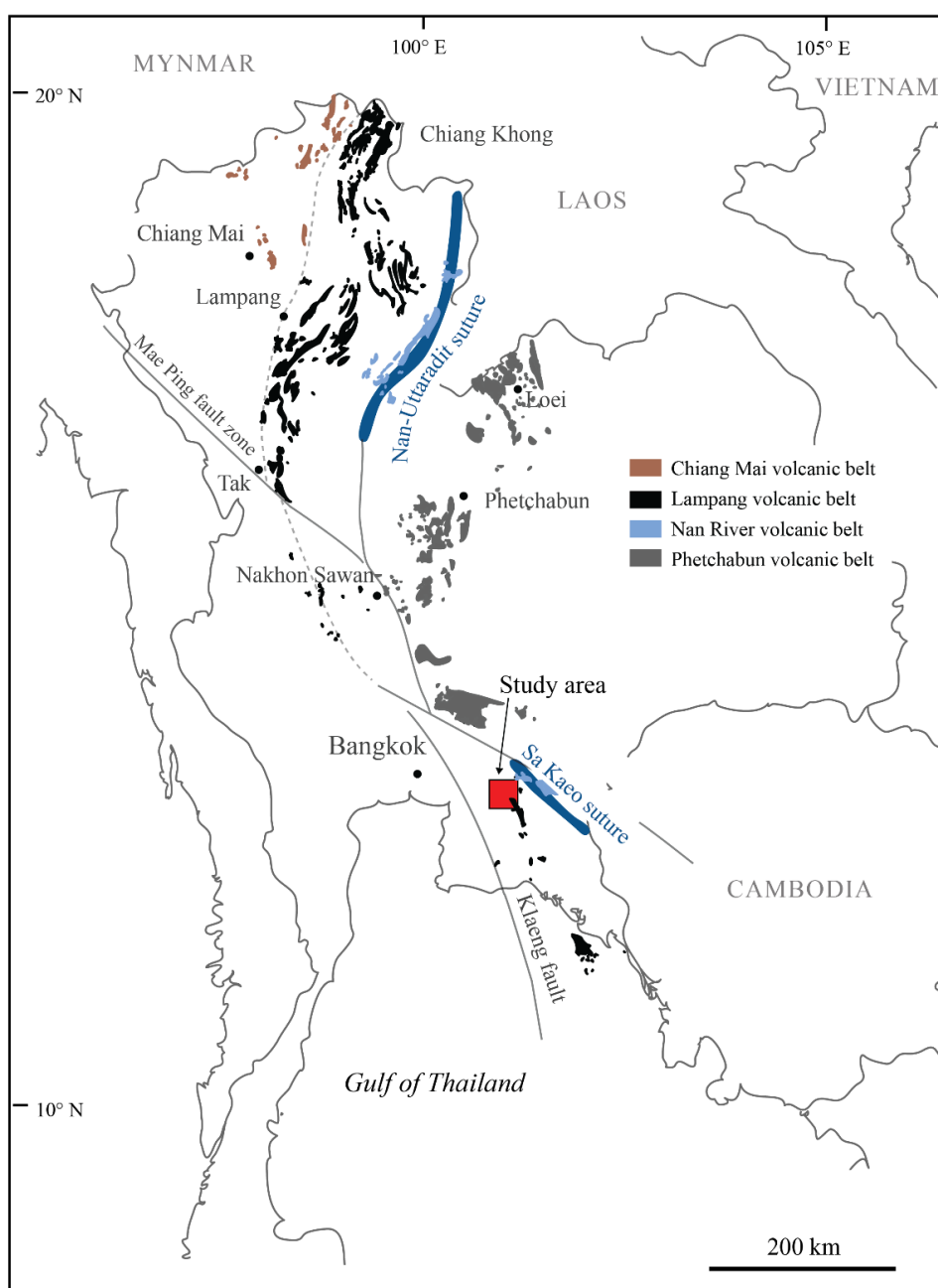


Fig. 2.2 Map showing the location of study area (red square) and the distribution of pre-Cenozoic volcanic rocks in Thailand (after Barr and Macdonald, 1991; Sone and Metcalfe, 2008).

2) Lampang volcanic belt

The Lampang volcanic belt is also known as Chiang Khong-Tak volcanic belt (Panjasawatwong, 2003). It is overlapping with the Sukhothai arc extending from northern, through central and to eastern Thailand (Barr and Charusiri, 2011; Barr and Macdonald, 1991; Baum et al., 1982; Baum and Hanh, 1977; Chaodumrong, 1992; Hara et al., 2009; Piyasin, 1972; Sone et al., 2012; Sone and Metcalfe, 2008). The Lampang volcanic belt is trending almost N-S in the northern part then to NW-SE in the south. It is widely distributed mainly in the north, central, and eastern parts of the country. This belt's volcanic rocks can be found from Chiang Khong district in Chiang Rai province through Lampang, Phrae, Tak, Nakhon Sawan, and Chanthaburi province in the eastern part of the country. Panjasawatwong (2003) studied the petrochemistry of volcanic rocks in the northern part of the Chiang Khong area and reported that they consist of dacite to tholeiite basalt forming in a continental arc setting. Subsequently, Barr et al. (2006) worked on the volcanic rocks in the same areas. They suggested that the volcanic rocks occur as lava flow and dykes ranging in composition from basaltic to rhyolitic calc-alkaline affinity. They interpreted these volcanic rocks have been formed in a subduction-related environment. Moreover, Barr et al. (2006) also dated volcanic rock using the U-Pb zircon age dating method and obtained 232 Ma (Middle Triassic). Furthermore, Srichan et al. (2009) reported that the volcanic rocks in the Chiang Khong area mainly occur as lava flow and dykes of basaltic to the rhyolitic composition. Petrochemical and U-Pb zircon age dating studied indicating that these volcanic rocks have a calc-alkaline affinity and could have formed from 223 to 220 Ma (Late Triassic) post-collisional basin. Similarly, Qian et al. (2016) studied petrochemistry and age dating of these volcanic rocks. They concluded that the rocks are ranging in composition from andesitic to alkali basalt of calc-alkaline affinity with low Mg content. They also confirmed that the age of the volcanic rocks is 229 Ma (U-Pb zircon age dating), which has similar age to the rhyolitic rocks from the northern area (Qian et al., 2017) that has an age of 230 Ma (U-Pb zircon age dating method). Hence, Qian et al. (2017) identified calc-alkaline and tholeiite transitional to alkaline.

In the central part of the Lampang volcanic belt, Wipakul et al. (2012) studied volcanic sequence. They reported that the rocks are mainly of ignimbrite depositing in subaerial to the subaqueous environment. Besides, Barr et al. (2000) said that lava flow

and tuff of dacitic to rhyolitic composition dated to 240 Ma (U-Pb zircon age dating). Similar age (240 Ma; U-Pb zircon age dating) of volcanic rocks ranging in composition from andesitic to rhyolitic of calc-alkaline affinity also reported Qian et al. (2017). Further south of the Lampang volcanic belt in the Tak area, petrochemistry was studied, revealing that the rhyolitic to basaltic rocks have formed in various tectonic settings, including active continental margin, back-arc basin, and post-collision (Phajuy and Singtuen, 2019). In Nakhon Sawan and Uthai Thani areas, the rhyolitic and gabbroic rocks identified as calc-alkaline to shoshonitic affinity forming in subduction-related settings (Jundee et al., 2017).

In the southern portion of the Lampang volcanic belt (e.g., Rayong, Chanthaburi, Trad, and Ko Chang area), the volcanic rocks are partly characteristic by rhyolitic flows with high K and low Ti composition (Barr and Charusiri, 2011; Grace, 2004; Jungyusuk and Khositantont, 1992; Paipana, 2014). At Ko Chang, dating of zircons from rhyolitic flow using LA ICP-MS U-Pb technique obtained an age of 258 Ma (Khin Zaw unpublished data in Ridd, 2012).

3) Nan river volcanic belt

Nan river volcanic belt is also known as the Nan-Uttaradit and Sa Kaeo suture volcanic belts) trends NE to SW consisting of Nan-Uttaradit in the north and Sa Kaeo province in eastern Thailand. Barr and Macdonald (1987) proposed the Nan river volcanic zone comprises ophitic mafic and ultramafic rocks formed in a back-arc or inter-arc setting during the Permian age. Subsequently, Panjasawatwong and Yaowanoyothin (1993) suggested that the ultramafic zone formed as a block in mélangé, including ocean-island basalt, back-arc basin basalt, and andesite, which took place during the Carboniferous to Permo-Triassic.

4) Phetchabun volcanic belt

Phetchabun volcanic belt (or Loei-Phetchabun-Phai Sali volcanic belt of Jungyusuk and Khositantont, 1992) is a volcanic belt trending N-S from Loei, through Phetchabun, Nakhon to Nayok and Sa Kaeo provinces. Jungyusuk and Khositantont (1992) reported that these volcanic rocks crosscut the Permian limestone, mainly composed of lava flows and volcanoclastic rocks rhyolitic to andesitic composition, and inferred Middle Permian age.

Intasopa and Dunn (1994) studied the volcanic rocks in the Loei area and classified them into two magmatic episodes. The first one comprises of calc-alkaline rhyolite to tholeiitic basalt of Devonian to Lower Carboniferous (Rb-Sr isotopic age 374 Ma and 361 Ma age), and the second is mainly of andesite of Permo-Triassic age ($^{40}\text{Ar}/^{39}\text{Ar}$ age 238 Ma and 237 Ma). Subsequently, Panjasawatwong et al. (2006) studied volcanic rocks in the Pak Chom area and reported that they comprise basaltic and andesitic flow depositing in the subaqueous environment. Petrochemical data suggest they are calc-alkaline, transitional tholeiite, and tholeiite forming in mid-oceanic ridge and island-arc setting. While, Khositantont (2008) studied volcanic rocks from the same area and suggested they are calc-alkaline developed on the ocean floor. The ages of these volcanic rocks dated to 434 Ma (U-Pb zircon age dating).

Kamvong et al. (2006) studied volcanic rocks in the Wang Pong area (Phetchabun province). They consist of andesite porphyry, crystal tuff, and agglomerate, and have a source similar to OIB-type mantle. Intasopa (1993) reported that the andesite dyke crosscut the Permian limestone has an age of 238 Ma ($^{40}\text{Ar}/^{39}\text{Ar}$). At Chatree gold mine, most studies focused on petrochemistry of host volcanic sequences and post-mineralization dykes (e.g., Boonsoong et al., 2011; Cumming, 2005; Tangwattananukul et al., 2008), and reported that both volcanic host sequences and post-mineralization dykes are ranging in composition from mafic to felsic and tholeiite to calc-alkaline affinity. Salam (2013) and Salam et al. (2014) described the Chatree host volcanic sequence to consist predominantly of basaltic andesite, andesite, monomictic andesite breccia, and polymictic breccia. The felsic variety is apparently to occur at the top of stratigraphy, mainly identified as crystal-rich fiamme breccia and lithic rich fiamme breccia. Salam et al. (2014) revealed that the Chatree host volcanic sequence comprises two suites, namely Suite I: 258 to 250 Ma tholeiite affinity, and Suite II: 250-240 Ma calc-alkaline affinity. Most dykes are andesite and have about 238 Ma (Salam et al., 2014).

2.4 Regional geology of study area

The oldest rocks in and around the study area are Carboniferous sedimentary rocks. It distributes mainly in the central part of the study area (Fig. 2.3). This Carboniferous unit comprises laminated limestone, laminated sandstone, limestone breccia, and laminated mudstone. The laminated limestone contains some fossils, including brachiopods, foraminifers, crinoids, and corals). Locally, low graded metamorphic rocks such as meta-sandstone, slaty mudstone are reported in the western part of the study area (Tiyapirach, 1996). Fontaine et al. (1999) suggested that shallow marine fauna at the Khao Yai Mo Noi and Khao Noi (this study area) inferred of Carboniferous age. Later, Paipana (2014) dated the oldest sedimentary rocks using detrital zircon and obtained the maximum age of 328 Ma (Late Carboniferous).

The second oldest rock unit is Permo-Triassic volcanic rocks, which are exposed at the Khao Yai Mo Noi in the west and Khao Noi in the middle and east of the study area. The Permo-Triassic volcanic unconformably overlies the Carboniferous rocks (Tiyapirach, 1996). They comprise rhyolitic tuff, andesite, and andesitic breccia. Paipana (2014) reported that the Bo Thong host volcanic rocks were intruded by syenite intrusion and were also crosscut by basaltic dykes. The LA ICP-MS U-Pb zircon age dating obtained 254 Ma (Late Permian). The granite unit exposed in the northern part of the study area, N-S trends, comprised of biotite granite and syenite (Department of Mineral Resources (DMR), 2007; Paipana, 2014; Tiyapirach, 1996). The Quaternary sediments cover an undulating terrace, comprise alluvium and terrace sediments. Both Carboniferous sedimentary rock and Permo-Triassic volcanic rocks are gently dipping to the east. Faults and lineaments in the area are generally trending NW-SE (Morley, 2002; Palin et al., 2013; Sone and Metcalfe, 2008) (Fig. 2.3).

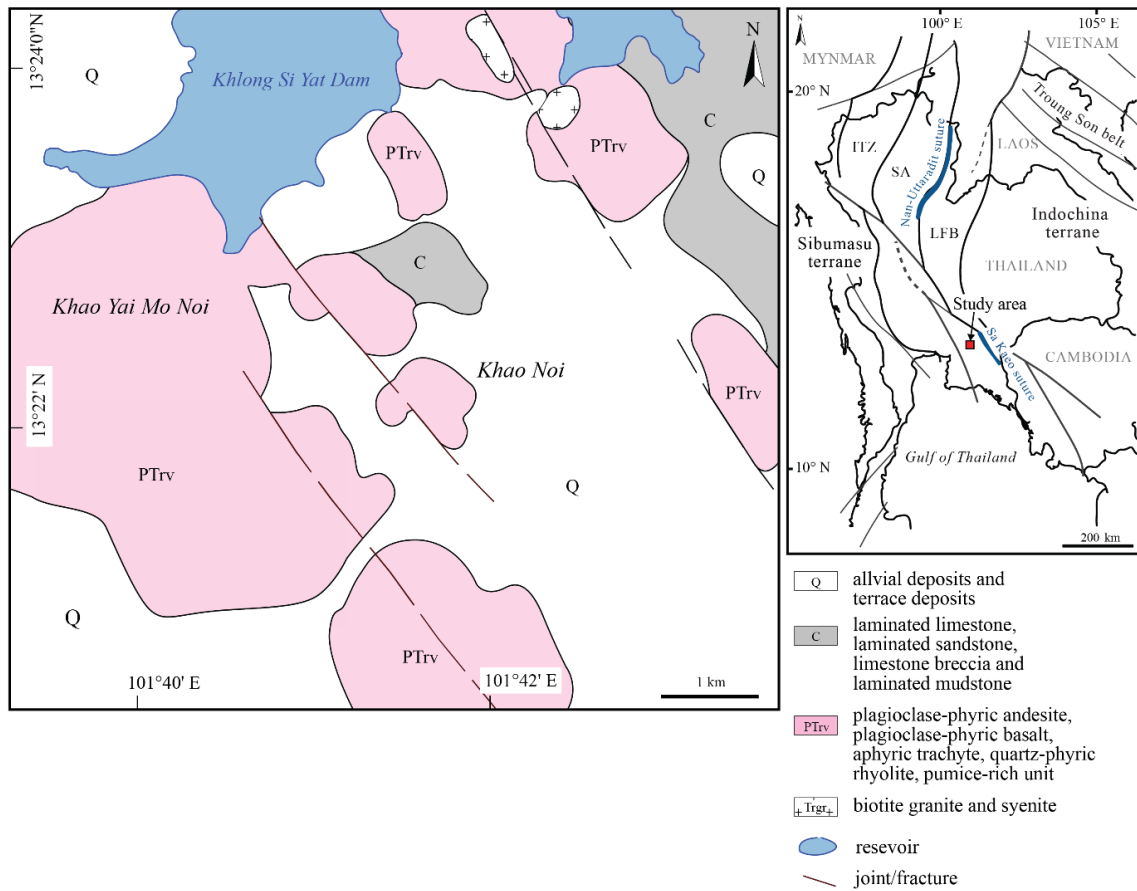


Fig. 2.3 Geological map of the Khao Noi area (modified from Tiyaiprach, 1996).

CHAPTER 3

STRATIGRAPHY, VOLCANIC FACIES AND ARCHITECTURE

3.1 Introduction

In this chapter based on field investigation (outcrop exposure), drill holes logging and sampling of drill holes obtaining from the Mineral Resources Exploration and Evaluation Project of the Department of Minerals Resources (DMR). This chapter provides the volcanic stratigraphy, volcanic facies and interpretation the depositional environment of volcanic rocks.

3.2 Stratigraphy of the Khao Noi area

In this study, criteria use in the identification of classifying volcanic rocks, lithofacies, and volcanic facies is based on the scheme provided by McPhie et al. (1993). The classification is based on lithofacies, petrography, and the relationship between drill holes. Drillcores from 28 drill holes have been briefly investigated (Fig. 3.1). However, only the cores from 9 drill holes were selected for this study. The list of selected drill holes includes DDH08, DDH09, DDH16, DDH17, DDH21, DDH23, DDH24, DDH26, and DDH27 with a total of 553.3 meters (table 3.1; Fig. 3.2). It generally strikes northwest with a shallow to moderate dip to the northeast (Fig. 3.3). The stratigraphy has been divided into three units; from lower to upper (oldest to youngest) as follows (Fig. 3.4).

Unit 1 (Sedimentary unit)

This unit forms a basement for the Khao Noi volcanic sequence. It comprises laminated limestone, laminated sandstone, limestone breccia, and laminated mudstone, estimate 40–60 m thick (Fig. 3.4). The lower part of Unit 1 mainly consists of laminated limestone up to 40 m thick, minor laminated sandstone, limestone breccia, and thin laminated mudstone at topmost. Unit 1 is overlain by Unit 2 with sharp contacts. It should be noted that the coherent rocks (e.g., plagioclase-phyric basalt, aphyric trachyte, and quartz-phyric rhyolite) cut through Unit 1 were interpreted as dykes.

Table 3.1 List of selected drill holes and outcrop description of the Khao Noi volcanic

Study point	Easting	Northing	Description
<i>Selected drill holes</i>			
DDH08	791390	1480429	
DDH09	791558	1480307	
DDH16	791762	1479539	
DDH17	791599	1479455	
DDH21	791609	1479328	
DDH23	791929	1479381	
DDH24	791748	1479355	
DDH26	791801	1479465	
DDH27	791719	1480238	
<i>Outcrop stop</i>			
KN1	791835	1479290	Fine-sandstone, massive
KN2	791355	1479251	Crystal-rich sandstone
KN3	791467	1479720	Polymictic breccia
KN4	791419	1479956	Polymictic breccia
KN5	791658	1480008	Fine-sandstone with fossil fragments
KN6	790183	1481047	Polymictic breccia
KN7	789632	1481067	Crystal-rich sandstone
KN8	788037	1480136	Crystal-rich sandstone
KN9	788005	1479948	Crystal-rich sandstone
KN10	788104	1478857	Crystal-rich sandstone
KN11	790620	1477625	Crystal-rich sandstone
KN12	787059	1472733	Sandstone conglomerate
KN13	797102	1482080	Limestone, pale gray, massive

Unit 2 (Mafic to intermediate volcanic unit)

The mafic-intermediate volcanic unit is estimate 60–80 m thick, consists mainly of plagioclase-phyric andesite, monomictic andesite breccia, plagioclase-phyric basalt and aphyric trachyte (Fig. 3.4). The upper contacts between plagioclase-phyric andesite and monomictic andesitic breccia with gradational contacts. The lower contacts have sharp unbrecciated contacts with sedimentary units (Unit 1). The monomictic andesitic breccia interbedded laminated mudstone with sharp contacts observed at drill hole DDH17 (Fig. 3.2).

The Mafic to intermediate volcanic unit also comprise plagioclase-phyric basalt, and aphyric trachyte commonly sharp contacts and chilled margins with their hosts, it was observed at drill hole DDH09 (Fig. 3.2 and 3.11). The mafic rocks are only a few meters thick, typical tabular shape, a gentle dip, and crosscut the whole succession.

Unit 3 (Felsic volcanic unit)

This unit is the youngest stratigraphic interval and best exposed in the field of the Khao Noi area. It consists mainly of crystal-rich pumice breccia, lithic-rich pumice breccia, and quartz-phyric rhyolite (Fig. 3.4). The felsic volcanic unit is estimated 60–80 m thick, which directly overlies the mafic-intermediate volcanic unit (Unit 2).

The lower contact with Unit 2 is gradational. Unit 3 also contains beds of normal graded crystal-rich pumice breccia and lithic pumice breccia. The quartz-phyric rhyolite occurs in the middle part of Unit 3 and displays quenched fragmental breccia. The quartz-phyric rhyolite commonly cross-cut the whole succession.

3.2 Facies and Facies associations of Khao Noi volcanic

The stratigraphy of Khao Noi volcanic comprises of facies and facies associations. This study identified 11 facies which are grouped into texturally and compositionally distinct facies associations included 1) Laminated limestone facies; 2) Laminated sandstone facies; 3) Limestone breccia facies; 4) Laminated mudstone facies; 5) Plagioclase-phyric andesite facies associations; 6) Plagioclase-phyric basalt; 7) Aphyric-trachyte facies; 8) Quartz-phyric rhyolite facies associations. The detailed description of each lithofacies will be described and discussed in the following sections.

1) Laminated limestone facies

The laminated limestone is mainly of a marine sedimentary rock unit, is exposed in the eastern part of the Khao Noi area in outcrops, and mostly observe in drill holes DDH08, DDH26, DDH16, and DDH24 (Fig. 3.5). They common diffusively stratified, thin to lamination, planar-bedded with intercalated siltstone to mudstone, and fine-grained, which occur in drill hole DDH24 at depth 124.4 m (Fig. 3.5A), and it dark gray to black in colors. This laminated limestone associated with microfossil, brachiopods, and crinoids occur in drill hole DDH24 at depth 124.4 m (Fig. 3.5B). The grains have different sizes in the range of 0.25–1 mm and well-sorted. The matrix is typically less

cement than mud. Locally has boundstone with closely packed of coral mounds which exposed at Wat Khao Tham Raet (KN13; 797102E/1482080N) eastern of Khao Noi volcanic (Fig. 3.5C).

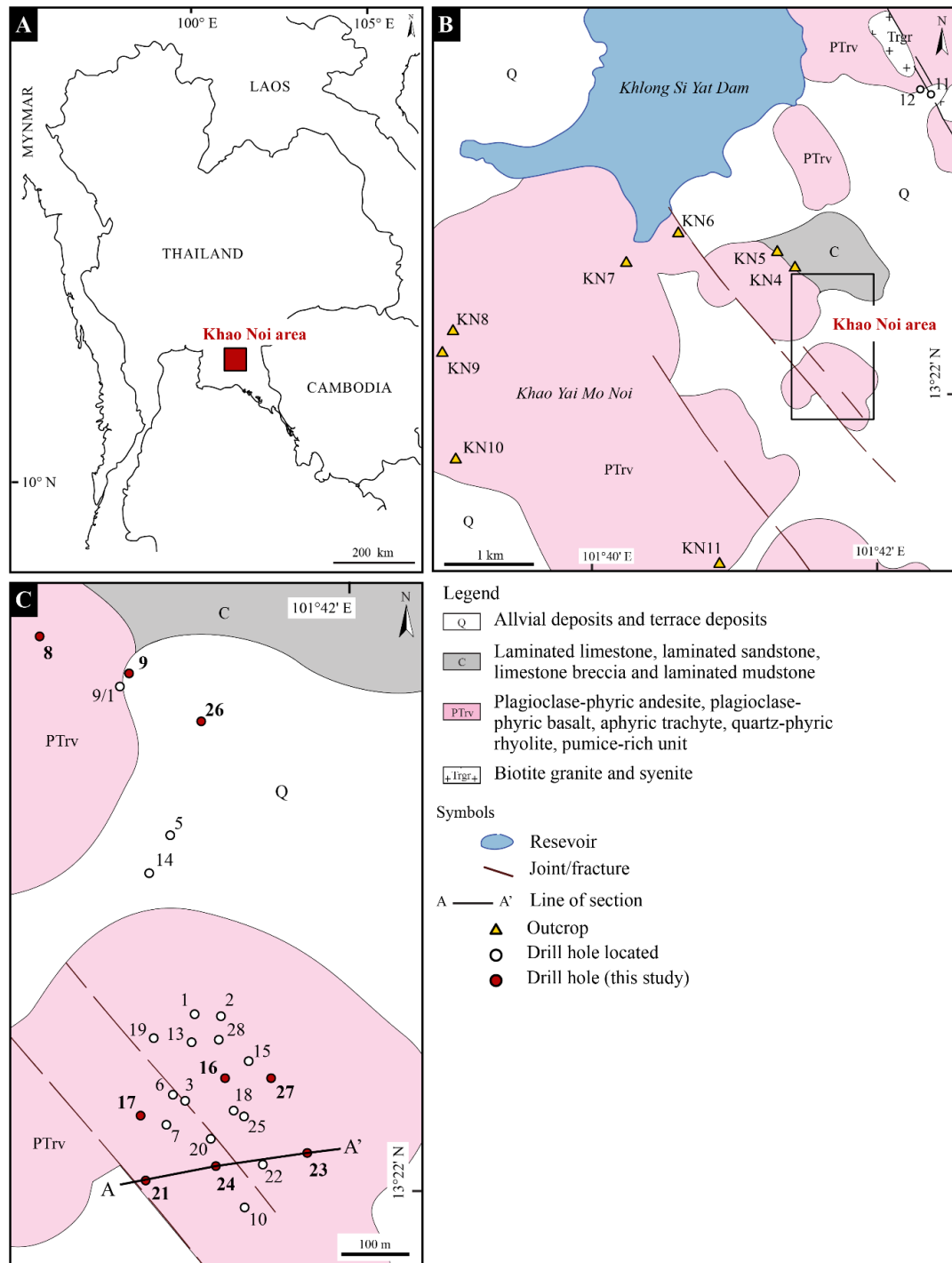


Fig. 3.1 (A) The Khao Noi volcanic located in east of Thailand. (B) Geological map showing outcrop location and (C) Drill holes location of the Khao Noi volcanic, Tha Takiap district, Chachoengsao province.



Fig. 3.2 Simplify graphic log of selected drill holes, in geographic order from northernmost at the left to the southernmost at the right. See **Fig. 3.1C** for location of drill holes.

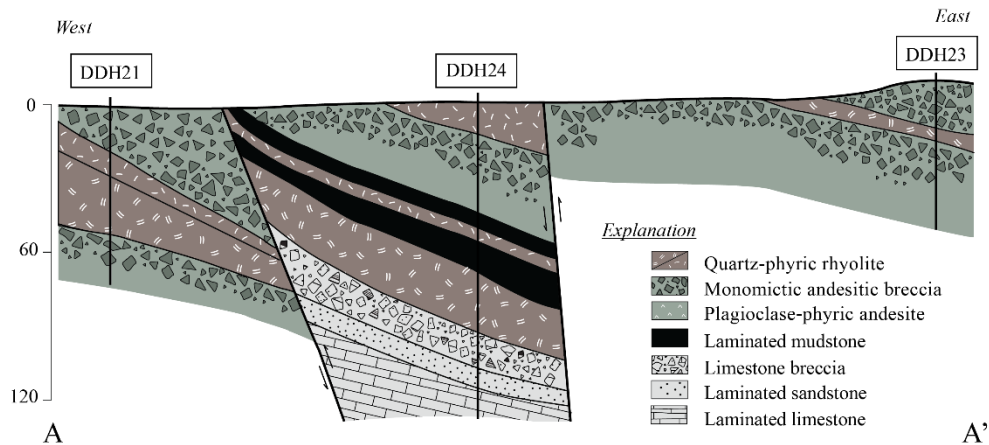


Fig. 3.3 Preliminary schematic cross-section (A-A') of the Khao Noi volcanic, showing lithofacies relationships, and somewhat oblique to be trends, display east-trending inclining in cross-section. See Fig. 3.1C for location of drill holes (after DMR, 2007).

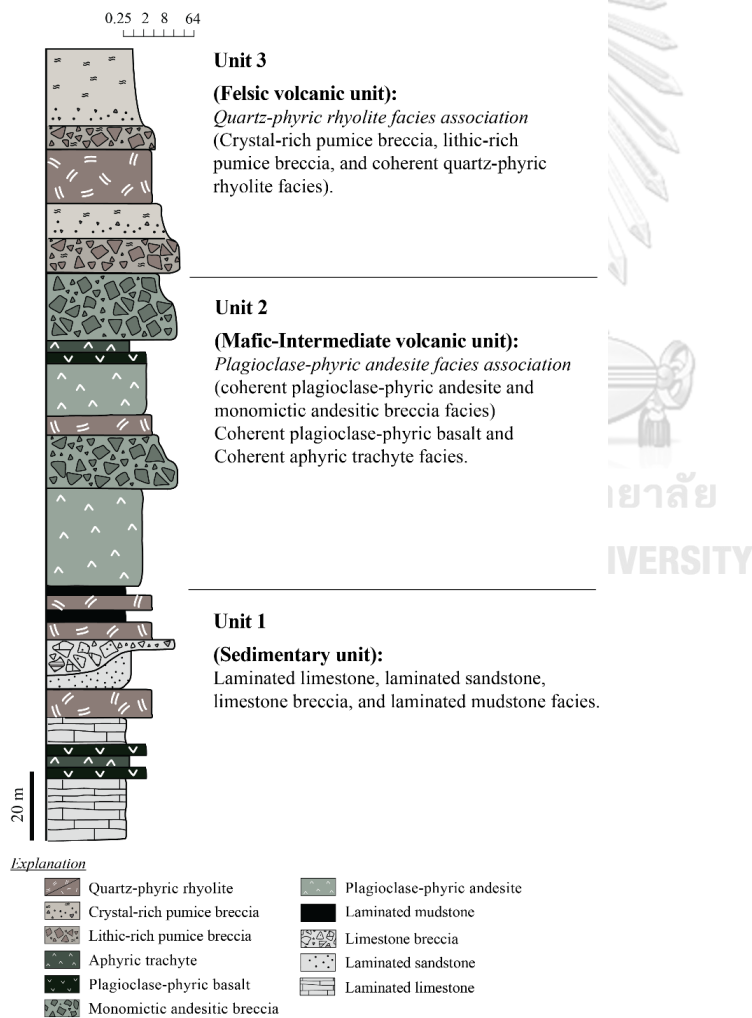


Fig. 3.4 Simplify composite stratigraphy of the Khao Noi volcanic, Chachoengsao province, eastern Thailand.

2) Laminated sandstone facies

Laminated sandstone exposed in northern and eastern of Khao Noi and a few occurs in drill holes and in outcrops. This facies contains fine sandstone. It is mainly massive and occurs in 20 to 30 m thick. The laminated sandstone is gray-dark gray in colors, and also occurs as lamina (<1 mm) to thin bed (1–3 cm) interlaminated with laminated siltstone and mudstone (Fig. 3.6A). The fine-grained sandstone beds have sharp bases, locally with small load structure, and have diffuse tops. They commonly normal graded from fine sand to mud sized, and comprise of quartz and feldspar grains (Fig. 3.6B). Locally, this laminated sandstone occur as thick to massive (Fig. 3.6C), and associated with fossil fragments such as coral and brachiopod in the north of Khao Noi volcanic (KN5; 791658E/1480008N) (Fig. 3.6D).

3) Limestone breccia facies

The limestone breccia commonly massive and thick beds intercalated/or overlain laminated sandstone and limestone. Beds are laterally continuous over several 100 m, which are well exposed in eastern and southern parts of the Khao Noi volcanic as well as in drill holes DDH16 and DDH24 (Fig. 3.1). The limestone breccia mainly of clast-to matrix-supported, poorly sorted, and associated weakly to grading (Fig. 3.7A). The clast consists of limestone, sandstone, and mudstone. Mostly limestone clasts are abundant in fossil fragments and include brachiopods, foraminifers, and corals (Fig. 3.7B). Clasts in the range 2 mm to 25 cm, angular to subround in the lower part (Fig. 3.7C), whereas upper part clasts are smaller and subround. The matrix is sand size comprises of lithic clasts, quartz, feldspar, and clay minerals.

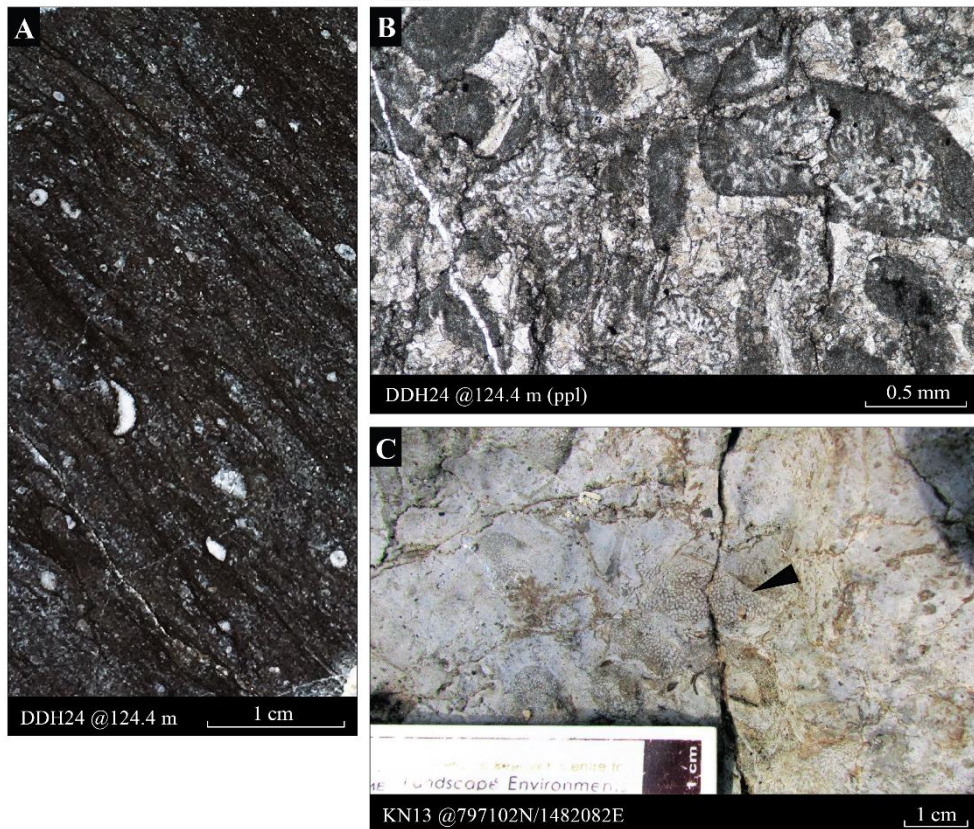
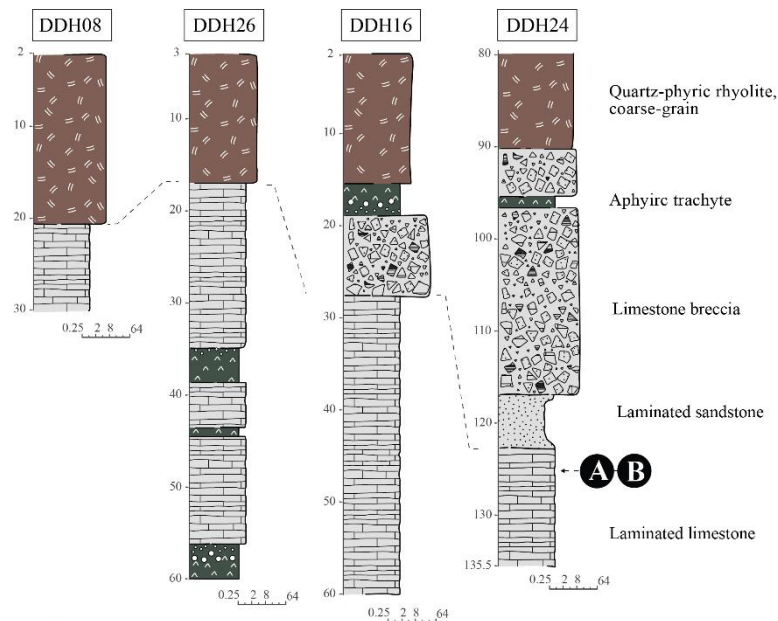


Fig. 3.5 Graphic log for drill holes DDH08, DDH26, DDH16 and lower part of DDH24, which intersects a thick interval of quartz-phyric rhyolite, aphyric trachyte, laminated sandstone and limestone. (A) Hand specimen of limestone interbedded with mud layer and inclined bed (40°, dip angle; DDH24 at depth 124.4 m). (B) Polarized photomicrograph of fossil fragment (foraminifera?) set in less carbonate cement. (C) Photograph of boundstone in Wat Tham Raet (KN13) adjacent area contains abundant of coral mounds. See Fig. 3.1C for location of drill holes and outcrops.



Fig. 3.6 (A) Photographs showing core sample laminated sandstone and limestone breccia (B) Hand specimen showing laminated sandstone interlayer with mud layer and inclined bed (60° , dip angle; DDH24 at depth 111.5 m). (C) Cross-polarized photomicrograph showing subangular sand size-grains with mostly clear quartz, feldspar, and clay. (D) Hand specimen of fine sandstone associated with fossil fragments. (E) Photograph of an outcrop of fine sandstone at the north of Khao Noi. See Fig. 3.1C for location of drill holes and outcrops.

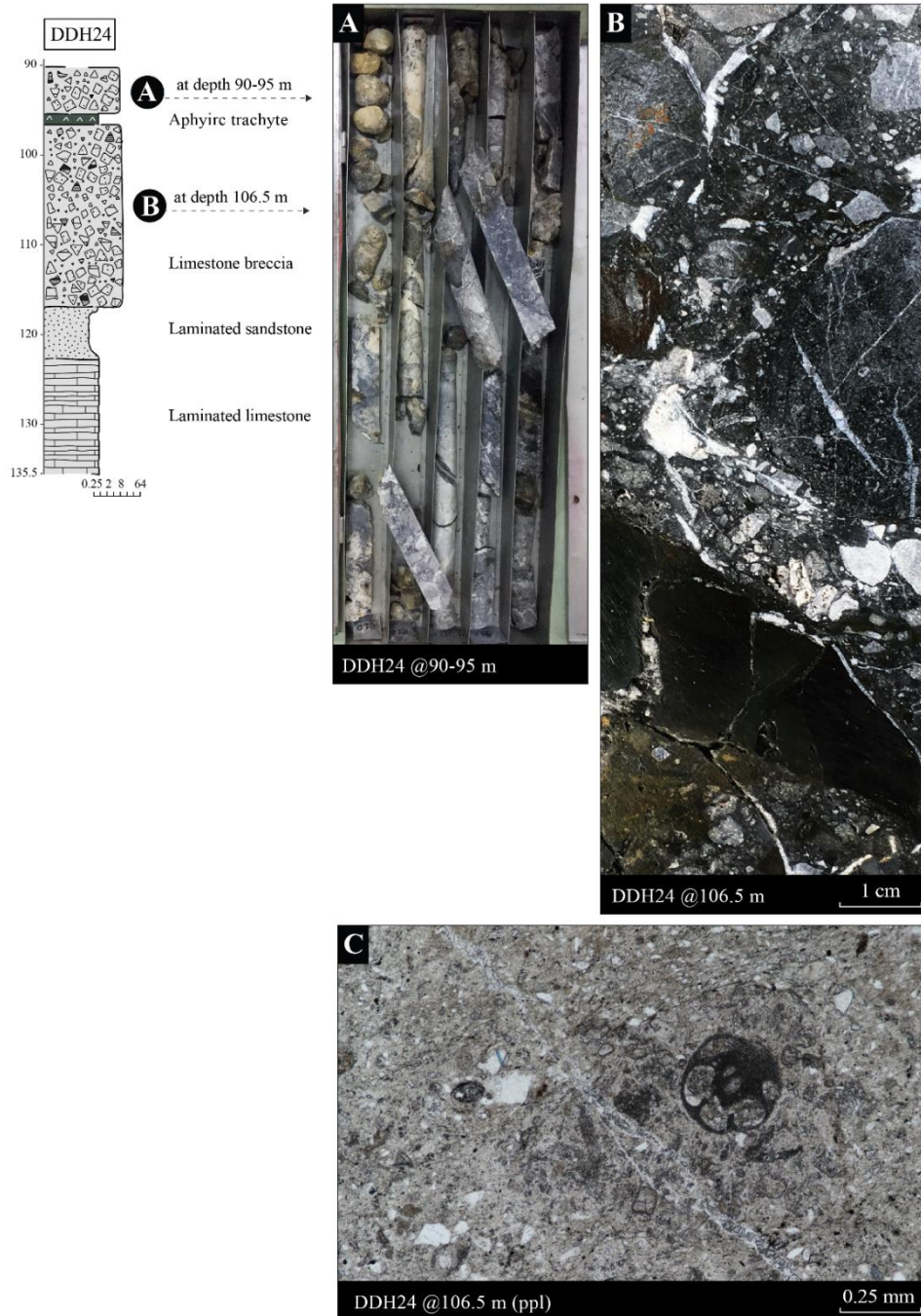


Fig. 3.7 The graphic log of lower part of drill hole DDH24, which interbedded a thick interval of limestone breccia, laminated sandstone and laminated limestone. **(A)** Hand specimen showing clast-supported of limestone breccia, mostly clasts of irregular limestone clasts, sandstone and few of mudstone surrounded by mud-matrix breccia (at depth 106.5 m). **(B)** Polarized photomicrograph showing fossils fragment (foraminifera?) in limestone clasts. See **Fig. 3.1C** for location of drill holes.

4) Laminated mudstone facies

The laminated mudstone occurs at the upper part of Unit 1 and is interbedded with quartz-phyric rhyolite (Fig. 3.3). Intervals contain massive to normal graded, moderately to well-sorted, thinning, and fining upward sequences (Fig. 3.8A). At the base of siltstone and laminated mudstone with massive conglomerate and pebbly clasts with subangular phyric pyroclasts occur only in drill hole DDH24 (Fig. 3.8B). Beds are 5 to 20 cm thick, poorly sorted, and are diffusely stratified with pebble-rich horizons (Fig. 3.8C). The succession mix of quartz-phyric rhyolite clast that slightly hydrothermal alteration, and pumice fragments in the matrix of feldspar grains, minor quartz crystal fragments, and sulfide grains.

5) Plagioclase-phyric andesite facies association

This facies association consists of two facies: Plagioclase-phyric andesite facies, and monomictic andesitic breccia facies.

Plagioclase-phyric andesite facies

The Plagioclase-phyric andesite is the main facies that mainly intersected only in drill holes DDH17, DDH21 DDH23 and DDH24 of the Khao Noi volcanic (Fig. 3.1). It has a thickness 2 to 30 meters. This facies is characteristic by fine-grained, porphyritic to seriate texture. The rock occasionally show porphyritic are common (Fig. 3.9A), the phenocrysts are plagioclase and hornblende, that occurs as isolated crystals, some rounded, sieve textures, embayed, and as hornblende-plagioclase cumulo-crysts (Fig. 3.9B). The groundmass includes microlite plagioclase, a variable proportion of hornblende, Fe-Ti oxide, and glass. The individual phenocrysts are twin and determination of Anorthite-contents ranging from An38 to An45 (Andesine). The rock contains some vesicles (3–5 vol. % of the rock) usually infilled with calcite. The size of vesicle size ranging from 0.2 to 0.5 mm, subrounded and elongate to moderate sphericity, which commonly occurs near margins (Fig. 3.9C).

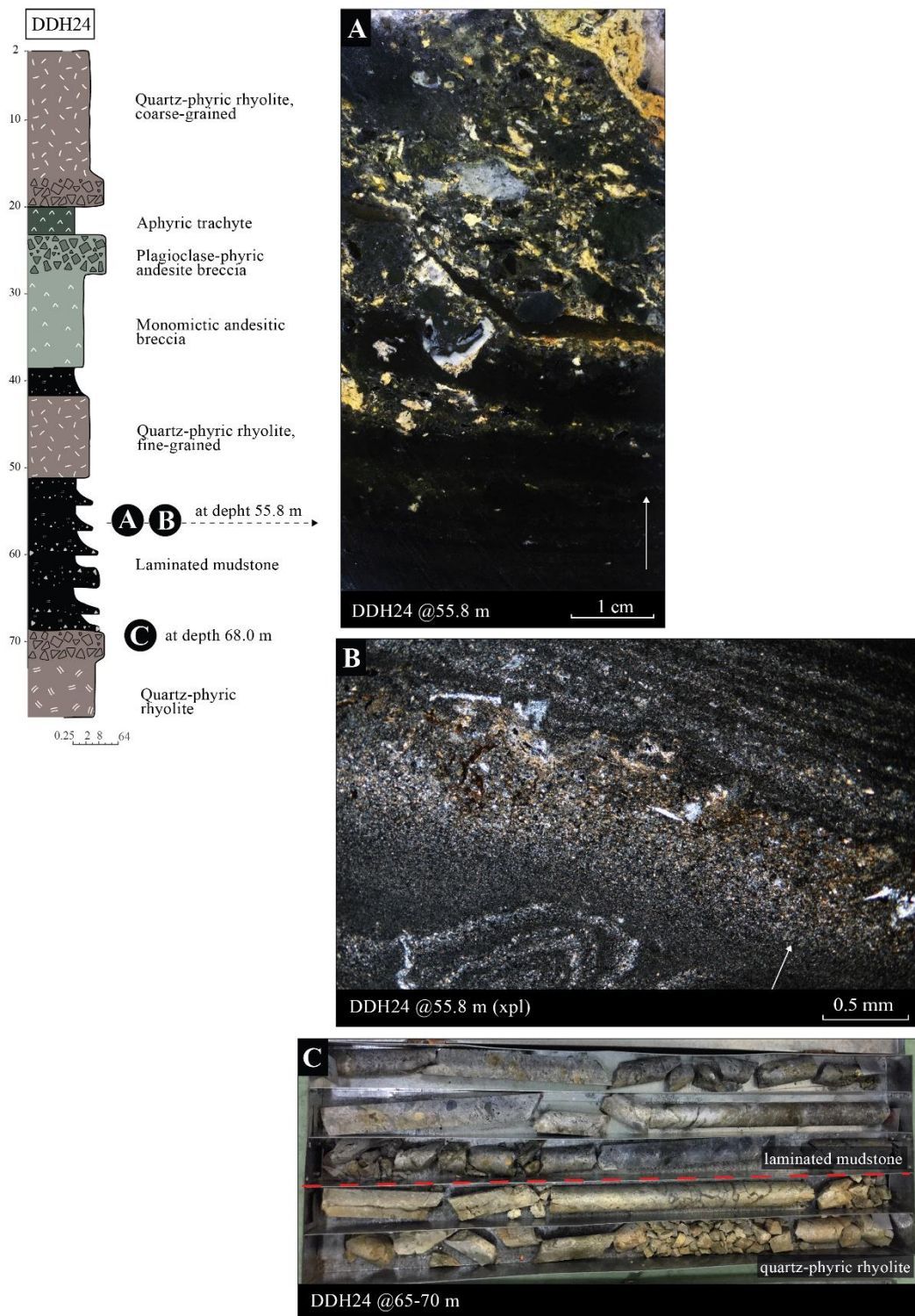


Fig. 3.8 The graphic log upper part of drill hole DDH24 through a laminated mudstone intersected by Quartz-phyric rhyolite with sharp contacts. (A) Hand specimen of laminated mudstone with fine-grained layers. (B) Cross-polarized photomicrograph laminated mudstone in normal graded fine-grained of crystal and lithic fragment and minor opaque mineral and pyrite crystal (arrow). (C) Beds of lithic and volcaniclastic clasts rich at basal at interval 65-70 meters. See **Fig. 3.1C** for location of drill holes.

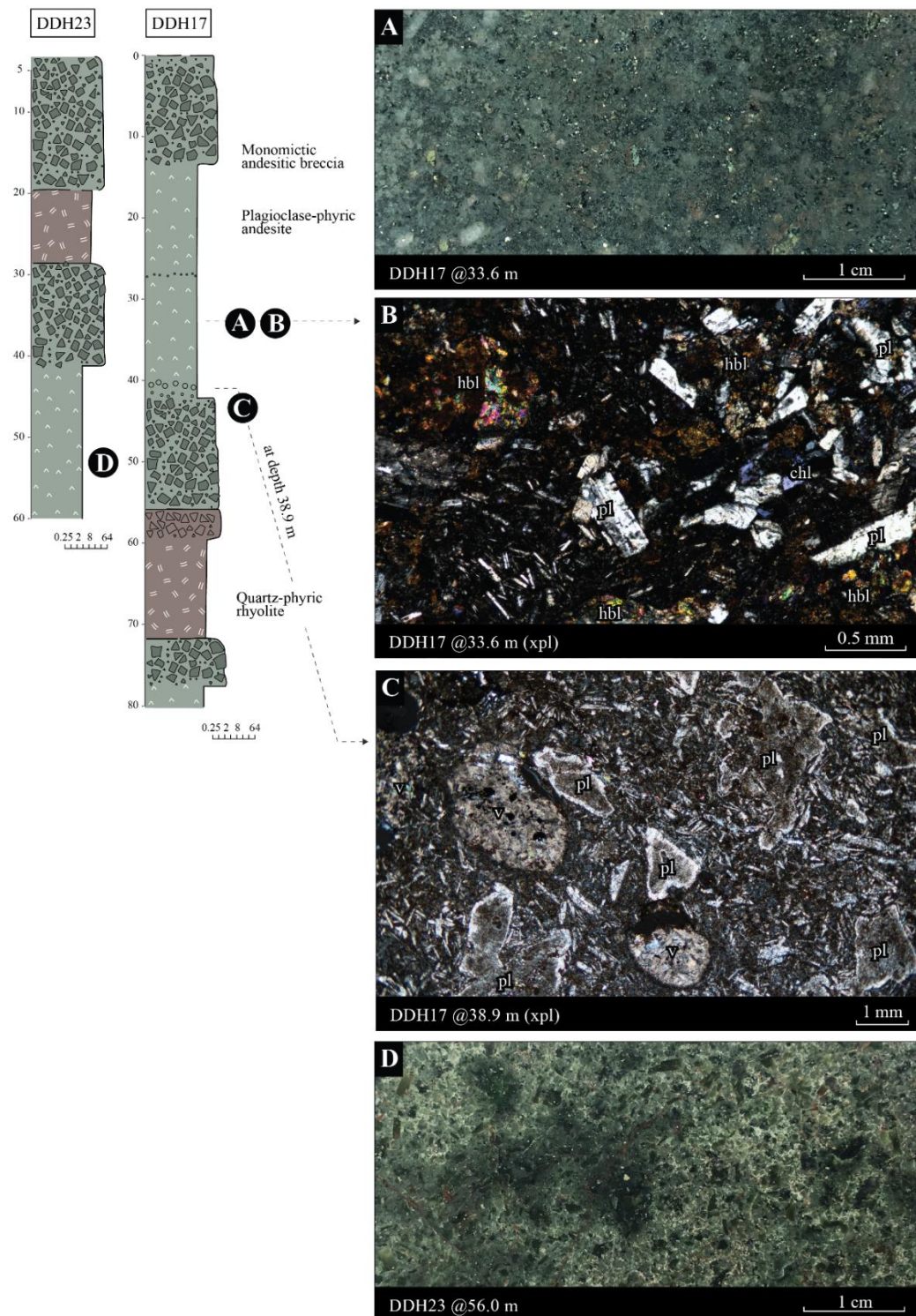


Fig. 3.9 The graphic log through a plagioclase-phyric andesite. (A) Plagioclase-phyric andesite showing fine-grain, that contains plagioclase phenocrysts. (B) Cross-polarized photomicrograph showing hornblende (hbl) and plagioclase phenocrysts (pl) in microlite plagioclase groundmass. (C) Cross-polarized photomicrograph of plagioclase phenocrysts (pl) in a holocrystalline groundmass and vesicle (V) and quartz. (D) Hand specimen of plagioclase-phyric andesite containing plagioclase phenocrysts. See **Fig. 3.1C** for location of drill holes.

6) Monomictic andesitic breccia facies

The monomictic andesitic breccia is voluminous facies that identified only in the drill holes DDH17, DDH21, DDH23, and DDH24. It have a thickness ranges from 2 to 30 meters, and is characterized by clast-supported breccia typical jigsaw-fit texture, rotated clasts of andesitic clasts on topmost (Fig. 3.10A) and irregular clasts in the lower part (Fig. 3.10B). The clast is slightly alteration with dominant of greenish-gray coloring. Clasts ranging in size from granules to cobbles (2 mm to 20 cm), which possible grading in coarse and fine breccia. The boundary of clast is sharp and fine-grained set in the matrix contains consists of juvenile clasts and crystals fragments that show flow band (Fig. 3.10D and 3.10E). In the lower part, clasts appeared as blocky clasts with chilled-margins that set in fine-grained fragments layers with no sediments.

The clast composition is porphyritic andesite clasts with plagioclase, hornblende phenocrysts. The phenocrysts are largely subhedral to anhedral that occurs as isolated crystals, glomerocrysts; some rounded edges. The groundmass constituents show a microlite texture that makes up of crystal of plagioclase and volcanic glass. The matrix comprises similar to breccia clasts, glassy fragments, and crystals fragments (hornblende and plagioclase).

7) Plagioclase-phyric basalt facies

The plagioclase-phyric basalt is exposed in several discontinuous outcrops, and intersected drill holes DDH09, DDH16, DDH21, DDH24, and DDH26 in the northern part of the Khao Noi volcanic (Fig. 3.1). They are typically tabular bodies, massive, and thickness ranging from 2 to 5 meters. The least-altered sample of plagioclase-phyric basalt is dominated by medium to coarse-grained, display green-gray to dark in color, with white to pink colored phenocrysts, show slightly porphyritic texture (Fig. 3.11A). Most phenocrysts are plagioclase. The groundmass consists of mafic minerals that are replaced by chlorite, felted plagioclase laths, glass, and opaque minerals (Fig. 3.11C).

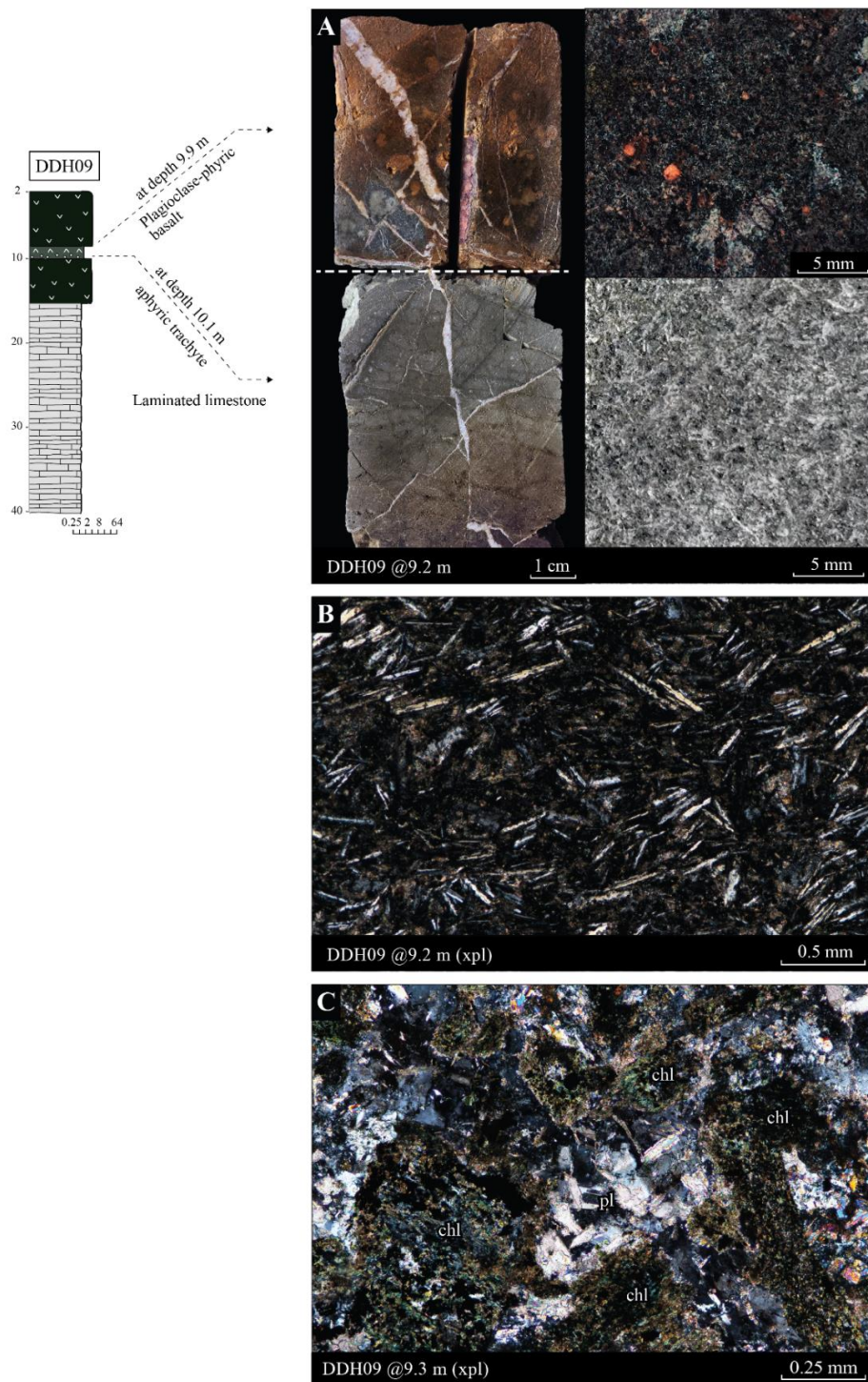


Fig. 3.11 The graphic log through plagioclase-phyric basalt and aphyric trachyte intersected limestone (drill hole DDH09). (A) Fine-grained margins of aphyric trachyte (up) showing aphanitic texture and plagioclase-phyric basalt (down) showing sparsely phenocrysts with medium grained. (B) Cross-polarized photomicrograph aphyric trachyte showing microlite plagioclase of trachytic texture. (C) Cross-polarized photomicrograph of plagioclase-phyric basalt showing mafic mineral phenocrysts which is partly pseudomorphs by chlorite (chl) with felty-texture groundmass of plagioclase. See Fig. 3.1C for location of drill holes.

8) Aphyric trachyte facies

The aphyric trachyte contains 5 vol. % of the rock that has been intersected in drill holes DDH09, DDH24, and DDH26 (Fig. 3.3). It is 2 to 5 meters thick, typically formed as tabular shape, which intersected monomictic andesitic breccia, and laminated limestone. Locally vesicles near the contacts with plagioclase-phyric basalt (Fig. 3.11A). This facies is characterized by pale greenish-gray to dark colors, fine-grained to sparsely phenocryst, and is non-to very poorly vesicular. Vesicles range in size from 0.2 to 2 mm, are subrounded to angular, and irregular to moderate sphericity, which typically occurs near the margins of this facies (Fig. 3.11A).

The aphyric trachyte show trachytic and porphyritic textured. The trachytic texture shows sub-parallel orient, comprises of plagioclase, alkaline-feldspar (<0.2 mm), dark brown glass, and Fe-Ti oxide. Whereas, sparsely porphyritic textured with 1-3 vol. % plagioclase phenocrysts; minor hornblende and ferromagnesian minerals.

9) Quartz-phyric rhyolite facies association

The quartz-phyric rhyolite facies association is the most abundant facies association exposed in the Khao Noi volcanic. This facies comprise lithic-rich pumice breccia, crystal-rich pumice breccia and quartz-phyric rhyolite.

Lithic-rich pumice breccia facies

The lithic-rich pumice breccia is assigned to have occurred as at the base of pyroclastic facies that commonly clast-supported. It exposes in eastern of the Khao Noi volcanic, south of the Khao Yai Mo Noi, and only drill hole DDH26 occurs in centimeters to meters thick bed (50 cm to 1 m thick).

They are massive to diffusively stratified, poorly sorted, a few intervals with irregular scatted juvenile clasts (3–5 % vol.), and clast in the range 1–30 cm in size. The uppermost of sequence commonly showing the laminated fine-sandstone (Fig. 3.12A). This facies mainly of juvenile clast, comprises pumice, phyric rhyolitic and lithic clast, angular to subangular. Pumice, white-pale gray in colors with highly vesicular and mostly have the irregular shape (20–30 vol. %) that resembles the texture of quartz-phyric rhyolite and hydrothermal alteration (Fig. 3.12B), all set in a fine shard, feldspar grains,

and Fe-Ti oxide grains (Fig. 3.13C). It is lightly-colored that contrasts with the dark-colored of a matrix.

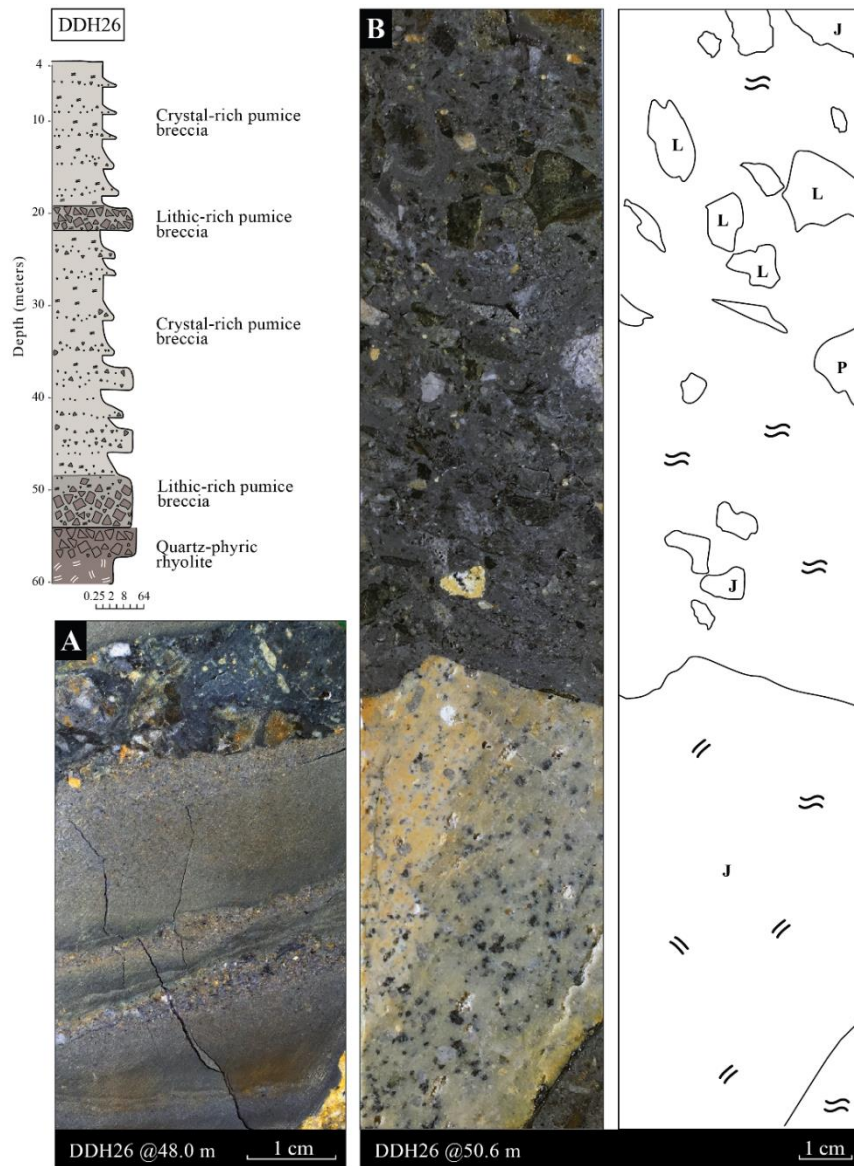


Fig. 3.12 The graphic log in drill hole DDH26 through lithic-rich pumice breccia overlying on quartz-phyric rhyolite with sharp contacts. The sequence of the pumice-rich unit base on breccia grading to the finer grain of sand size rich. (A) The uppermost sequence of lithic-rich pumice breccia showing fine-grained lamination interlayer coarse-grained and breccia. (B) Hand specimen of lithic-rich pumice breccia, clasts mainly of pumice clast (P) and lithic clasts (L). Large silicified quartz-plagioclase-phyric rhyolite clast (J) with sericite alteration (at depth 44.6 m). See Fig. 3.1C for location of drill holes.

Quartz-phyric rhyolite facies

The quartz-phyric rhyolite occurred as coherent texture, including two compositions that separate into the lower and upper unit, which coarser-grained varies in the lower part, and finer-grained phyric rhyolite in the upper part (Fig. 3.3). The quartz-phyric rhyolite exposed along the rural road NO.3259 (Sri Yat Dam to Ban Nong Kok) eastern of Khao Yai Mo Noi and in drill holes DDH08, DDH16, DDH17, DDH21, DDH24, DDH26, and DDH27 (Fig. 3.1). They have irregular tabular geometries that locally cross-cut stratigraphy (Fig. 3.2). Intervals of quartz-phyric rhyolite from discontinuous band to vary in thickness up to 26 m and extend up to several hundred meters laterally.

They display in pale gray color, and rare flow banding occurs (Fig. 3.14A). The phyric texture ranging from moderately to highly of phenocrysts/xenocrysts (Fig. 3.14B). That mixture of phenocrysts and xenocrysts, where the ratio of phenocrysts to xenocrysts is greater than 2:3. The lower part is coarse-grained phenocrysts (2 mm up to 8 mm), commonly plagioclase phenocrysts with rare hornblende (Fig. 3.14C). Feldspar phenocrysts, up to 11 mm long, subhedral to anhedral, and difficult identified. Quartz phenocrysts are subhedral to anhedral that occurs both as individual crystals and clustered xenocrysts. Quartz crystals are typically clear, embayed edge, and show the fine-grain boundary layer that formed around the crystals (Fig. 3.14D). The upper part, finer-grained, subangular quartz xenocrysts (1–3 mm), is set in a microcrystalline groundmass (<0.2 mm) of quartz and sericite.

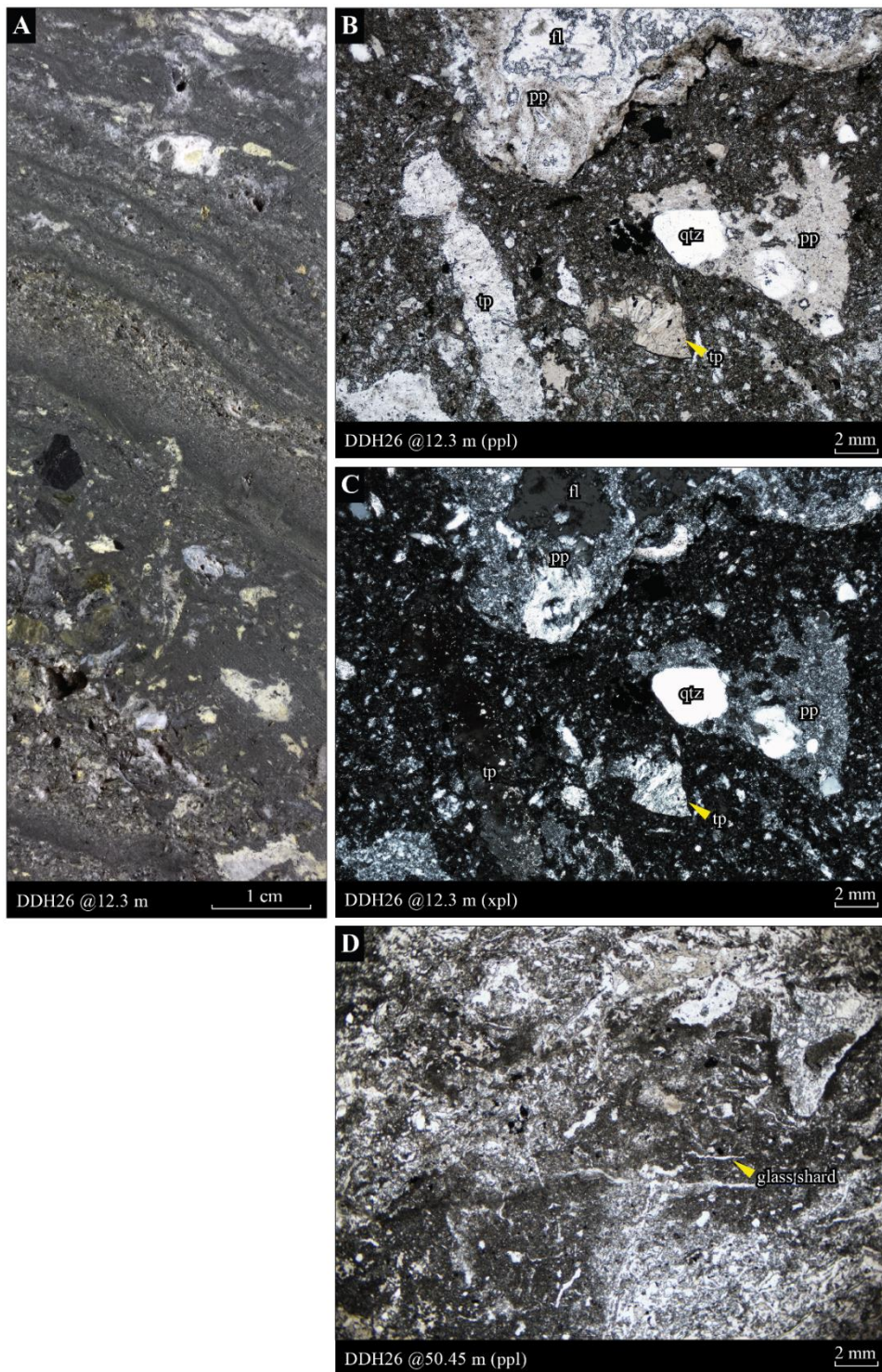


Fig. 3.13 Hand specimen of crystal-rich pumice breccia showing many pumice clasts have an irregular shape, surrounding by crystal fragments. (A) Polarized Photomicrograph showing phytic pumice (pp) contains quartz, feldspar, and tube pumice (tp) (arrow). (B) Cross-polarized photomicrograph of pumice clast and fluorite (fl) infill within the association of the fine-grained matrix and shard. (C) Polarized Photomicrograph showing glass shard and fine-grained pumice fragments.

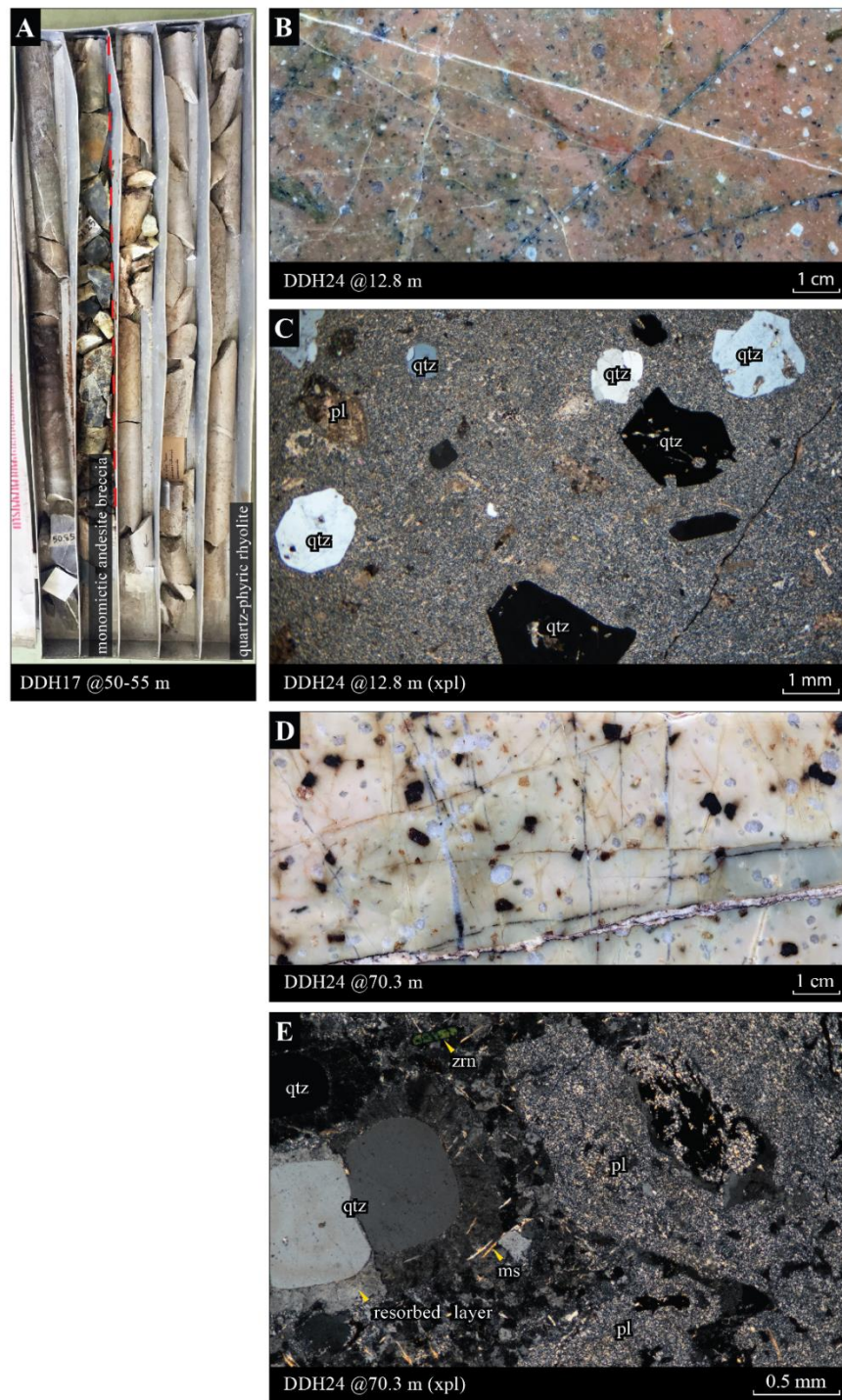


Fig. 3.14 (A) Fine-grained quartz-phyric rhyolite containing an abundance of quartz (qtz) and plagioclase (pl) phenocrysts. (B) Cross-polarized photomicrograph showing large subhedral quartz xenocrysts with irregular embayed edges set in the cryptocrystalline groundmass. (C) Coarse-grained composed of quartz xenocrysts and plagioclase phenocrysts with iron oxide. (D) Cross-polarized photomicrograph showing plagioclase phenocrysts, cluster of quartz xenocrysts with an irregular resorbed layer in quartz microcrystalline groundmass and zircon grain (zrn). See **Fig. 3.1C** for location of drill holes.

3.4 Interpretation of volcanic facies

Plagioclase-phyric andesite facies association comprises of coherent facies and autoclastic facies. They have passive contacts and are closely spatially associated. The coherent and monomictic breccia are similarly mineralogical and texture, suggests genetically related and a part of the same eruptive. *Plagioclase-phyric andesite* commonly porphyritic texture that shows euhedral phenocrysts set in microlite groundmass. The geometry of tabular and generally discontinuous, with upper and lower with fine-grained margins, indicated that they are coherent facies formed as lava domes and sill that are associated with hyaloclastite breccia, indicate that deposits in subaqueous lava (Allen et al., 1996). *Monomictic andesitic breccia* usually clast-supported, jigsaw-fit texture, irregular clast shape, pebble to cobble clast size, clasts population that interpreted as hyaloclastite breccia. The morphology of clasts that irregular shape with fine-grain margins, blocky clasts, flow-banded, and rotated clasts interpreted as juvenile clasts formed by quench fragmentation. The lack of evidence of transport and reworks of post-eruptive re-sedimentation with the matrix no sediments indicate that breccia that made during the emplacement of the plagioclase-phyric andesite lavas.

Plagioclase-phyric basalt and aphyric trachyte are commonly sharp contacts with their host rocks. They are showing fine-grain chilled margin, and vesicles imply that mafic magma was a shallow intrusion. They cut the whole stratigraphy imply that intrude after the lithification of host rocks. And both are interpreted that shallow intrusion sill and dykes.

Quartz-phyric rhyolite facies association occurs as pyroclastic facies, which spatially related, similar composition, and texturally. *Lithic-rich pumice breccia* is laterally continuous at the base of crystal-rich pumice breccia. The clast is sharp and angular shape indicated that brittle fragmentation. Moreover, the phyric-rhyolite clast population implies that few or no transport post-fragmentation, interpreted as pyroclastic facies. *Crystal-rich pumice breccia* contains fluidal rhyolitic pumice clasts, which evidence for plastic deformation upon impact with the substrate. The pyroclastic progressive movement of the water-supported pyroclastic flows during hot and unconsolidated. The characteristics of pyroclasts suggest they were fed from fire fountain eruption and derived not far from a source (cf. Allen, 1992; Cas and Wright, 2012;

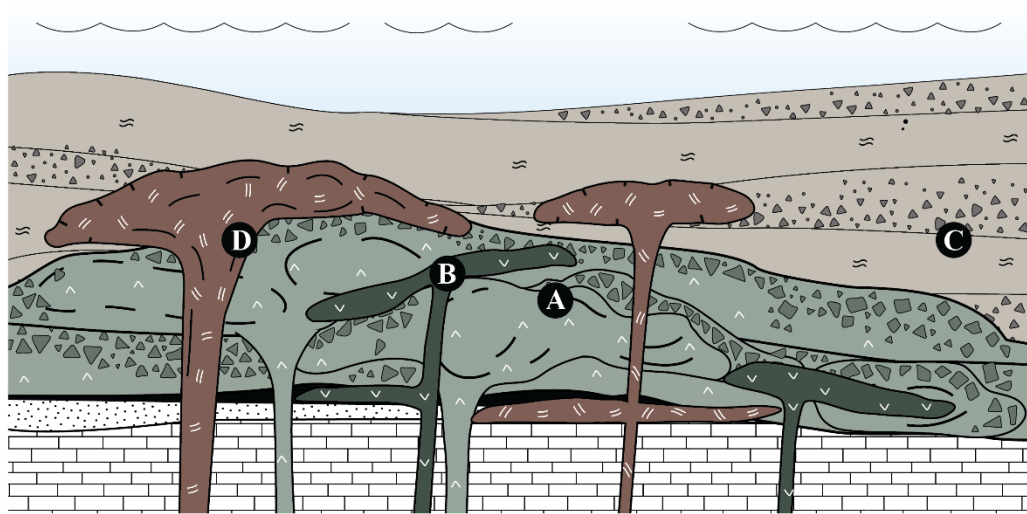
McPhie et al., 1993; Simpson and McPhie, 2001). The many crystal-rich pumice cycle suggests that they are related to one more single eruption. *Quartz-phyric rhyolite* has variations in phenocrysts type, abundance, and size, which forming during more than one process crystallization. All of the features suggest they are syn-volcanic intrusion, cryptodomes or sills (cf. McPhie et al. (1993)). In the lower sequences show sharp contacts implying that felsic magma intrudes after the lithification of host rocks. Whereas, the upper part shows quench fragments dominated, imply that emplace wet unconsolidated sediments.

3.5 Facies architecture of the Khao Noi area succession

The Khao Noi volcanic record two distinctive styles of eruptions are effusive eruption and explosive eruption (Fig. 3.15). The products of these two eruption styles intercalated with submarine sediments. The coherent facies (plagioclase-phyric andesite), autoclastic facies (monomictic andesitic breccia) record effusive volcanism. The pyroclastic facies and syn-volcanic intrusion that evidence of explosive volcanism.

Effusive volcanism is contained of proximal volcanic facies by the effusive eruption and shallow intrusions: the andesite lavas and dome in Khao Noi volcanic are massive core, flow banded rind, and in-situ hyaloclastite margins are common in other ancient submarine volcanic successions (Fig. 3.15A) (cf. Cas and Wright (2012); McPhie et al. (1993)). The syn-volcanic intrusion are mafic dykes, is typical concordant and discordant contacts that cut in sedimentary rocks and monomictic andesitic breccia (Fig. 3.15B).

Explosive volcanism dominant pyroclasts comprise of pumice-rich with high vesicle and fluidal clasts that produce from gas-and water-supported pyroclastic current, which explodes of the subaqueous volcanic (cf. McPhie et al. (1993); Simpson and McPhie (2001)) (Fig. 3.15C). The syn-volcanic intrusion is rhyolitic, is typically concordant and discordant contacts, tabular and mushroom-like, which occurs in association with extrusion andesitic lava in the proximal section. They display similar texture and internal structure that they are intruding in the shallow intrusion (Fig. 3.15D).



Explanation












	Laminated mudstone		Plagioclase-phyric andesite		Quartz-phyric rhyolite
	Limestone breccia		Aphyric trachyte		Crystal-rich pumice breccia
	Laminated sandstone		Plagioclase-phyric basalt		Lithic-rich pumice breccia
	Laminated limestone		Monomictic andesite breccia		

Fig. 3.15 Schematic cross-section through the Khao Noi area. **(A)** Subaqueous, andesite lava domes and sills volcano; Unit 2. **(B)** The syn-volcanic intrusion of the basalt dykes and aphyric trachyte dykes (Unit 2). **(C)** Subaerial to shallow marine pyroclastic eruptions generate subaqueous syn-volcanic mass-flow deposits; Unit 3, and **(D)** The syn-volcanic intrusion of rhyolite sills (Unit 3).

CHAPTER 4

GEOCHEMISTRY

4.1 Introduction

This chapter describes whole-rock geochemistry of volcanic rock in the Khao Noi area to identify its composition, fractional crystallization, magma affinity, and tectonic setting.

4.2 Sample preparation and analytical techniques

Least altered seventeen samples were selected previously discussed in Chapter 3. The selected samples were prepared for whole-rock chemical analysis by firstly reducing-sized fragments into small chips (5 mm across) using a Rocklabs hydraulic crusher. These crushed fragments cautiously were chosen to avoid vesicles, amygdale minerals, veinlets, xenoliths, and weathering surfaces. Approximately 100 g were grounded to a fine powder (63 microns) for a few minutes by using a Rocklabs tungsten-carbide ring mill. All of above procedures were examined at the Department of Geological Sciences, Chulalongkorn University.

The 1 g of powder sample was heated at 110 °C for an hour for the moisture content of rocks, and then was heated at 1050 °C for 2 hours to determine Loss in the ignition (LOI) for volatile matter. This procedure was done at the Department of Mineral Resources, Bangkok.

1) Major element analyses

All major- and minor-oxides (SiO_2 , TiO_2 , Al_2O_3 , total iron oxide as $\text{Fe}_2\text{O}_3^{(\text{total})}$, MnO , MgO , Na_2O , K_2O , P_2O_5 and Loss in ignition), were determined by using a PANalytical (Zetium) X-ray fluoresces (XRF) spectrometer installed at the Department of Mineral Resources, Bangkok, Thailand. The instrumental parameters are made up of Rhodium tube (used in an element range of Na to U) and flow proportion detectors, X-ray tube operated at 60 kV and current of up to 160 mA at maximum power level of 4 kW. These oxides were measured from the fuse bead, prepared by mixed of 1 g fine-powdered sample with flux agent in a ratio of 1:5 by weight. The flux agent is the mixture of di-lithium tetraborate (99.9%) and lithium metaborate (99.9%) (66:34) (by weight).

The sample was dissolved in a platinum crucible at 1015 °C for 20 min by using a fusion machine (Claisse the Ox Advanced electric fusion). The standards are used including JG-2 (granite), G-2 (Granite), JB-1a (basalt), JG-1a (granodiorite), and JGb-1 (gabbro). All the major-and minor-oxides were recalculated to 100 wt. % and reported in Table 4.2.

Table 4.1 List of rock sample from Khao Noi area for whole-rock geochemistry.

Sample No.	Location (drill hole)	Depth (m)	Facies	Unit
KNC4	DDH21	69.15–69.40	Plagioclase-phyric andesite	2
KNC17	DDH17	33.70–33.90	Plagioclase-phyric andesite	2
KNC44	DDH17	75.25–75.40	Plagioclase-phyric andesite	2
KNC45	DDH21	67.70–67.85	Plagioclase-phyric andesite	2
KNC49	DDH23	48.00–48.15	Plagioclase-phyric andesite	2
KNC30	DDH23	52.50–52.70	Plagioclase-phyric andesite	2
KNC40	DDH17	25.40–25.50	Plagioclase-phyric andesite	2
KNC46	DDH21	68.30–68.45	Plagioclase-phyric andesite	2
KNC47	DDH23	38.25–38.35	Plagioclase-phyric andesite	2
KNC26	DDH17	75.50–75.70	Plagioclase-phyric basalt	2
KNC27	DDH17	77.70–77.85	Plagioclase-phyric basalt	2
KNC37	DDH09	10.0–10.20	Plagioclase-phyric basalt	2
KNC21	DDH17	42.20–42.80	Plagioclase-phyric basalt	2
KNC22	DDH17	48.80–49.00	Plagioclase-phyric basalt	2
KNC25	DDH17	73.00–73.35	Plagioclase-phyric basalt	2
KNC19	DDH24	95.00–95.50	Aphyric trachyte	2
KNC20	DDH09	9.50–9.80	Aphyric trachyte	2

2) Trace and Rare earth element analyses

A number of selected trace elements (Ba, Rb, Sr, Th, Y, Zr, Nb, Ni, Cr, and V), and Rare Earth Elements (La, Ce, Pr, Sm, Eu, Gd, Tb, Dy, Ho, Er, Tm, Yb, and Lu) were determined by using inductively coupled plasma mass spectrometry (ICP-MS). The solution for measuring was prepared according to ASTM D3976-92 by dissolving the fuse bead, which was a mixing fine-powdered sample with sodium peroxide flux with acid. The solution was prepared and analysed by SGS laboratory, Canada.

4.3 Rock types and Magmatic affinities

The three coherent volcanic rock types of the Khao Noi area classified by lithofacies and petrography show different types of REE patterns, N-MORB normalized multi-element patterns, and variation diagram.

1) Plagioclase-phyric andesite

Plagioclase-phyric andesite is plotted in the trachyte-andesite and basanite field of the chemical classification by Winchester and Floyd (1977) (Fig. 4.1). The samples show relatively high Nb/Y ratio while low Zr/TiO₂ ratio in the range of 0.60–5.52 and 0.0016–0.0021, respectively, following alkaline series. The plagioclase-phyric andesite shows SiO₂ content ranging from 54.88 to 61.86 wt. %, MgO (0.85–3.60 wt. %), K₂O (2.77–5.09 wt. %), Al₂O₃ (15.32–18.26 wt. %), Na₂O (1.84–3.34 wt. %), and Fe₂O₃^(total) (3.49–8.76 wt. %) contents. These major oxides slightly increase with relative MgO content, while TiO₂ (0.86–1.11 wt. %) and CaO (2.74–5.09 wt. %) contents are constant (Fig. 4.2). LOI vary in 4.03–6.13 wt. % related to their secondary minerals (calcite infilling). In addition, AFM diagram is used to characterize magma affinity. The diagram shows that the plagioclase-phyric andesite is tholeiite magmatic which evolves from the F (Fe₂O₃^(total)) toward the alkaline magma series (Fig. 4.3).

By plotting transition and trace elements against the MgO content, the plagioclase-phyric andesite shows enrich in transition elements characterized by a high concentration of transition elements and can be divided into 2 group: Suite I and Suite II.

Suite I is characterized by a slightly negative trend of Ni (18–44 ppm) and Sr, high V (76–134 ppm), low Zr (232–337 ppm), low Y (2.9–36.5 ppm), and low Zn (22–54 ppm) content compare with Suite II (Fig. 4.4).

The REE concentration with chondrite-normalized by Sun and McDonough (1989) of the suite I shows enrichment of LREE (La–Nd) and MREE (Sm–Dy). The REE patterns of the suite I have flatter pattern of HREE (Ho–Lu) than the suite II with (La/Yb)_{cn} = 6.28 to 11.81; (La/Sm)_{cn} = 4.20 to 6.38; (Sm/Yb)_{cn} = 1.10 to 1.86. The weak negative Eu anomalies which is typical of plagioclase less in magma source are found (Eu/Eu* = 0.027 to 0.031). These REE pattern might present characteristic of mildly calc-alkaline series which is enriched in LREE and flat HREE distribution (Fig. 4.5).

Table 4.2 Whole-rock major element oxide (wt. %), trace and rare earth elements (ppm).

Sample no.	KNC4	KNC17	KNC44	KNC45	KNC49	KNC30	KNC40	KNC46	KNC47	KNC26
Rock type	PPA	PPA	PPA	PPA	PPA	PPA	PPA	PPA	PPA	PPA
<i>Major element (wt. %)</i>										
SiO ₂	55.76	56.96	61.86	56.92	54.88	56.89	58.59	55.70	52.14	54.15
TiO ₂	1.00	0.86	1.11	0.99	0.94	0.98	0.92	0.98	0.94	1.41
Al ₂ O ₃	16.33	15.32	18.26	16.16	16.76	17.15	16.79	16.53	17.12	21.92
Fe ₂ O ₃ ^(total)	7.20	6.93	3.49	7.73	8.76	10.32	6.83	8.33	13.85	6.29
MnO	0.13	0.14	0.03	0.13	0.13	0.15	0.13	0.15	0.20	0.06
MgO	3.26	2.17	0.85	3.60	2.94	2.20	1.58	3.97	2.66	1.98
CaO	5.00	5.09	3.50	3.44	2.74	2.27	3.60	3.89	2.26	2.22
Na ₂ O	3.34	2.82	<0.1	3.20	1.84	2.26	3.39	2.63	1.12	<0.1
K ₂ O	3.16	2.77	5.09	2.90	3.74	2.43	2.41	3.05	2.62	5.57
P ₂ O ₅	0.23	0.21	0.22	0.24	0.23	0.24	0.22	0.23	0.24	0.28
LOI	4.03	6.13	4.72	4.06	6.04	4.52	4.83	4.02	6.17	5.12
Total	99.44	99.39	99.23	99.37	98.99	99.41	99.28	99.48	99.31	99.11
<i>Trace element and REE compositions determine by ICPMS (ppm)</i>										
mg#	56	39	53	59	44	33	31	56	31	45
Li	40	40	70	30	<10	30	110	110	40	390
V	134	134	82	80	76	18	9	45	24	<5
Sc	17	17	17	13	11	7	7	8	7	<5
Cr	110	80	70	40	60	10	<10	40	20	<10
Ni	29	38	44	18	28	13	9	19	17	8
Cu	28	30	55	22	17	7	42	13	13	12
Co	11.6	5.6	30.0	37.2	23.5	1.5	1.7	5.2	2.5	1.8
Zn	44	54	38	22	34	43	252	79	28	71
Ga	31	30	21	23	22	43	44	29	51	61
Rb	220	86	40	91	26	315	257	458	392	1210
Sr	12.5	11.9	14.5	6.5	6.5	11.2	5.2	14.8	10.2	15.4
Y	36.5	11.6	10.0	13.0	2.9	35.1	49.1	94.1	27.0	26.2
Zr	259	337	287	232	269	401	331	243	103	268
Sn	28	79	8	7	15	81	83	46	39	449
Sb	0.9	1.3	0.6	0.6	0.5	0.7	0.5	0.6	1.8	0.5
Cs	19.0	28.3	6.2	8.3	4.6	33.4	36.7	55.4	30.3	126.0
Ba	372.0	89.1	129.0	21.7	3.1	35.5	13.9	202.0	23.1	39.2
La	52.1	18.4	24.7	22.8	11.4	38.5	100.0	42.0	10.0	36.3
Ce	133.0	113.0	104.0	148.0	57.9	184.0	264.0	96.0	19.4	71.5
Pr	11.2	3.7	4.7	5.8	2.1	9.6	18.6	10.8	2.4	8.7
Nd	40.1	12.0	14.7	21.1	6.6	32.7	55.5	40.0	8.6	27.
Sm	7.5	2.3	2.5	3.5	1.3	7.4	10.8	10.6	3.2	7.3
Gd	6.3	1.8	1.6	2.6	0.7	5.8	8.9	11.3	3.7	6.2
Tb	1.0	0.3	0.3	0.4	0.1	1.0	1.5	2.3	0.9	1.2
Dy	6.5	2.0	1.8	2.5	0.7	6.1	8.4	14.4	5.6	6.4
Ho	1.3	0.5	0.4	0.6	0.1	1.2	1.6	3.1	0.9	0.9
Er	3.9	1.6	1.2	1.7	0.5	3.6	4.7	8.9	2.3	2.6
Tm	0.6	0.3	0.2	0.3	0.1	0.6	0.7	1.4	0.4	0.5
Yb	3.8	2.1	1.5	2.0	0.7	3.7	4.6	10.0	3.1	3.5
Lu	0.6	0.4	0.2	0.3	0.1	0.6	0.7	1.5	0.5	0.5
Nb	22	24	15	14	16	49	54	34	33	161
Ta	3.0	8.8	1.5	1.5	1.8	10.5	9.3	8.8	4.8	87.5
Pb	61	39	324	55	27	64	222	103	51	185
Th	37.9	32.3	26.1	27.8	26.7	165.0	156.0	57.0	17.2	38.4
U	5.5	5.0	6.5	3.7	11.9	19.0	17.5	18.7	22.4	23.0
Eu	1.1	0.4	0.4	0.5	0.2	0.2	0.2	0.6	0.2	0.2
Hf	8	10	9	7	8	14	12	9	3	9
Ge	2	2	2	1	2	2	3	3	3	5
Tl	1.5	0.9	<0.5	0.6	<0.5	1.9	1.6	2.8	1.9	8.3
La/Yb _{cn}	9.83	6.28	11.81	8.18	11.68	7.46	15.59	3.01	2.31	7.44
La/Sm _{cn}	4.48	5.16	6.37	4.21	5.66	3.36	5.98	2.56	2.01	3.21
Sm/Yb _{cn}	1.97	1.10	1.67	1.75	1.86	2.00	2.35	1.06	1.03	2.09
Eu/Eu*	0.0271	0.0303	0.0326	0.0300	0.0312	0.0049	0.0034	0.0100	0.0093	0.0042

Note: Fe₂O₃^(total) = total iron, Fe₂O₃ is derived from the subtraction of Fe₂O₃^(total) by the XRF method, LOI = loss on ignition, Eu/Eu* = (Eu_{cn})/1/2(Sm_{cn} x Gd_{cn}); cn = Chondrite normalized from Sun and McDonough, 1989 (McLennan, 1989).

Abbreviation: HPPA = Hornblende-plagioclase-phyric andesite, PPA = Plagioclase-phyric andesite, PPBD = Plagioclase-phyric basalt dyke, ATD = Aphyric trachyte dyke.

Table 4. 2 (Continued)

Sample no.	KNC27	KNC37	KNC21	KNC22	KNC25	KNC19	KNC20
Rock type	PPBD	PPBD	PPBD	PPBD	PPBD	ATD	ATD
<i>Major element (wt. %)</i>							
SiO ₂	43.04	42.05	42.61	37.71	44.94	48.21	46.13
TiO ₂	1.52	1.28	1.46	1.52	1.58	1.43	1.50
Al ₂ O ₃	16.44	19.80	15.65	16.85	16.78	17.72	18.68
Fe ₂ O ₃ ^(total)	11.82	10.43	11.16	11.38	10.46	12.15	13.15
MnO	0.21	0.20	0.19	0.22	0.17	0.21	0.18
MgO	4.25	1.90	6.35	5.52	5.66	2.68	2.99
CaO	7.99	9.30	8.20	9.73	6.45	4.54	3.73
Na ₂ O	0.43	2.15	1.89	0.61	1.27	3.90	4.34
K ₂ O	3.07	4.04	1.37	1.97	2.55	1.63	1.64
P ₂ O ₅	0.54	0.61	0.25	0.27	0.54	0.51	0.53
LOI	9.89	7.45	10.43	13.32	8.65	6.39	6.27
Total	99.19	99.20	99.56	99.11	99.04	99.35	99.14
<i>Trace element and REE compositions determine by ICPMS (ppm)</i>							
mg#	46	39	59	54	56	34	39
Li	40	90	60	60	20	7	110
V	9	11	<5	<5	6	12	17
Sc	<5	7	<5	6	<5	6	8
Cr	<10	<10	<10	<10	<10	<10	<10
Ni	9	10	7	7	8	9	15
Cu	<5	34	8	31	11	10	10
Co	37.1	32.1	1.3	2.2	21.9	1.2	2.2
Zn	22	26	46	70	33	100	67
Ga	32	38	49	60	43	45	43
Rb	259	302	1540	1400	538	369	285
Sr	11.6	10.8	22.0	19.7	14.6	13.1	12.2
Y	19.8	31.2	81.4	119.0	44.8	32.1	63.9
Zr	123	210	240	240	79	864	689
Sn	63	121	144	224	325	116	68
Sb	1.0	0.6	0.5	0.8	0.8	1.7	1.3
Cs	21.6	41.7	136.0	130.0	33.0	64.7	55.0
Ba	34.0	34.8	80.0	56.8	40.6	23.0	26.5
La	23.7	30.2	39.7	83.9	73.7	37.6	141.0
Ce	63.3	153.0	99.9	168.0	132.0	104.0	439.0
Pr	4.9	6.5	11.4	22.4	17.5	8.01	32.3
Nd	15.1	21.8	40.8	75.1	49.9	26.9	109.0
Sm	3.3	4.6	12.0	20.7	12.5	5.4	20.7
Gd	2.7	4.3	11.4	18.3	8.7	4.7	16.0
Tb	0.5	0.8	2.4	3.7	1.7	0.9	2.4
Dy	3.0	5.0	14.2	21.6	9.2	5.3	12.8
Ho	0.6	1.1	2.8	3.8	1.5	1.1	2.3
Er	2.0	3.2	8.3	11.6	4.1	3.5	6.2
Tm	0.3	0.5	1.3	1.9	0.7	0.5	0.9
Yb	2.0	3.3	9.6	13.4	5.3	3.8	5.6
Lu	0.3	0.5	1.3	1.9	0.8	0.6	0.9
Nb	36	52	40	98	85	64	58
Ta	7.1	9.2	12.7	38.2	35.0	15.6	9.2
Pb	60	47	259	303	422	36	73
Th	95.7	140.0	54.1	64.1	30.8	111.0	236.0
U	10.1	11.2	27.4	42.0	13.1	22.7	27.1
Eu	0.1	0.1	0.3	0.6	0.4	0.1	0.2
Hf	5	8	8	8	4	25	23
Ge	2	3	3	3	2	3	3
Tl	1.5	1.8	10.5	10.5	4.3	2.0	1.8
La/Yb _{cn}	8.50	6.56	2.97	4.49	9.97	7.10	18.06
La/Sm _{cn}	4.64	4.24	2.14	2.62	3.81	4.50	4.40
Sm/Yb _{cn}	1.65	1.39	1.25	1.54	2.36	1.42	3.70
Eu/Eu*	0.065	0.0028	0.0050	0.0052	0.0061	0.0032	0.0019

Note: Fe₂O₃^(total) = total iron, Fe₂O₃ is derived from the subtraction of Fe₂O₃^(total) by the XRF method, LOI = loss on ignition, Eu/Eu* = (Eu_{cn})/1/2(Sm_{cn} x Gd_{cn}); cn = Chondrite normalized from Sun and McDonough, 1989 (McLennan, 1989).

Abbreviation: HPPA = Hornblende-plagioclase-phyric andesite, PPA = Plagioclase-phyric andesite, PPBD = Plagioclase-phyric basalt dyke, ATD = Aphyric trachyte dyke.

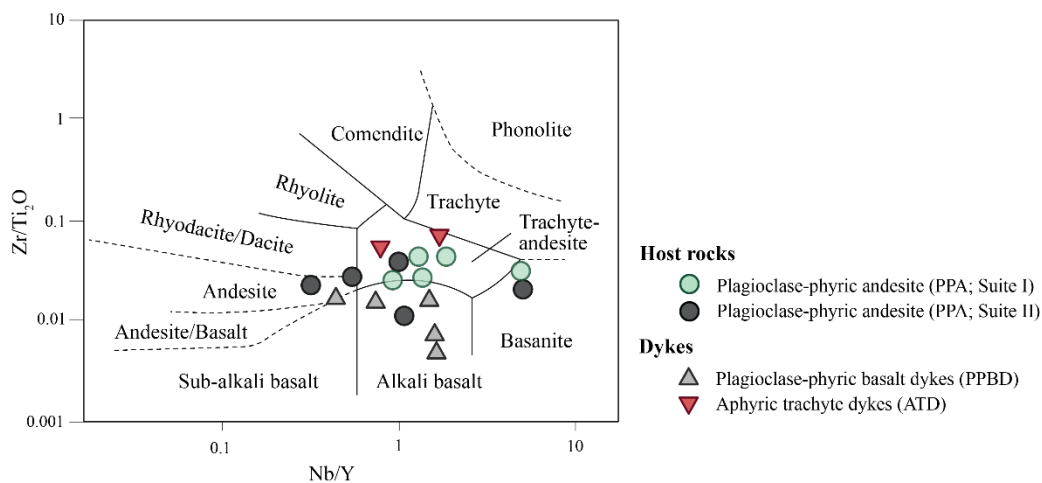


Fig. 4.1 Discrimination diagram of Nb/Y and Zr/TiO_2 (after Winchester and Floyd, 1977).

The N-MORB-normalized multi-elements patterns are plotted to the average of Sun and McDonough (1989). All patterns of rock samples show enrichment in LILE such as Cs, Rb, Pb, U, Li, and LREE in comparison to HFSE (Nb, Ta, Zr, Hf, Ti, and Y) (Fig. 4.6). The enrichment is typical enriched by crust composition while the low concentration of Nb is characteristics of magma associated subduction-related (McCulloch, 1991; Pearce, 1996, 1982, p. 198).

Suite II of plagioclase-phyric andesite is mostly plotted into andesite, trachyte-andesite, and basanite (Fig. 4.1). The Nb/Y ratio against Zr/TiO_2 ratio are ranging in 0.002–1.40 and 0.90–6.44, respectively, corresponding to subalkaline and alkaline series. The suite II has lower concentration of Ni and V than the Suite I while the Y concentration is slightly higher (Fig. 4.4).

The REE concentration with chondrite-normalized by Sun and McDonough (1989) of the suite II shows higher REE ratios and more steeply dipping REE patterns than the Suite I. The REE patterns show slightly flat in LREE and HREE with $(La/Yb)_{cn} = 2.31$ to 15.59; $(La/Sm)_{cn} = 2.02$ to 5.98; $(Sm/Yb)_{cn} = 1.03$ to 2.35. The strong negative Eu anomalies which indicate the relative equilibrium of melts with amphibole, garnet and the absence of plagioclase from the magma source are also found ($Eu/Eu^* = 0.003$ –0.02) (Fig. 4.3). The Suite II characteristics might present typical of mildly alkaline series.

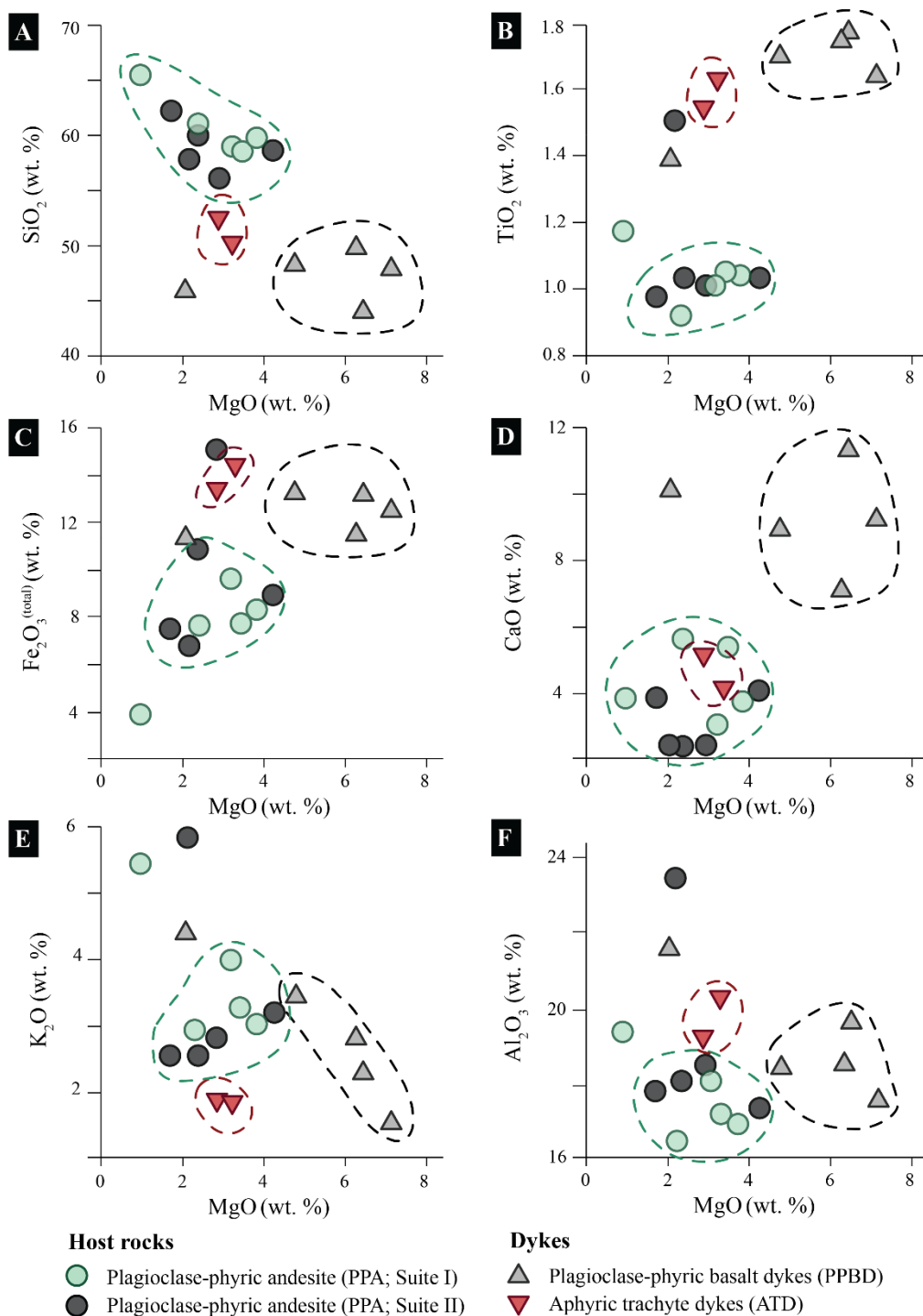


Fig. 4.2 Major element bivariate diagrams plotted against MgO for volcanic rocks from Khao Noi area. (A) SiO₂ vs. MgO showing a slightly negative trend to more mafic composition, (B) TiO₂ vs. MgO showing low concentrate and relatively high Ti for dykes, (C) Fe₂O₃ (total) vs. MgO showing low Fe concentrate and high Fe concentrate in dykes, (D) CaO vs. MgO showing slightly low Ca and relatively high for plagioclase-phyric basalt dyke, (E) K₂O vs. MgO showing low concentrate for the volcanic rocks, and (F) Al₂O₃ vs. MgO showing low concentrate for the volcanic rocks.

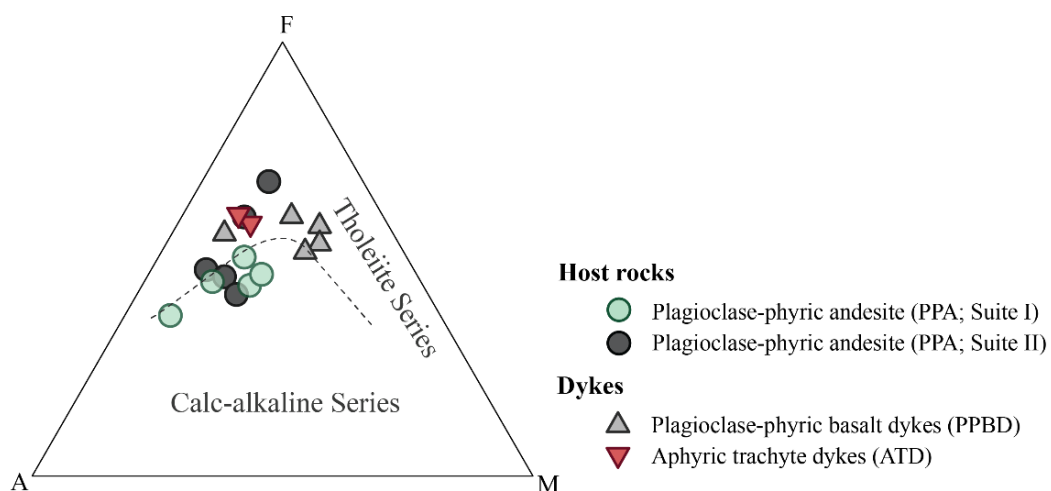


Fig. 4.3 AFM diagram for tholeiite and calc-alkaline magma series with divide line from Irvine and Baragar (1971); dash gray line) showing trend to calc-alkaline and tholeiite series for the volcanic rocks.

The N-MORB-normalized multi-elements patterns are plotted to the average of Sun and McDonough (1989). All patterns of rocks present the enrichment in LILE such as Cs, Rb, Pb, U, Li, and LREE in comparison to HFSE (Nb, Ta, Zr, Hf, Ti, and Y) (Fig. 4.4).

2) Plagioclase-phyric basalt dyke

Plagioclase-phyric basalt dyke is classified chemically by the diagram of Winchester and Floyd (1977) as sub-alkaline basalt and alkaline basalt (Fig. 4.1). The samples show Nb/Y ratio and Zr/TiO₂ ratio in range of 0.49–1.90 and 0.17–0.80, respectively, with alkaline and sub-alkaline series. The plagioclase-phyric basalt dyke is characterized by SiO₂ content ranging from 37.71 to 44.94 wt. %. All of samples show slightly high concentration of TiO₂ (1.28–1.58 wt. %), Fe₂O₃^(total) (10.43–11.82 wt. %), CaO (6.45–9.73 wt. %) and decreasing of K₂O (1.37–4.04 wt. %) content during MgO increase (Fig. 4.2). In addition, the AFM diagram shows trend of plagioclase-phyric basalt dyke toward F (Fe₂O₃^(total)) suggesting the tholeiite magma series (Fig. 4.3).

The plagioclase-phyric basalt dyke is characterized by low concentration of Ni (7–10 ppm), V (6–11 ppm), and Zr (79–240 ppm) content. While Y concentration (19.8–119 ppm), and Sr concentration (14.6–22 ppm) are slightly higher than the other rock types (Fig. 4.4).

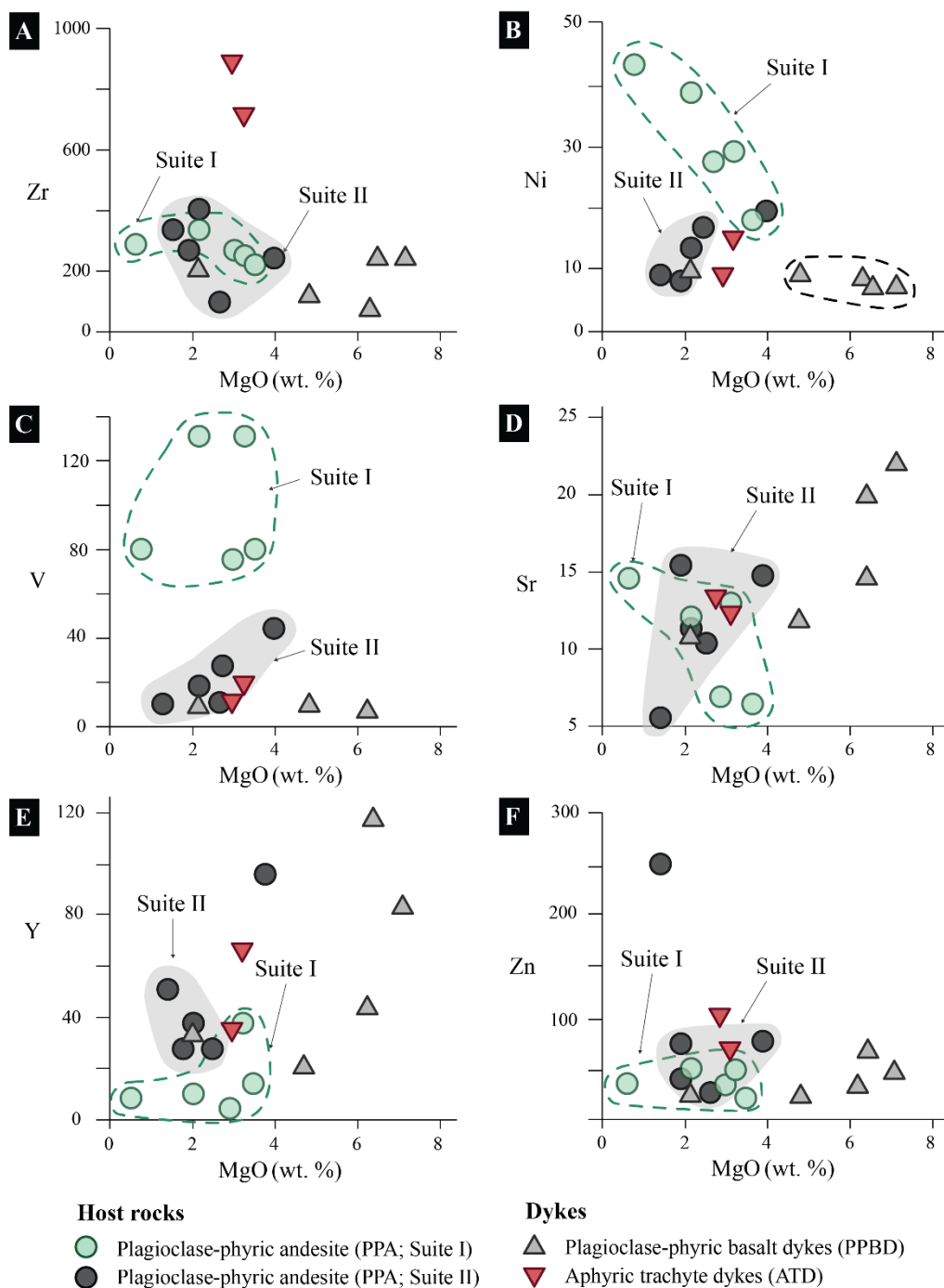


Fig. 4.4 Trace element bivariate diagrams plotted against MgO for coherent rocks from the Khao Noi area. **(A)** Zr vs. MgO showing low Zr concentrate, **(B)** Ni vs. MgO showing low concentrate except the Suite I of plagioclase-phyric andesite showing a negative trend, **(C)** V vs. MgO showing high V for Suite I and low concentrate for all volcanic rocks, **(D)** Sr vs. MgO showing a slightly positive trend for volcanic rocks, **(E)** Y vs. MgO showing low concentrate, and **(F)** Zn vs. MgO showing low concentrate.

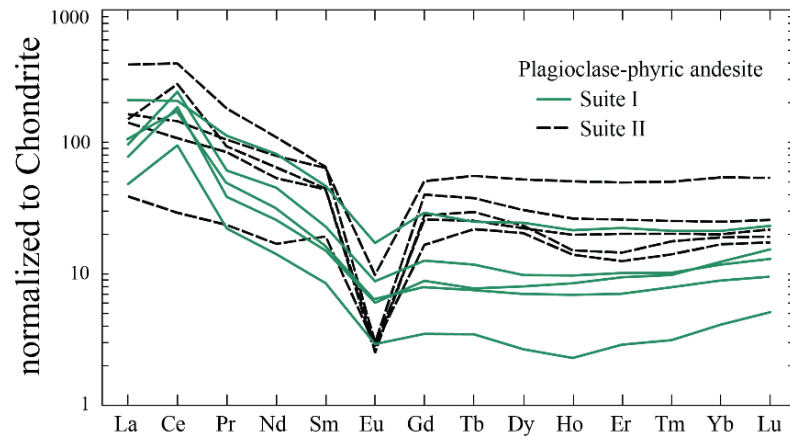


Fig. 4.5 Chondrite-normalized REE patterns for the plagioclase-phyric andesite, the Chondrite-normalized value from Sun and McDonough (1989).

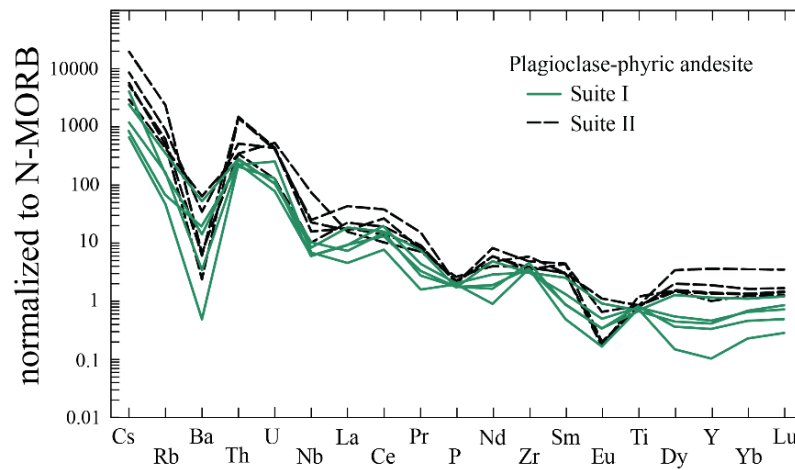


Fig. 4.6 N-MORB normalized multi-element for plagioclase-phyric andesite, the N-MORB normalized value from Sun and McDonough (1989).

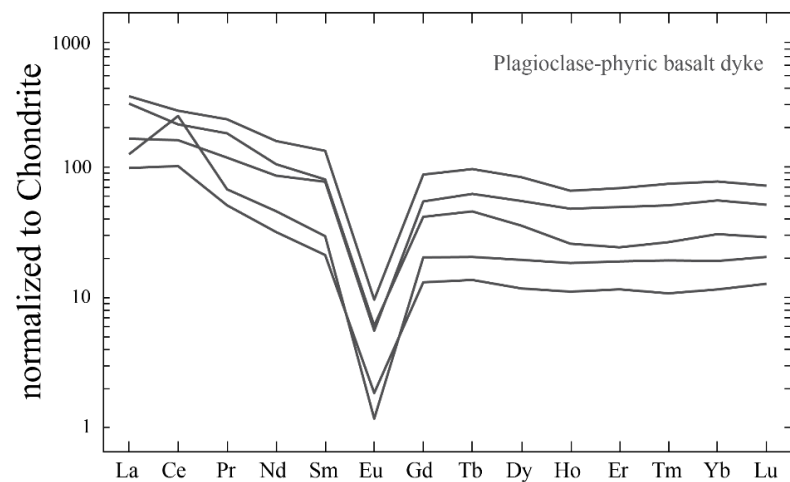


Fig. 4.7 Chondrite-normalized REE patterns for the plagioclase-phyric basalt dyke, the Chondrite-normalized value from Sun and McDonough (1989).

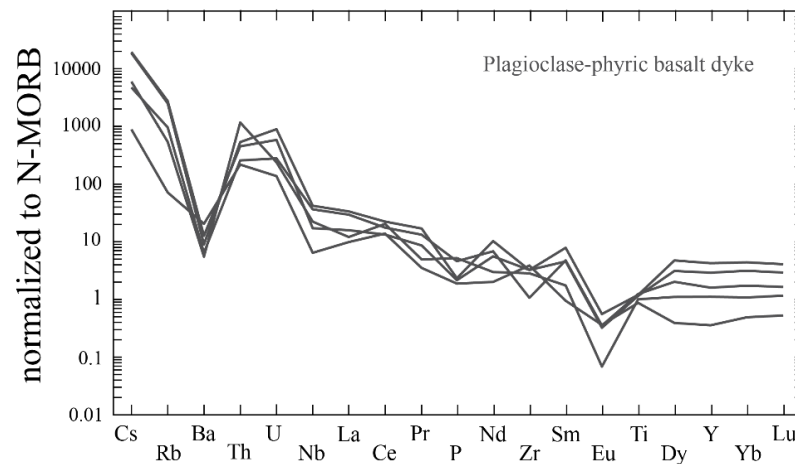


Fig. 4.8 N-MORB normalized multi-element for plagioclase-phyric basalt dyke, the N-MORB normalized value from (Sun and McDonough, 1989).

The REE patterns of the plagioclase-phyric basalt dyke, Chondrite-normalized of Sun and McDonough (1989), show sloping trends. They show slightly steep in LREE and flat HREE pattern with $(La/Yb)_{cn} = 2.96–9.97$; $(La/Sm)_{cn} = 2.13–4.63$; $(Sm/Yb)_{cn} = 1.25–2.36$. The strong negative Eu anomalies are also presented ($Eu/Eu^* = 0.002–0.006$) (Fig. 4.6). The REE patterns are typical of mildly alkaline series.

The N-MORB-normalized multi-elements patterns are plotted to the average of Sun and McDonough (1989). The rocks present the enrichment in LILE such as Cs, Rb, U, and LREE in comparison to HFSE (Nb, Zr, Ti, and Y) (Fig. 4.7).

3) Aphyric trachyte dyke

Aphyric trachyte dyke are plotted in trachyte-andesite field to Winchester and Floyd's chemical classification diagram (1977) (Fig. 4.2). The Nb/Y ratio and the Zr/TiO₂ ratio are in range of 0.91–1.99 and 1.32–2.26, respectively, following alkaline series. The aphyric trachyte shows SiO₂ contents varying from 46.13 to 48.21 wt. %, moderate TiO₂ concentration (1.43–1.50 wt. %), slightly high Fe₂O₃^(total) (12.15–13.15 wt. %). While the CaO (3.73–4.54 wt. %) and K₂O (1.63–1.64 wt. %) content are slightly low (Fig. 4.2). In AFM diagram, the aphyric trachyte dyke display enrichment in Fe₂O₃^(total) content plot, thus the rock samples are plotted in tholeiite magma series (Fig. 4.3).

The bivariate diagrams of transitional elements vs. MgO show that the aphyric trachyte dyke is characterized by high Zr (689–864 ppm). On the other hand, The Ni

(9–15 ppm), V (6–8 ppm) and Zn (22–70 ppm) are slightly low. The bivariate diagrams show moderate concentration of Sr (12.3–13.1 ppm) and Y (32.1–63.9 ppm) (Fig. 4.4).

The aphyric trachyte dyke shows slightly steep in LREE and flat HREE trend of chondrite-normalized pattern. The REE patterns are characterized by $(La/Yb)_{cn} = 7.09–18.06$; $(La/Sm)_{cn} = 4.39–4.49$; $(Sm/Yb)_{cn} = 1.42–3.69$ and strong negative Eu anomalies ($Eu/Eu^* = 0.001–0.003$). The REE patterns of the aphyric trachyte dyke are typical of mildly alkaline series (Fig. 4.9).

The N-MORB-normalized multi-elements patterns are plotted to the average of Sun and McDonough (1989). The rocks present the enrichment in LILE such as Cs, Rb, U, and LREE in comparison to HFSE (Nb, Zr, Ti, and Y) (Fig. 4.10)

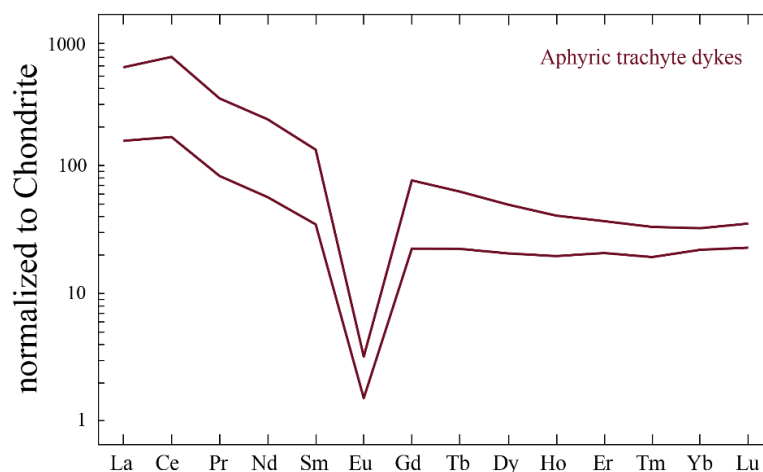


Fig. 4.9 Chondrite-normalized REE patterns for the aphyric trachyte, the Chondrite-normalized value from Sun and McDonough (1989).

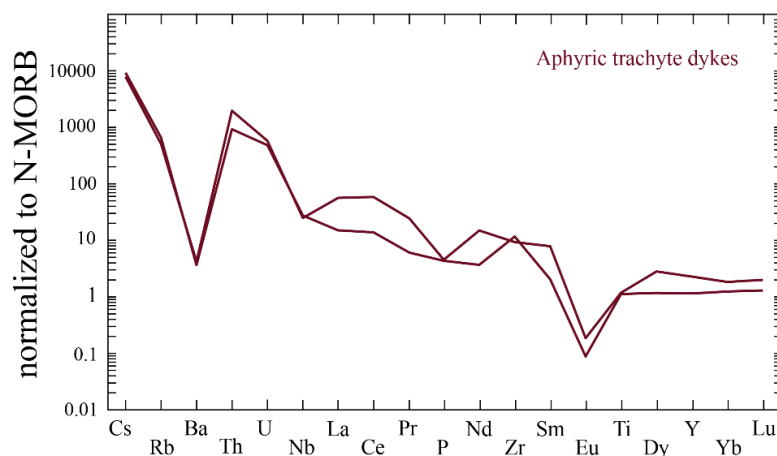


Fig. 4.10 N-MORB normalized multi-element for aphyric trachyte, the N-MORB normalized value from Sun and McDonough (1989).

4.4 Tectono-magmatic Discrimination Diagrams

The diagrams, used to discriminate tectonic environments of the studied rocks, include TiO_2 vs. Al_2O_3 , FeO^T (as $\text{Fe}_2\text{O}_3^{\text{total}}$)- MgO - Al_2O_3 , and Ta/Yb vs. Th/Yb diagram. All of the rock groups are plotted into the arc-related environment of the TiO_2 vs. Al_2O_3 diagram (Müller et al., 1992) (Fig. 4.11A). Moreover, Nb/Yb vs. Th/Yb diagram (Pearce, 1983) show the sample plotted into Continental arc and alkaline oceanic arcs with enriched mantle characteristics (Fig. 4.11B).

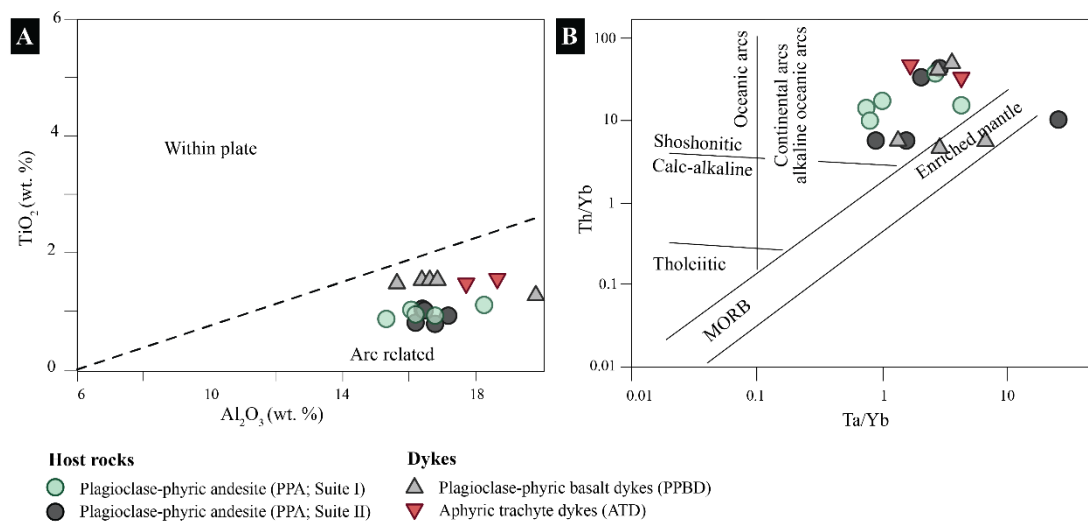


Fig. 4.11 (A) Al_2O_3 vs. TiO_2 (after Müller et al., 1992); (B) Ta/Yb vs. Th/Yb diagram (after Pearce, 1983) the volcanic rocks are distinguishing all group generally shoshonitic series show the field for Continental arcs and alkaline oceanic arcs.

Besides, the Chondrite and N-MORB normalized multi-elements patterns of modern volcanic rocks are used to clarify tectonic settings of formation. Suite I of plagioclase-phyric andesite respectively is chemically similar to high-K calc-alkaline volcanic rocks from the East Java arc (Edwards et al., 1994) which related the subduction zone. For the representative of the Suite II of plagioclase-phyric andesite, the plagioclase-phyric basalt, and aphyric trachyte, the most similar in chemical composition of the modern volcanic rock is the high-K calc-alkaline volcanic rocks from Vulcano from the Aeolian arc (De Astis et al., 2000) (Fig. 4.12A). However, all of the studied volcanic rocks samples show significantly the negative Eu anomaly in REE patterns and fractionated patterns in trace elements diagrams compared to high-K calc-alkaline rocks of East of Java and Aeolian (Fig. 4.12B). The negative Eu anomaly might suggest that

volcanic rocks at the Khao Noi area are formed as highly fractionated high-K calc-alkaline magma related subduction.

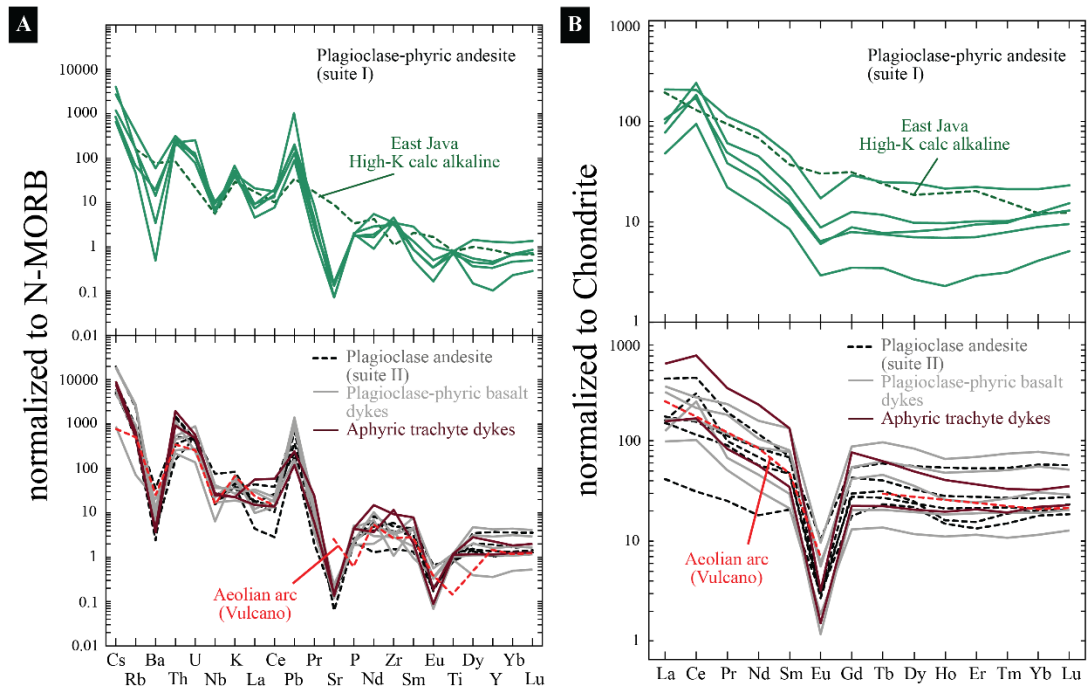


Fig. 4.12 (A) N-MORB normalized multi-element patterns and (B) Chondrite-normalized REE patterns for the studied, least-altered volcanic rocks and their modern analogue.

CHAPTER 5

DISCUSSION AND CONCLUSION

5.1 Introduction

Based on results given in chapters 3 (volcanic stratigraphy and facies architecture) and chapter 4 (geochemistry of volcanic rocks), the environmental of volcanic deposition and tectonic implication are discussed below:

5.2 Stratigraphy

The Khao Noi area in Tha Takiap district, Chachoengsao province is part of the Lampang volcanic belt, which has been erupted in Late Permian (254 Ma) comprising mainly lava and associated products covering an area of about 5 km². Based on field investigation and drill core logging, the volcanic sequence at Khao Noi has a thickness of 150 meters. The lowest unit is represented by the sedimentary unit (Unit 1), which forms as a basement for the Khao Noi area sequence, is characterized by laminated limestone, laminated sandstone, limestone breccia, and laminated mudstone. This unit is equivalent to the Carboniferous marine sedimentary unit of Tiya Pirach (1996). The volcanic sequence can be divided into two units; namely, 1) Mafic-intermediate volcanic unit (Unit 2) consisting of plagioclase-phyric andesite, monomictic andesitic breccia, plagioclase-phyric basalt, and aphyric trachyte. Unit 2 is characterized by products of effusive volcanism and erupted in a submarine setting. 2) Felsic volcanic unit (Unit 3) comprises lithic-rich pumice breccia, crystal-rich pumice breccia, and quartz-phyric andesite. Unit 3 usually represents the products of explosive volcanism that possibly erupted in a submarine or subaerial setting. The contact between Unit 2 and Unit 3 is sharp and compositionally change from mafic-intermediate to felsic composition.

5.3 Volcanism

Event 1: The sedimentary unit at the Khao Noi area represents shallow marine depositional environment (Fig. 5.1A).

Event 2: The first andesitic lava and monomictic andesitic breccia are the products of effusive volcanism. The angular shapes are most consistent with brittle fracturing

generated by lava flow imply as quench fragmentation. However, the jigsaw-fit texture and lack of reworking of clasts suggest relatively proximal from sources (Fig. 5.1B).

Event 3: The second andesitic lava and monomictic andesitic breccia are the product of effusive volcanism. The clast-rotated shapes are common. The clast shows flow-banded and fine-grain margins, which formed cooling of outermost of the lava flow that eruption in the submarine. The lack of reworking of clasts suggests relatively proximal to andesitic lava flow (Fig. 5.1C).

Event 4: The mafic coherent is conformable to plagioclase-phyric andesite facies associations. They are interpreted to shallow intrusion rocks from their textures. Based on medium-to fine-grained crystals suggest that they fast cool and not explosive on the surface. They are interpreted to dykes and sills from their geometry that intrudes host rocks (Fig. 5.1D).

Event 5: The felsic facies associations are products of explosive eruptions. The pumice clasts, glass shards, and crystal fragments that typical release from the explosive eruption (Fig. 5.1E). The pyroclasts are not sure this felsic eruption explosive in a subaerial or submarine setting. The graded bedding and lamination are common, suggests that deposits from pyroclasts mass flow or pyroclastic surge. Their clasts represented fragments and juvenile clasts that imply transportation from the distal source (Fig. 5.1F). The location of these felsic sources is unknown.

Event 6: The felsic coherent show quench fragments contacts that intruded unconsolidated, suggests that syn-eruptive volcanism. The cross-cut whole succession includes basement rocks (Unit 1). Based on the geometry and sharp contact, these intrusions rocks have been interpreted as dykes and sills (Fig. 5.1G).

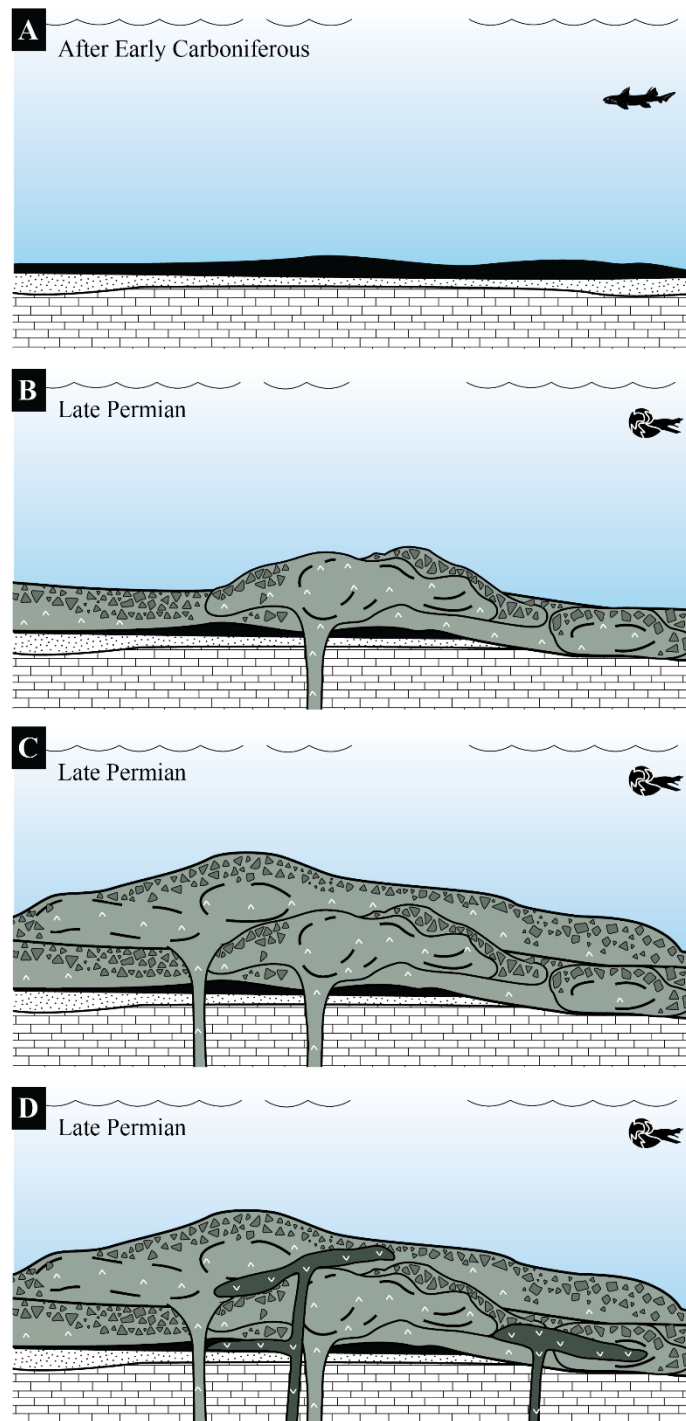


Fig. 5.1 Schematic of facies modal for the depositional environment. **(A)** The sedimentary rocks (Unit 1) were deposited after the Early Carboniferous age. **(B)** During the late Permian age, the first plagioclase-phyric andesite lava was effusive overlying basement sedimentary rocks and associated hyaloclastite (Unit 2). Then **(C)** the second of andesitic lava was effusive. **(D)** Emplacement of mafic-intermediate dykes.

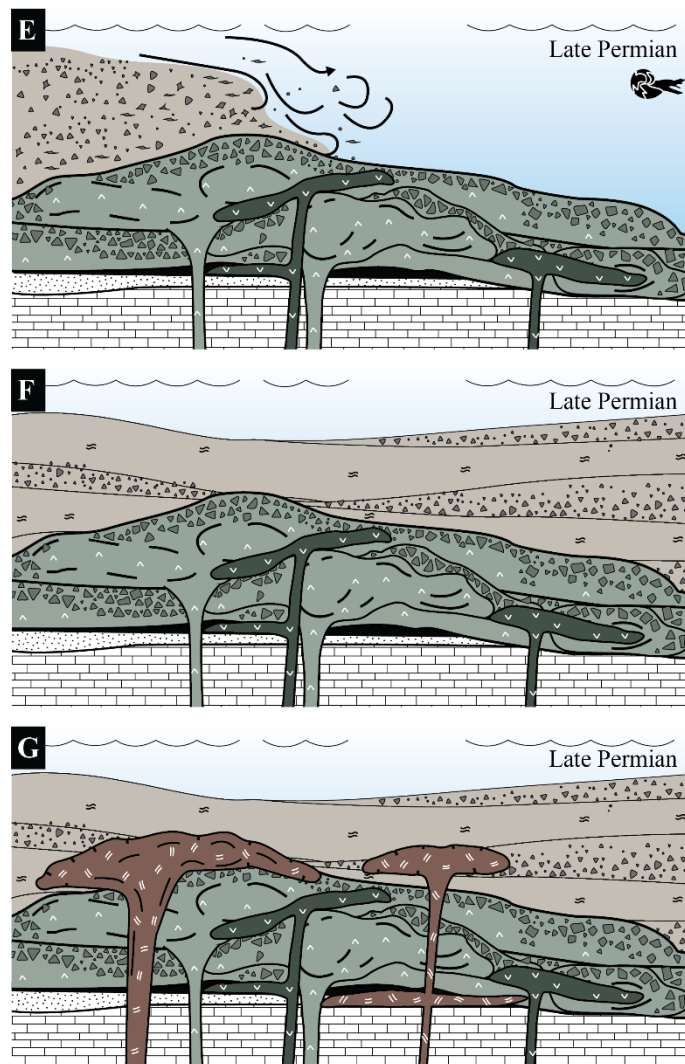


Fig. 5.2 Schematic of facies modal for depositional environment. **(E)** Syn-eruptive pyroclastic flow, pyroclastic surge and resedimented pyroclasts from distal source. **(F)** At least three sequence of felsic volcanism that deposited in the Khao Noi volcanic. And **(G)** the last events is syn-volcanic rhyolite dyke and sills.

5.4 Magmatic suite at Khao Noi volcanic

Petrography, the studied volcanic rock can be classified into three rock types (groups) for identifying the tectonic setting of the magmatic group as plagioclase-phyric andesite, plagioclase-phyric basalt, and aphyric trachyte. Based on chemical composition, the rocks are calc-alkaline and some of tholeiite series. Compositionally, they include andesite, trachyte-andesite, alkali basalt, and basanite. The characteristics for each rocks type: 1) Plagioclase-phyric andesite is characterized by low Ti, Zr, Sr, and Y, moderate Ni, and V, 2) Plagioclase-phyric basalt is characterized by high Ti and Sr, low Zr, Ni, V, and Zn, 3) Aphyric trachyte is characterized by high Zr and Sr, moderate

Y, and low Ni, V and Zn. Besides, the REE pattern divided into two magmatic suites, Suite I (plagioclase-phyric andesite I) is LREE enrichment, flat HREE, and minor negative Eu anomalies, while Suite II (plagioclase-phyric andesite II) and post volcanic sequence (plagioclase-phyric basalt and aphyric trachyte) more enrichment values of LREE>MREE>HREE than with strongly negative Eu anomalies.

5.5 Tectonic setting

The N-MORB normalized patterns of the Khao Noi volcanic rocks show relatively LILE enrichments, with low abundance of HFSE (especially Nb) which is characteristics of subduction-related magma (Stolz et al., 1996). The enrichment of Rb, K and Th is the enrichment of mantle source by aqueous fluids driven off subducted oceanic crust (Pearce, 1982).

Edwards et al., (1994) reported the Ringgit-Beser complex in East Java, Indonesia is a result of subduction between the Indo-Australian plate under Sunderland (Hall, 2012); subduction has produced a magma of calc-alkaline derived melts mantle fluxed by fluids from the subducted slab. Based on the similarity between the Ringgit-Beser complex and the Suite I volcanic of the Khao Noi area, it is inferred that the calc-alkaline rock of the Khao Noi area might form in a similar setting (the subduction environment).

Moreover, the plagioclase-phyric andesite (Suite II) and post-volcanic sequence (plagioclase-phyric basalt and aphyric trachyte) have a similar composition to high-K calc-alkaline from the Aeolian arc in the southern Tyrrhenian Sea that has been formed in an island arc setting along the northern and western margins of the Calabro Peroritano basement and European plate. In addition, the volcanic rocks in the Aeolian Arc are coexisting of calc-alkaline and shonshonitic to potassic alkaline affinity in a subduction-related environment (De Astis et al., 2000). The volcanic rocks of Suite II and post-volcanic sequence (plagioclase-phyric basalt and aphyric trachyte) from the Khao Noi area have similar geochemical characters that could well be formed in a similar tectonic environment.

Paipana (2014) dated detrital zircon from sandstone basement rocks (Unit 1) and reported that the depositional age of is not older than 328 Ma (Carboniferous). Salam (2013) reported rhyodacite from Khao Rabom Pran obtained U-Pb zircon age of 257.4 Ma suggesting the timing of Khao Noi volcanic could be formed during Late Permian

and it is further constrained by emplacement of the syenitic rocks north of Khao Noi which yielded U-Pb zircon age of 254 Ma (Late Permian; Paipana (2014)).

Moreover, since Khin Zaw unpublished data in Ridd (2012) reported the related age of 258 Ma from spherulitic rhyolite at the western part of Ko Chang (part of Sukhothai arc) about 100 km to the south of Khao Noi area, the implied age of the Khao Noi volcanic eruption and deposition are corresponding to be a part of Lampang volcanic belt which southern part of Sukhothai arc.

5.6 Regional tectonic setting

The N-MORB normalized trace element patterns distribution is analogous to the surrounding volcanic belts. In the Sukhothai arc, Barr et al. (2000) reported the volcanic rocks in the Lampang area have a calc-alkaline affinity of the Middle Triassic age. Srichan et al. (2009) studied basaltic dykes from the Chiang Khong area suggests that rocks have tholeiite affinity of Late Triassic age. In the Loei Fold Belt, Salam et al. (2014) reported the volcanic rocks in the Phetchabun area comprised of calc-alkaline dacitic dykes of Late Triassic. However, Arboit et al. (2016) suggested basaltic dykes have a calc-alkaline affinity of Late Triassic. Only limited geochemical data are available; most of the samples are close to data from the Lampang area of Sukhothai arc (Barr et al., 2000), that high alkalinity concentration. However, the Khao Noi volcanic have mildly calc-alkaline series, are identified to be Late Permian that the oldest volcanic rocks of Sukhothai arc (Fig. 5.3).

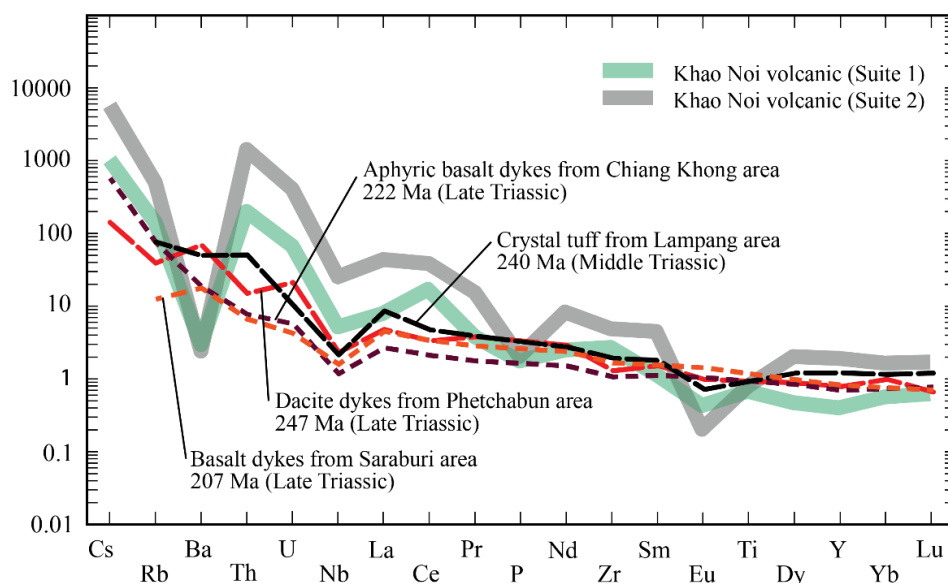


Fig. 5.3 N-MORB normalized multi-element diagram of Sun and McDonough (1989) displaying the patterns for two suite representative Khao Noi volcanic rocks compared with surrounding volcanic belt. **Note;** black dotted line data from Barr et al. (2000), purple dotted line data from Srichan et al. (2009), red dotted line data from Salam et al. (2014), orange dotted line data from Arboit et al. (2016).

5.7 Conclusion

Based on previous work, field investigation, lithofacies, stratigraphy, and geochemistry of the rocks of the Khao Noi volcanic, Chachoengsao Province, southeast Thailand. The key conclusion is defined below:

1. Based on field data, contact relationships in drill core logging, The Khao Noi area comprises mainly three units, namely, 1) Sedimentary unit, 2) Mafic-intermediate volcanic unit, and 3) Felsic volcanic unit.
2. Based on drill core logging, geochemical data, the volcanic sequence comprises five main eruptive events. The first event comprises plagioclase-aphyric andesite lava and quenches fragmentation (monomictic andesitic breccia), and the second event is mainly of andesitic lava and clast-rotated fragmentation. Both eruptions took place in a submarine environment. The third event involves the plagioclase-phyric basalt facies and aphyric trachyte facies as the intrusion of dykes. The fourth event is felsic-dominated compositions that comprise lithic-rich pumice breccia, crystal-rich pumice breccia representing the re-sediment products of a more explosive eruption a subaerial or submarine environment. Last events, quartz-phyric rhyolite

dykes, and sills show intrudes into unconsolidated sediment affected by mineralization.

3. Most coherent volcanic rocks in Khao Noi volcanic are mafic to intermediate consisting of basaltic, andesitic, and trachytic compositions that display porphyritic, aphyric, vesicular textures, which include plagioclase and hornblende phenocrysts. However, the latest sills occur as rhyolitic composition.
4. The magma affinity of volcanic rocks in the Khao Noi volcanic is high-K calc-alkaline affinity and most mafic to intermediate lavas, mafic dykes, and felsic sills.
5. There are two distinct types of volcanic composition that show similar geochemical characterized by LILE and LREE enrichment, which HREE and HFSE depletion with negative Eu anomalie. The geochemical characteristics suggest that these two groups were generated from the same parental magma, but they had two different fractional crystallization with minor contamination by upper crustal during volcanic rock evolution.
6. Characteristics of the REE and trace elements all indicate that subduction-related by enrichment of LILE and LREE relative to the HFSE. This subduction signature is thought to be formed in the pre-collision subduction event during the late Permian and end early Triassic. The oldest date of volcanic activity is about 258 Ma, very soon before the Paleo-Tethys closure.

REFERENCES

- Allen, R.L., 1992. Reconstruction of the tectonic, volcanic, and sedimentary setting of strongly deformed Zn-Cu massive sulfide deposits at Benambra, Victoria. *Econ. Geol.* 87, 825–854.
- Allen, R.L., Weihed, P., Svenson, S.-A., 1996. Setting of Zn-Cu-Au-Ag massive sulfide deposits in the evolution and facies architecture of a 1.9 Ga marine volcanic arc, Skellefte District, Sweden. *Econ. Geol.* 91, 1022–1053.
- Arboit, F., Collins, A.S., Morley, C.K., Jourdan, F., King, R., Foden, J., Amrouch, K., 2016. Geochronological and geochemical studies of mafic and intermediate dykes from the Khao Khwang Fold–Thrust Belt: Implications for petrogenesis and tectonic evolution. *Gondwana Res.* 36, 124–141.
- Barr, S.M., Charusiri, P., 2011. Volcanic rocks. *Geol. Thail. Geol. Soc. Lond.* 415–439.
- Barr, S.M., Macdonald, A.S., 1991. Toward a late Palaeozoic-early Mesozoic tectonic model for Thailand.
- Barr, S.M., Macdonald, A.S., 1987. Nan River suture zone, northern Thailand 4.
- Barr, S.M., Macdonald, A.S., 1979. Palaeomagnetism, age, and geochemistry of the Denchai Basalt, northern Thailand. *Earth Planet. Sci. Lett.* 46, 113–124.
- Barr, S.M., Macdonald, A.S., Dunning, G.R., Ounchanum, P., Yaowanoyothin, W., 2000. Petrochemistry, U–Pb (zircon) age, and palaeotectonic setting of the Lampang volcanic belt, northern Thailand. *J. Geol. Soc.* 157, 553–563.
- Barr, S.M., Macdonald, A.S., Ounchanum, P., Hamilton, M.A., 2006. Age, tectonic setting and regional implications of the Chiang Khong volcanic suite, northern Thailand. *J. Geol. Soc.* 163, 1037–1046.
- Barr, S.M., Tantisukrit, C., Yaowanoyothin, W., Macdonald, A.S., 1990. Petrology and tectonic implications of Upper Paleozoic volcanic rocks of the Chiang Mai belt, northern Thailand. *J. Southeast Asian Earth Sci.* 4, 37–47.
- Baum, F., Hanh, L., 1977. Geologic map of northern Thailand, Phayao Sheet, Scale 1:250,000.
- Baum, F., Von, B., Hess, A., Koch, K.E., 1982. Geological map sheet 5 (Chiang Mai) Northern Thailand map series, 1: 250,000.
- Boonsoong, A., Panjasawatwong, Y., Metparsopsan, K., 2011. Petrochemistry and tectonic setting of mafic volcanic rocks in the Chon Daen-Wang Pong area, Phetchabun, Thailand: Mafic volcanics of Phetchabun, Thailand. *Isl. Arc* 20, 107–124.
- Bunopas, S., 1981. Palaogeographic history of western Thailand and adjacent parts of Southeast Asia-A plate tectonics interpretation. *Geol. Surv. Pap.* 5, 810.

- Bunopas, S., Khositantont, S., 2008. Did Shan-Thai twice marry Indochina and then India?: A Review 27.
- Bunopas, S., Vella, P., 1983. Tectonic and geologic evolution of Thailand, in: Proceedings of a Workshop on Stratigraphic Correlation of Thailand and Malaysia. Geological Society of Thailand, Bangkok/Geological Society of Malaysia Kuala Lumpur, pp. 307–322.
- Cas, R., Wright, J., 2012. Volcanic successions modern and ancient: A geological approach to processes, products and successions. Springer Science & Business Media.
- Chaodumrong, P., 1992. Stratigraphy, sedimentology and tectonic setting of the Lampang Group, central north Thailand 247.
- Cumming, G.V., 2005. Analysis of volcanic facies at the Chatree gold mine and in the Loei-Petchabun Volcanic belt, central Thailand (honours). University of Tasmania.
- De Astis, G., Peccerillo, A., Kempton, P.D., La Volpe, L., Wu, T.W., 2000. Transition from calc-alkaline to potassium-rich magmatism in subduction environments: geochemical and Sr, Nd, Pb isotopic constraints from the island of Vulcano (Aeolian arc). *Contrib. Mineral. Petrol.* 139, 684–703.
- Department of Mineral Resources (DMR), 2007. Report of Mineral Resources Exploration and Evaluation Project: Area 4/2001 “Bo Thong.” Department of Mineral Resources, Bangkok, Thailand.
- Edwards, C.M.H., Menzies, M.A., Thirlwall, M.F., Morris, J.D., Leeman, W.P., Harmon, R.S., 1994. The Transition to Potassic Alkaline Volcanism in Island Arcs: The Ringgit-Beser Complex, East Java, Indonesia. *J. Petrol.* 35, 1557–1595.
- Fontaine, H., Salyapongse, S., Vachard, D., 1999. The Carboniferous of East Thailand—New Information from Microfossils.
- Gillespie, M.R., Kendall, R.S., Leslie, A.G., Millar, I.L., Dodd, T.J., Kearsy, T.I., Bide, T.P., Goodenough, K.M., Dobbs, M.R., Lee, M.K.W., 2019. The igneous rocks of Singapore: new insights to Palaeozoic and Mesozoic assembly of the Sukhothai Arc. *J. Asian Earth Sci.* 183, 103940.
- Grace, V., 2004. Analysis of volcanic facies at the Chatree gold mine and in the Loei-Phetchabun volcanic belt, central Thailand. Tasmania.
- Hall, R., 2012. Late Jurassic–Cenozoic reconstructions of the Indonesian region and the Indian Ocean. *Tectonophysics* 570–571, 1–41. <https://doi.org/10.1016/j.tecto.2012.04.021>
- Hara, H., Wakita, K., Ueno, K., Kamata, Y., Hisada, K., Charusiri, P., Charoentitirat, T., Chaodumrong, P., 2009. Nature of accretion related to Paleo-Tethys subduction recorded

- in northern Thailand: Constraints from mélange kinematics and illite crystallinity. *Gondwana Res.* 16, 310–320.
- Intasopa, S., 1993. Petrology and geochronology of the volcanic rocks of the Central Thailand Volcanic Belt, unpublished Ph. D (PhD. Thesis). Thesis, The University of New Brunswick, Canada.
- Intasopa, S., Dunn, T., 1994. Petrology and Sr-Nd isotopic systems of the basalts and rhyolites, Loei, Thailand. *J. Southeast Asian Earth Sci.* 9, 167–180.
- Irvine, T.N., Baragar, W.R.A., 1971. A Guide to the Chemical Classification of the Common Volcanic Rocks. *Can. J. Earth Sci.* 8, 523–548.
- Jundee, P.K., Limtrakun, P., Boonsoong, A., Panjasawatwong, Y., 2017. Felsic to Mafic Volcanic /Hypabyssal Rock in Nakhon Sawan and Uthai Thani Provinces, Central Thailand. *Chiang Mai J Sci* 13.
- Jungyusuk, N., Khositantont, S., 1992. Volcanic rocks and associated mineralization in Thailand, in: *Proceedings of a National Conference on Geologic Resources of Thailand: Potential for Future Development*. Department of Mineral Resources, Bangkok. p. 538.
- Kamvong, T., Charusiri, P., Intasopa, S.B., 2006. Petrochemical characteristics of igneous rocks from the Wang Pong Area, Phetchabun, North Central Thailand: implications of tectonic setting. *J. Geol. Soc. Thail.* 1, 9–26.
- Khin Zaw., Santosh, M., Graham, I.T., 2014. Tectonics and metallogeny of mainland SE Asia: Preface. *Gondwana Res.* 26, 1–4.
- Khositantont, S., 2008. Gold and iron–gold mineralization in the Sukhothai and Loei–Phetchabun Fold Belts. PhD Thesis Chiang Mai Univ. Chiang Mai Thail. Univ. Tasman. Hobart Aust. 185.
- Khositantont, S., Khin Zaw, Ounchanum, P., 2009. Mineralization characteristics and ore fluid of Huai Kham On gold deposit, northern Thailand, in: *Advances in Geosciences: Volume 13: Solid Earth (SE)*. World Scientific, pp. 1–12.
- McCulloch, M.T., 1991. Geochemical and geodynamical constraints on subduction zone magmatism 17.
- McLennan, S.M., 1989. Rare earth elements in sedimentary rocks: influence of provenance and sedimentary processes. *Geochem. Mineral. Rare Earth Elem. Rev. Mineral.* 21 169–200.
- McPhie, J., Doyle, M., Allen, R.L., 1993. Volcanic textures: a guide to the interpretation of textures in volcanic rocks.
- Morley, C.K., 2002. A tectonic model for the Tertiary evolution of strike–slip faults and rift basins in SE Asia. *Tectonophysics* 347, 189–215.

- Müller, D., Rock, N.M.S., Groves, D.I., 1992. Geochemical discrimination between shoshonitic and potassic volcanic rocks in different tectonic settings: a pilot study. *Mineral. Petrol.* 46, 259–289.
- Paipana, S., 2014. Geology and Mineralization Characteristics of Bo Thong Antimony+-Gold Deposit, Chonburi Province, Eastern Thailand. BSc Hons Thesis Univ. Tasman. Hobert Aust. 100.
- Palin, R.M., Searle, M.P., Morley, C.K., Charusiri, P., Horstwood, M.S.A., Roberts, N.M.W., 2013. Timing of metamorphism of the Lansang gneiss and implications for left-lateral motion along the Mae Ping (Wang Chao) strike-slip fault, Thailand. *J. Asian Earth Sci.* 76, 120–136.
- Panjasawatwong, Y., 2003. Tectonic Setting of the Permo-Triassic Chiang Khong Volcanic Rocks, Northern Thailand Based on Petrochemical Characteristics. *Gondwana Res.* 6, 743–755.
- Panjasawatwong, Y., Danyushevsky, L.V., Crawford, A.J., Harris, K.L., 1995. An experimental study of the effects of melt composition on plagioclase-melt equilibria at 5 and 10 kbar: implications for the origin of magmatic high-An plagioclase. *Contrib. Mineral. Petrol.* 118, 420–432.
- Panjasawatwong, Y., Yaowanoyothin, W., 1993. Petrochemical study of post-Triassic basalts from the Nan Suture, northern Thailand. *J. Southeast Asian Earth Sci.* 8, 147–158.
- Panjasawatwong, Y., Khin Zaw, Chantaramee, S., Limtrakun, P., Pirarai, K., 2006. Geochemistry and tectonic setting of the Central Loei volcanic rocks, Pak Chom area, Loei, northeastern Thailand. *J. Asian Earth Sci.* 26, 77–90.
- Pearce, J.A., 1996. A user's guide to basalt discrimination diagrams. *Trace Elem. Geochem. Volcan. Rocks Appl. Massive Sulphide Explor. Geol. Assoc. Can. Short Course Notes* 12, 113.
- Pearce, J.A., 1983. Role of the sub-continental lithosphere in magma genesis at active continental margins, in: Hawkesworth, C.J., Norry, M.J. (Eds.), *Continental Basalts and Mantle Xenoliths*. Shiva Publications, Nantwich, Cheshire, pp. 230–249.
- Pearce, J.A., 1982. Trace element characteristics of lavas from destructive plate boundaries. *Andesites* 525–548.
- Phajuy, B., 2008. Petrochemistry and tectonic significance of mafic volcanic rocks in the Chiang Rai-Chiang mai volcanic belt, Northern Thailand (PhD. Thesis). Chiang Mai: Graduate School, Chiang Mai University, 2008.
- Phajuy, B., Panjasawatwong, Y., Osataporn, P., 2005. Preliminary geochemical study of volcanic rocks in the Pang Mayao area, Phrao, Chiang Mai, northern Thailand: tectonic setting of formation. *J. Asian Earth Sci.* 24, 765–776.

- Phajuy, B., Singtuen, V., 2019. Petrochemical characteristics of Tak volcanic rocks, Thailand: Implication for tectonic significance. *ScienceAsia* 45, 350–360.
- Piyasin, S., 1972. Geology of Changwat Lampang Sheet (NE47-7), scale 1: 250,000.
- Qian, X., Wang, Y., Feng, Q., Zi, J.-W., Zhang, Y., Chonglakmani, C., 2016. Petrogenesis and tectonic implication of the Late Triassic post-collisional volcanic rocks in Chiang Khong, NW Thailand. *Lithos* 248–251, 418–431.
- Qian, X., Wang, Y., Srithai, B., Feng, Q., Zhang, Y., Zi, J.-W., He, H., 2017. Geochronological and geochemical constraints on the intermediate-acid volcanic rocks along the Chiang Khong–Lampang–Tak igneous zone in NW Thailand and their tectonic implications. *Gondwana Res.* 45, 87–99.
- Ridd, M.F., 2012. The role of strike-slip faults in the displacement of the Palaeotethys suture zone in Southeast Thailand. *J. Asian Earth Sci.* 51, 63–84.
- Salam, A., 2013. A geological, geochemical and metallogenic study of the Chatree epithermal deposit, Phetchabun Province, central Thailand (PhD. Thesis). University of Tasmania.
- Salam, A., Khin Zaw, K., Meffre, S., McPhie, J., Lai, C.-K., 2014. Geochemistry and geochronology of the Chatree epithermal gold–silver deposit: Implications for the tectonic setting of the Loei Fold Belt, central Thailand. *Gondwana Res.* 26, 198–217.
- Shen, S., Feng, Q., Zhang, Z., Chongpan, C., 2009. Geochemical characteristics of the oceanic island-type volcanic rocks in the Chiang Mai zone, northern Thailand. *Chin. J. Geochem.* 28, 258–263.
- Simpson, K., McPhie, J., 2001. Fluidal-clast breccia generated by submarine @re fountaining, Trooper Creek Formation, Queensland, Australia. *J. Volcanol. Geotherm. Res.* 17.
- Singharajwarapan, S., Berry, R., 2000. Tectonic implications of the Nan Suture Zone and its relationship to the Sukhothai Fold Belt, Northern Thailand. *J. Asian Earth Sci.* 18, 663–673.
- Sone, M., Metcalfe, I., 2008. Parallel Tethyan sutures in mainland Southeast Asia: New insights for Palaeo-Tethys closure and implications for the Indosinian orogeny. *Comptes Rendus Geosci.* 340, 166–179.
- Sone, M., Metcalfe, I., Chaodumrong, P., 2012. The Chanthaburi terrane of southeastern Thailand: Stratigraphic confirmation as a disrupted segment of the Sukhothai Arc. *J. Asian Earth Sci.* 61, 16–32.
- Srichan, W., Crawford, A.J., Berry, R.F., 2009. Geochemistry and geochronology of Late Triassic volcanic rocks in the Chiang Khong region, northern Thailand. *Isl. Arc* 18, 32–51.

- Stolz, A.J., Jochum, K.P., Spettel, B., Hofmann, A.W., 1996. Fluid-and melt-related enrichment in the subarc mantle: evidence from Nb/Ta variations in island-arc basalts. *Geology* 24, 587–590.
- Sun, S. -s., McDonough, W.F., 1989. Chemical and isotopic systematics of oceanic basalts: implications for mantle composition and processes. *Geol. Soc. Lond. Spec. Publ.* 42, 313–345.
- Tangwattananukul, L., Lunwongsa, W., Mitsuta, T., Ishiyama, H., Takashima, I., Won-In, K., Charusiri, P., 2008. Geology and petrochemistry of dike rocks in the Chatree gold mine, central Thailand: Implication for tectonic setting, in: *Proceedings of the International Symposia on Geoscience Resources and Environments of Asian Terranes (GREAT 2008)*, 4th IGCP. pp. 299–311.
- The Royal Thai Survey Department, 2008. AMPHOE THA TAKIAP (Sheet 5335IV). L7018.
- Tiyapirach, S., 1996. Geological map of Amphoe Tha Takiap (5335 IV)-1:50,000 scale. Bureau of Geological Survey, Department of Mineral Resources, Bangkok, Thailand.
- Ueno, K., Hisada, K., 2001. The Nan-Uttaradit-Sa Kaeo Suture as a Main Paleo-Tethyan Suture in Thailand: Is it Real? *Gondwana Res.* 4, 804–806.
- Wang, Y., He, H., Zhang, Y., Srithai, B., Feng, Q., Cawood, P.A., Fan, W., 2017. Origin of Permian OIB-like basalts in NW Thailand and implication on the Paleotethyan Ocean. *Lithos* 274–275, 93–105.
- Winchester, J.A., Floyd, P.A., 1977. Geochemical discrimination of different magma series and their differentiation products using immobile elements. *Chem. Geol.* 20, 325–343.
- Wipakul, U., Tiangtham, C., Srithai, B., Panjasawatwong, Y., 2012. Volcanic Facies of the Doi Phra Baht Volcanic Deposits, Mueang District, Lampang Province, Thailand 5, 9.
- Zhang, G., Qu, H., Liu, S., Xie, X., Zhao, Z., Shen, H., 2016. Hydrocarbon accumulation in the deep waters of South China Sea controlled by the tectonic cycles of marginal sea basins. *Pet. Res.* 1, 39–52.

VITA

NAME Amporn Chaikam

DATE OF BIRTH 15 February 1986

PLACE OF BIRTH Chiang Mai

**INSTITUTIONS
ATTENDED** Bachelor of Sciences in Geology, Chiang Mai University,
Chiang Mai, Thailand

HOME ADDRESS 14/8 Nantaram Rd., Hayya Subdistrict, Muang District,
Chiang Mai Province.



จุฬาลงกรณ์มหาวิทยาลัย
CHULALONGKORN UNIVERSITY